UNIVERSITY OF CALIFORNIA
RIVERSIDE

Immunoregulatory Mechanisms in a Mouse Model of Hookworm Infection

A Dissertation submitted in partial satisfaction
of the requirements for the degree of

Doctor of Philosophy

in

Microbiology

by

Hashini M. Batugedara

December 2018

Dissertation Committee:
Dr. Meera Nair, Chairperson
Dr. Emma Wilson
Dr. Adler Dillman

The Dissertation of Hashini M. Batugedara is approved:

Committee Chairperson

University of California, Riverside

ACKNOWLEDGEMENTS

I want to express sincere gratitude to my advisor Dr Meera Nair. Meera, thank you for allowing me to work on these research projects and for motivating me throughout my graduate career. This work was only possible because of your vision and guidance.

I also want to thank my thesis committee, Dr Emma Wilson and Dr Adler Dillman. Thank you for your continued support and guidance throughout my thesis work.

A most heartfelt thank you to my lab mates, past and present. I could not have asked for a better group of people to work with day after day. Your friendship and support has meant the world to me.

Finally, I need to thank my family and friends. I would not be where I am today without you.

The text of this dissertation, in part or in full, is a reprint of the material as it appears in "Here, there and everywhere: Resistin-like molecules in infection, inflammation, and metabolic disorders" in Cytokine, 2018. Gabrielle Pine and Hashini Batugedara, wrote the article. Meera Nair listed in that publication wrote, directed and supervised the research which forms the basis for this dissertation.

The text of this dissertation, in part or in full, is a reprint of the material as it appears in "Hematopoietic cell-derived RELMα regulates hookworm immunity through effects on macrophages" in the Journal of Leukocyte Biology, 2018. Hashini Batugedara, Jiang Li, Gang Chen, Dihong Lu, Jay Patel, Jessica Jang, Kelly Radecki and Abi Burr performed the

investigation, formal analysis and visualization. Adler Dillman and Meera Nair listed in that publication directed and supervised the research which forms the basis for this dissertation. The text of this dissertation, in part or in full, is a reprint of the material as it appears in "Host and helminth-derived endocannabinoids are generated during infection with effects on host immunity" in Infection and Immunity, 2018. Hashini Batugedara, Donovan Argueta, Jessica Jang, Dihong Lu, Marissa Macchietto, Jaspreet Kaur performed the investigation, formal analysis and visualization. Adler Dillman, Nicholas DiPatrizio and Meera Nair listed in that publication directed and supervised the research which forms the basis for this dissertation.

.

DEDICATION

For ammi, thaththi and akki and jojo.

ABSTRACT OF THE DISSERTATION

Immunoregulatory Mechanisms in a Mouse Model of Hookworm Infection

by

Hashini M. Batugedara

Doctor of Philosophy, Graduate Program in Microbiology
University of California, Riverside, December 2018
Dr. Meera Nair, Chairperson

Parasitic worms infect billions of people worldwide. In humans, these infections and inflammation are chronic and debilitating. Therefore, it is imperative to explore host factors that regulate immunity and promote parasite clearance and host protection. In this thesis we discuss two such host factors; resistin like molecules and endocannabinoids.

We describe here that during infection with the rodent hookworm *Nippostrongylus brasiliensis* (*Nb*), a host molecule named RELMα dampens Th2 inflammatory responses. We use bone marrow (BM) chimera technology to show that RELMα from BM-derived cells and not non BM cells dampens Th2 immunity and prevents worm clearance. We show that of the BM cells, $CD11c^+$ lung macrophages are the dominant source of RELMα. Next, we employ a macrophage-worm co-culture system and found that RELMα impairs the ability of macrophages to attach to and kill worms. By conducting gene expression analysis, we show that RELMα decreased cell adhesion and Fc receptor signaling pathways, which are associated with macrophage-mediated helminth killing.

Second, we explored how endocannabinoid signaling influences host immunity to helminths. Endocannabinoids are lipid-derived signaling molecules that function in feeding behavior and metabolism. Following *Nb* infection, we detected elevated levels of endocannabinoids 2-AG and AEA in the worm infected mouse lung and intestine. To test how endocannabinoids influence helminth infection, we utilized pharmacological inhibitors of cannabinoid receptors. We found inhibition of CB_1R resulted in higher worm and eggs burdens which was correlated with decreased amounts of the Th2 cytokine IL-5 in the host. Interestingly, bioinformatic analysis revealed putative genes encoding endocannabinoid biosynthetic and degradative enzymes in many parasitic nematodes. Additionally, we found that all lifecycle stages of Nb produce endocannabinoids. Therefore, we report for the first time that helminth and host-derived endocannabinoids promote host immune responses and reduce parasite burden.

Collectively, these studies demonstrate two mechanisms of immunomodulation during helminth infection. In the first mechanism, BM-derived RELMα dampens immune responses and inhibits macrophage killing of worms. In the second mechanism, we describe how host and parasite-derived endocannabinoids promote host immunity by upregulating Th2 immunity which drives parasite clearance. In summary, we have identified key regulators of immune responses in helminth infection.

TABLE OF CONTENTS

LIST OF FIGURES

LIST OF TABLES

CHAPTER ONE – Introduction: Resistin-Like Molecules and Endocannabinoids Regulate Inflammation and Immunity During Helminth Infections

Hashini M. Batugedara[1] and Meera G. Nair[2]

[1]Department of Microbiology, University of California Riverside, Riverside, CA, USA.

[2]Division of Biomedical Sciences, School of Medicine, University of California Riverside, Riverside, CA, USA

A version of this chapter was published in *Cytokine*, 2018.

Abstract

Infections with parasitic worms are met with a T helper type 2 (Th2) immune response by the host. Th2 immunity is important for controlling parasite burdens during primary infections and for developing immunity to subsequent secondary infections. Parasitic worm infections are typically chronic in nature where worms persist within the host for long periods of time causing physical damage as they migrate through tissues. Th2 immunity has evolved to rapidly repair tissue damage caused by parasites and is critical for restoring tissue integrity and homeostasis. However, due to the chronicity of helminth infections, tissue repair processes can be persistent and can ultimately lead to debilitating fibrosis. Therefore, Th2 immunity needs to be delicately regulated to clear infection and protect the host from excessive inflammation.

In this chapter, we will introduce the significance of studying helminth infections, a laboratory model for studying helminth infections and the host immune response generated against parasitic worms. We will conclude with a review of resistin-like molecules and endocannabinoids, two host factors found to be immunoregulatory during helminth infection, for their multifaceted roles in physiology and specifically in the immune system.

Helminth infections

Helminth infections as a public health concern

Parasitic worms, known scientifically as helminths, are a global health concern as they cause devastating disease in an estimated two billion of the world's poorest populations. Nematodes (intestinal and filarial worms) and platyhelminths (trematodes, flukes and cestodes) constitute the two phyla of helminths [1]. The major intestinal helminth infections of humans are caused by *Ascaris lumbricoides* (roundworm), *Trichuris trichiura* (whipworm), *Necator americanus* and *Ancylostoma duodenale* (hookworm) [2]. While roundworm and whipworm are transmitted by swallowing parasite eggs, hookworms enter the host by infectious larvae penetrating the skin (Table 1). Once in the host, roundworms and whipworms hatch, mature and propagate in the small and large intestine, respectively. Hookworms that penetrate the skin travel through vasculature and the lungs, then mature and lay eggs in the intestine. The adult parasite tenure within the host is species dependent but ranges from 1 to 7 years. All three intestinal parasites complete their lifecycle by being passed in feces as eggs that then survive in contaminated soil until they come in contact with a suitable human host [3]. Therefore, diseases associated with intestinal helminths are prevalent in sub-tropical areas with poor sanitation conditions that cause infections and re-infections to be common.

Clinical manifestations of helminth infection

Due to the chronic nature of most helminth infections, helminthiasis is not associated with high mortality but rather, with high morbidity. Acute disease symptoms caused by parasitic worm infections include anemia, weight loss and swelling of extremities or more severely, chronic helminth infections have been associated with life-long morbidity including growth retardation and organ failure [4, 5]. Containment of helminth infections currently rely on

treatment with anti-parasitic drugs such as ivermectin, mebendazole and albendazole [2]. An interesting feature of helminth infection is that worm burdens are not equally distributed in a given population [6]. This led to coining the term “wormy persons”, suggesting that differences in host biology may contribute to the magnitude of infection. Further, there is no clear evidence that the infected host develops lasting protective immunity to helminths. Therefore, in endemic regions, even with the availability of anti-parasitic drugs, re-infections occur. To this end, investigating host factors that contribute to and regulate immunity to helminths is critical.

Table 1. Characteristics of nematodes that commonly infect humans

	Ascaris lumbricoides	*Trichuris trichiura*	*Necator americanus Ancylostoma duodenale*
Disease	Roundworm infection/Ascariasis	Whipworm infection/Trichuriasis	Hookworm infection
Population infected (millions)	807-1221	604-795	576–740
Route of infection	Ingestion of eggs	Ingestion of eggs	L3 larvae skin penetration
Site of infection	Small intestine	Caecum and colon	Lungs and small intestine
Lifespan in host (years)	1	1.5-2	5-7

***Nippostrongylus brasiliensis* as a model of hookworm infection**

Nippostrongylus brasiliensis (*Nb*) is widely used as a model to study human hookworm infection. *Nb* is a natural parasite of rodents which shares homology to human hookworms *Necator americanus* and *Ancylostoma duodenale*. In laboratory studies, mice are infected with *Nb* by subcutaneous injection. Similar to the human hookworm lifecycle, the *Nb* larvae enter the vasculature of the mouse and then enter the lungs at 1-2 days post infection. While in the lungs *Nb* burrow through the tissue causing massive hemorrhaging [5]. Importantly for the worm, they undergo development from L3 to L4 larvae. Starting at day 3 post infection, worms travel via the trachea and esophagus of the mouse and enter the stomach and small intestine. In the small intestine, the worms mature to their adult stage, propagate, and produce thousands of eggs per day. These eggs are passed in the feces starting at day 6 post infection and persists until worms are cleared by day 9 post infection [7]. The eggs that pass in the mouse feces can be collected and cultured in the laboratory using fecal culture methods [8]. In the fecal culture, eggs hatch within 24 h and undergo two molts to develop into L3 infectious stage larvae. To isolate L3 larvae for experiments, L3 from fecal cultures can be extracted using a Baermann apparatus [8]. Of note, the *Nb* lifecycle differs from human hookworms in that the mice can clear the worms from their system by approximately day 10 post infection with immunity developed for challenge secondary infections [7]. In contrast, human hookworms are retained in the host small intestine for 1-5 years with little to no immunity developed for re-infection. Due to the ease of maintaining the lifecycle and susceptibility of laboratory mice and rats, *Nb* is currently widely used to as a model for studying host responses to hookworms.

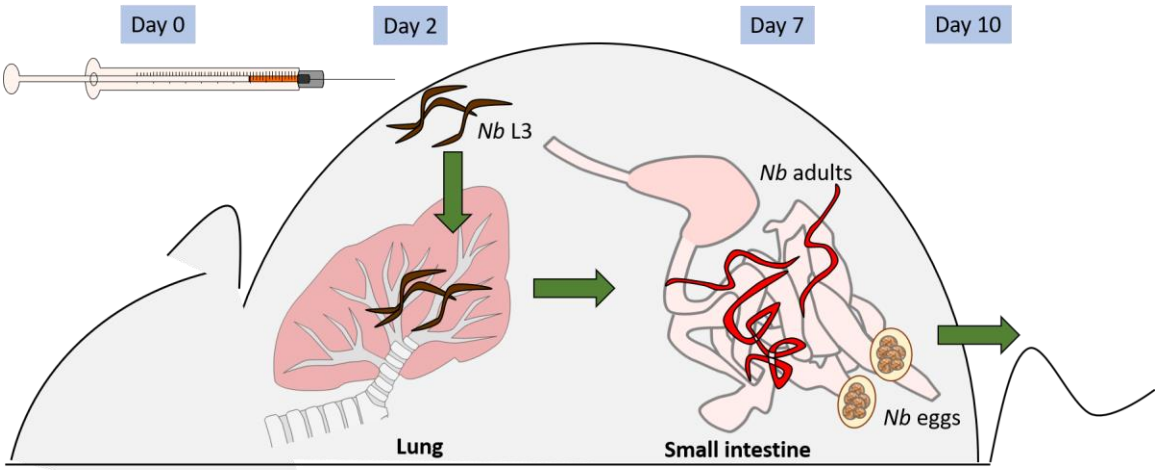

Figure 1. ***Nippostrongylus brasiliensis*** **lifecycle in the mouse used for laboratory studies.**

Host immunity to helminth infections

The host immune response against invading pathogens can be characterized broadly as type 1 (Th1) or type 2 (Th2). Th1 responses are host responses against bacteria, viruses and intracellular parasites. In contrast, the host launches a Th2 responses against helminths and extracellular parasites. Each type of immune response is characterized by a specific set of cytokines unique to the relevant inflammatory milieu. The primary Th1 cytokines are IFNγ, TNFα and IL-2, whereas the primary Th2 cytokines are IL-4, IL-5, IL-9 and lL-13 [9]. Once initiated by the appropriate pathogen, the immune response and associated cells and cytokines interact in a coordinated effort to clear the pathogen and return the host back to homeostasis.

Th2 activation

In contrast to Th1 immunity that is triggered by pathogen associated molecular pattern (PAMP) signaling by immune cells, Th2 immunity is trigged by danger associated signaling patterns (DAMPS) by damaged tissue. Specifically, during hookworm infection, damaged barrier tissues of the skin and lung produce DAMPS such as Trefoil factor 2 [9, 10]. DAMPS can then drive damaged epithelial cells to produce molecules known as alarmins such as thymic stromal lymphopoietin (TSLP), IL-33 and IL-25. IL-33 and IL-25 produced by damaged epithelial cells initiates the recruitment of innate lymphoid cell type 2 (ILC2), which contribute large quantities of Th2 cytokines IL-5 and IL-13 [9, 11]. Eosinophils and basophils that are recruited in response to these cytokines bind circulating IgE bound to parasites with their receptor FcεRI. This granulocyte-IgE interaction causes cell activation that leads to degranulation and effector molecule release for parasite damage [12]. Eosinophils and basophils play additional role as they are important innate sources of IL-4. These innate sources of IL-4 in addition to IL-33 and IL-25

help activate T helper 2 cells which then in turn produced more IL-4 and IL-13 that further intensifies the Th2 milieu [9].

Alternatively activated macrophages

Th2 cytokines activate B cells, antibody production and differentiation of alternatively activated macrophages (AAMs; versus classically activated macrophages in Th1 settings). AAMs play an important role in promoting wound healing [13]. Parasite migration and exacerbated inflammation leads to tissue damage that is then repaired by products of alternatively activated macrophages. AAMs promote wound healing by regulating inflammatory responses, phagocytosing debris in the affected tissue and by expressing a number of genes involved in wound healing such as arginase-1 and RELMα [13, 14]. Multiple studies that depleted macrophages in a skin injury model found that AAMs function in downregulating hemorrhage and promoted fibrogenesis and reepithelization [15, 16].

Lung inflammation during hookworm infection

Specifically, during hookworm infections, the host suffers from severe lung hemorrhage as the worm migrates through lung tissue as a natural step in their lifecycle [5]. The immune response that is launched against the worms also contributes to tissue damage. Collectively, lung damage can lead to acute inflammation that develops into chronic inflammation [17]. This inflammation and tissue remodeling induced by hookworms shares characteristics with the lung pathology observed in allergy, asthma and chronic obstructive pulmonary disease [17-19].

Intestinal inflammation during hookworm infection

In the intestines, hookworms that arrive from the lungs attach to the intestinal epithelium and feed on host blood. Here, immune and non-immune cells alike respond to IL-4 and IL-13 produced during intestinal worm infection. IL-13 drives a mechanism known as " the epithelial escalator" and "weep and sweep" [20]. In the epithelial escalator, intestinal epithelial cells respond to IL-13 by undergoing excessive cell proliferation that leads to shedding of epithelial cells and the worms attached to them. In the weep and sweep mechanism, intestinal goblet cells produce excessive mucus and cause smooth muscle contraction to expel worms [20]. In a study where AAMs were depleted using clodronate liposomes it was shown that AAM products such as arginase-1 contribute to smooth muscle contraction and the weep and sweep method for parasite elimination from the intestines [21]. In both the lungs and the intestines, the process of immune clearance of pathogens is highly regulated where proinflammatory signaling for pathogen clearance is held in tight balance with immunoregulatory signaling to prevent host tissue damage.

In this thesis, we will discuss two mechanisms of Th2 immune regulation during helminth infections of mice. First, we will present a study on immune response downregulation by a host molecule known as RELMα that functions to impair macrophage functions against parasitic worms. The second study will detail host and parasite derived endocannabinoid production during hookworm infection, which contributes to an upregulated immune response important for worm clearance. Together, these studies will reveal the complex nature of immune responses during insult by parasitic worms and highlight the mechanisms by which two seemingly unrelated host molecules, RELMα and endocannabinoids, function in parallel for host protection during helminth infection.

Resistin-like molecules (RELMs)

Resistin-like molecules (RELMs) are mammalian secreted proteins, which were identified less than 20 years ago in different disease settings, leading to differing nomenclature. RELMα (*Retnla*) was the first RELM protein discovered in a mouse model of asthma, where it was named FIZZ1 for Found in Inflammatory Zone. Murine resistin (*Retn*/FIZZ3) was subsequently identified and functionally characterized in metabolic dysfunction, where it caused "resistance" to insulin, leading to the more common nomenclature for this protein family as 'RELMs'. Finally, RELMα was also investigated in hypoxia and named Hypoxia-Induced Mitogenic Factor (HIMF) [22]. The complex nomenclature demonstrates significant diversity in RELM expression pattern and functions, however, it may cause confusion and potential bias when searching for studies on this intriguing family of proteins.

RELM gene and protein structure

The RELM gene family (*Retn*) was originally identified in mice, but appears to be present in all mammals [23]. While mice and rats have four RELM genes *Retn*, *Retnla*, *Retnlb*, *Retnlg*; only *Retn* and *Retnlb* belong to a diverse taxonomic group, including humans, nonhuman primates, canines, cats and horses. In mice and rats, three of the four RELM genes, *Retnlb*, *Retlna* and *Retnlg*, are clustered together on chromosome 16 [24]. These genes share the most sequence homology and exhibit similar transcriptional regulation but are differentially expressed in cell-types and tissue. In comparison, mouse *Retn*, human *Retn* and human *Retnlb* exhibit greater diversity in transcriptional regulation and expression pattern, and are present on different chromosomes (chromosomes 8, 19 and 3 respectively). Sequence identity is high between human and mouse RELM proteins, with ~ 60% homology in amino acid sequence [25, 26].

RELM genes encode secreted proteins of 105-138 amino acids in size with 3 main domains: an amino (N) terminal signal sequence, a variable middle section, and a conserved carboxyl (C) terminal. The C terminal is comprised of a cysteine signature motif sequence shared by all RELM family members (C-X_{11}-C-X_8-C-X-C-X_3-C-X_{10}-C-X-C-X-C-X_9-CC-X_{3-6}-END), which is proposed to be critical for disulfide bond formation and protein folding [24, 27, 28]. The crystal structures of mouse resistin and RELMβ have been solved, revealing that they form trimers linked together via disulfide bonds to form hexameric assemblies [29]. Dimerization of RELMβ and resistin was dependent on a cysteine in the N-terminal. This cysteine is lacking in RELMα and RELMγ, suggesting that they may exist as monomers [30, 31], however their crystal structure has not been solved. A better understanding of the RELM protein structure may provide important information for identification of the receptors, which remain unknown for many of the RELM proteins.

Genetic regulation of RELM expression

The genetic regulation and expression profile of the RELM genes have been well characterized from several human and murine studies (Figure 2A). These studies reveal both shared and distinct cellular expression profiles within the RELM gene family (Figure 2B). While some RELM genes, such as RELMα, RELMγ and human resistin, are expressed by hematopoietic cells, mouse resistin, RELMα and RELMβ are expressed in non-hematopoietic cells. All mouse and human RELM proteins are detectable in the serum, offering the potential to utilize RELM levels as biomarkers [32-34].

RELMα/*Retnla* exhibits the greatest heterogeneity in expression within the RELM family. Under homeostatic conditions, *Retnla* mRNA is present at low levels in the lung, tongue, mammary tissue, and white adipose tissue [27]. Originally discovered as a secreted protein in the

bronchio-alveolar lavage of ovalbumin-challenged mice, the consensus from multiple studies using mouse asthma models is that RELMα is highly expressed by airway epithelial cells and type 2 pneumocytes [22, 35, 36]. Consistent with this, RELMα transcription is driven and critically dependent on a Th2 cytokine environment. Indeed, binding sites for the Th2 cytokine-induced transcription factor STAT6 are present within the *Retnla* promoter, and STAT6$^{-/-}$ or IL-4$^{-/-}$ mice exhibit reduced RELMα expression [37, 38]. In addition to expression by non-hematopoietic cells, RELMα is also recognized as a key signature gene of M2/alternatively activated macrophages that differentiate in chronic, Th2 cytokine-skewed conditions such as helminth or chronic protozoan parasite infection [38-41]. RELMα expression by other immune cells, eosinophils and dendritic cells (DC), has also been reported [39, 42]. RELMα is also expressed in lung and peritoneal injury models, and following hypoxic stress [22, 43, 44]. In these models, RELMα expression may rely on other transcription factors, such as CCAAT/enhancer-binding protein (C/EBP), which binds to its' specific motif adjacent to the STAT6 binding site in the *Retnla* promoter [37]. While RELMα induction can occur in the absence of Th2 cytokine signaling, likely through C/EBP, sustained RELMα expression requires Th2 cytokine stimulation [44]. Interestingly, functional transcription studies revealed that C/EBP binding to the *Retnla* promoter was necessary for IL-4/STAT6-induced *Retnla* expression, suggesting that the STAT6 and C/EBP work in tandem to activate the *Retnla* gene [37]. There are also putative binding sites for Ets family proteins and PPAR, upstream and downstream of the STAT6 binding site respectively [37]. Furthermore, transcription factor binding motifs for NF-κB, GAS, and C/EBP are present throughout the *Retnla* gene, both in the 5' and 3' flanking regions and in introns [22].

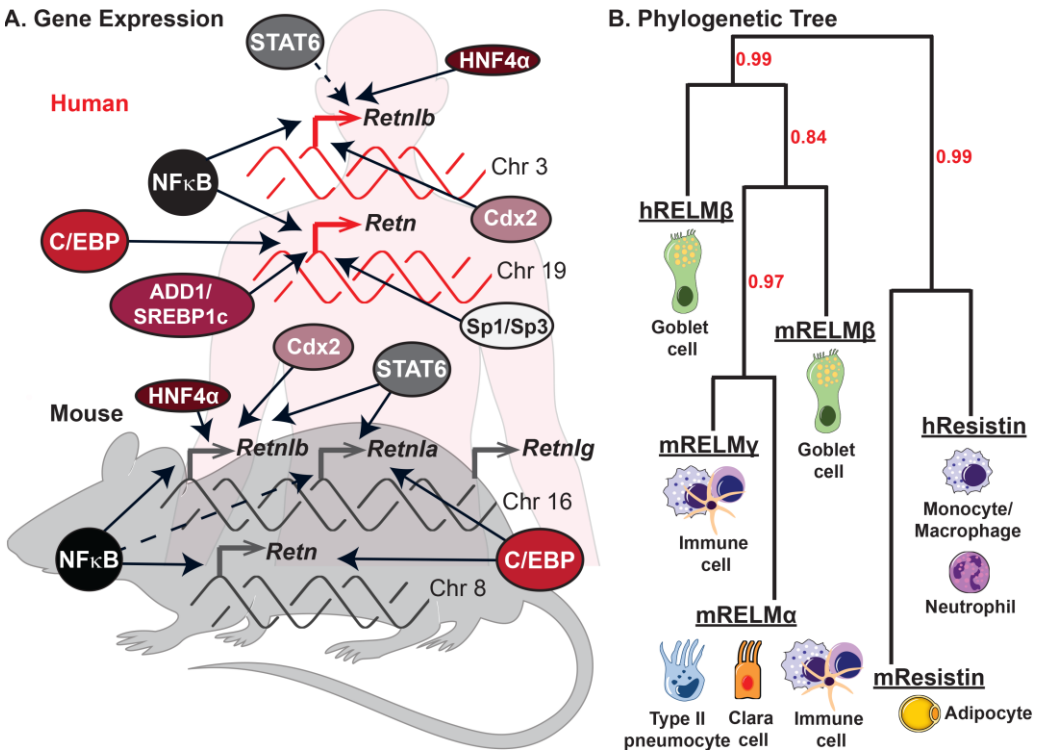

Figure 2. RELM expression in mouse and man. A) Genetic regulation and chromosome location of the human and murine RELM genes. Dashed arrows represent putative transcriptional regulation, while solid arrows represent molecularly confirmed transcription factors. B) Phylogenetic tree illustrating the relatedness of mouse and human RELMs was generated using http://www.phylogeny.fr software. Bootstrap values are indicated in red. The primary cell types that express each RELM are presented.

RELM putative receptors and downstream signaling

RELMs have been studied and implicated in diverse physiological functions. Surprisingly however, the RELM receptors and downstream signaling pathways are largely elusive. Of the four RELMs, resistin is the only member thus far with a confirmed receptor, whereas the rest of the members are associated with putative or unknown receptors. Figure 3 summarizes our current understanding of RELMα protein signaling and function.

Although extensively studied, the search for a RELMα receptor still continues (Figure 3). RELMα binding assays revealed that it selectively binds to $CD4^+$ Th2 cells, DCs and macrophages [45]. There is evidence that Bruton's tyrosine kinase (BTK), an important signaling molecule in B cell maturation, is a binding partner for RELMα [45, 46] (Figure 3, I). Immunofluorescent assays have shown that upon RELMα stimulation, BTK redistributes and anchors to the cell membrane where it then co-localizes with RELMα [46]. Given that BTK is an intracellular protein, the exact interaction between the secreted extracellular RELMα and intracellular BTK is unclear. Two distinct outcomes of RELMα binding associated with BTK signaling have been reported. First, RELMα induced BTK autophosphorylation stimulated myeloid cell chemotaxis. Second, in an *in vitro* CD4+ Th2 cell differentiation assay, RELMα downregulated Th2 cytokine production in a BTK-dependent manner [45, 46].

Several *in vitro* studies demonstrated a chemotactic and mitogenic function of RELMα, positing a function for RELMα in angiogenesis and tissue remodeling (Figure 3, II). In human pulmonary artery smooth muscle cells, RELMα increased intracellular Ca^{2+} concentrations by activating inositol 1,4,5-triphosphate receptor (IP_3R) in a phospholipase C dependent mechanism [47]. RELMα also stimulated proliferation of rat pulmonary microvascular smooth muscle cells via the PI3K/AKT signaling pathway, and induced expression of angiogenesis mediators: VEGF and MCP-1, and monocyte recruiting chemokine SDF-1x [22, 48]. In a lung fibrosis model,

RELMα was implicated in myofibroblast differentiation during lung fibrosis, likely through activation of Notch1 and Jagged1 [49]. While fibroblast activation is detrimental in pulmonary or liver fibrosis, it is a required wound healing process following tissue injury. Recent evidence supports a critical function for RELMα in wound healing through fibroblast activation. Following skin excision wounds in mice, RELMα induced fibroblast expression of lysyl hydrolase 2, an enzyme that mediates collagen cross-linking for skin repair and tissue regeneration [50-52]. Finally, RELMα also acts as an adipokine to regulate metabolic homeostasis [53]. RELMα increased expression of cholesterol-7-α-hydroxylase (Cyp7a1) in hepatocytes by inducing the transcriptional activator liver receptor homologue-1 (LRH-1). This effect was beneficial in hyperlipidemic mice as it promoted excretion of cholesterol in the form of bile acids (Figure 3, III).

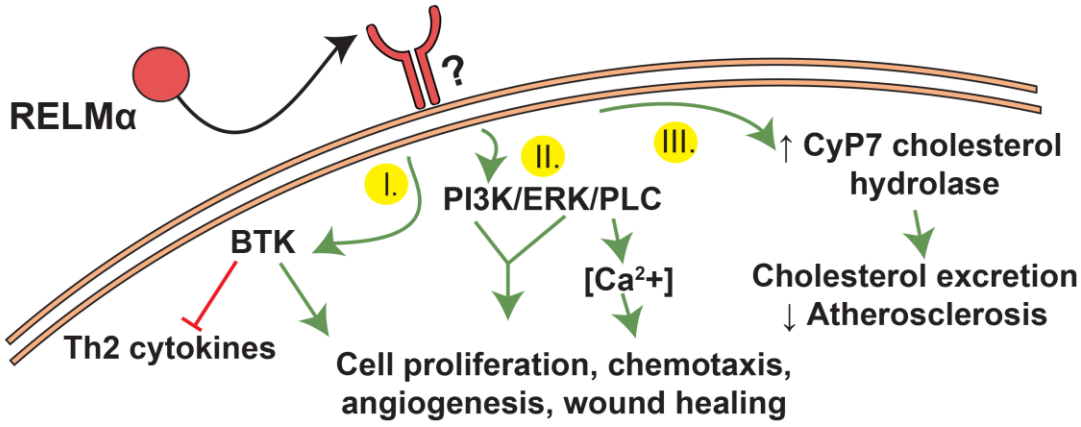

Figure 3. Proposed receptor and signaling of RELMα.

RELM function in mice and men

There have been a multitude of diverse studies investigating RELM protein function, some of which, reveal opposing functions. This section will review the functional studies on RELMs and their putative roles in infection, inflammatory and autoimmune diseases and metabolic function (summarized in Figure 4).

Microbial infection

The use of RELMα$^{-/-}$ mice in helminth and bacterial infection as well as helminth antigen sensitization models has revealed complex host immunomodulatory roles for this protein. Following infection with the rodent hookworm *Nippostrongylus brasiliensis*, RELMα suppressed Th2 cytokine responses through functional effects on CD4^{+} Th2 cells, which impaired optimal adult worm expulsion [32, 45, 54]. On the other hand, RELMα's suppression of Th2 inflammation had beneficial effects for the host as it prevented excessive and potentially fatal lung inflammation. It seems therefore that RELMα acts as a critical rheostat in the balance between host immunity and inflammation, preserving host immune homeostasis sometimes at the expense of optimal antimicrobial immunity. In addition to direct suppression of CD4^{+} Th2 cells, RELMα was also able to promote IL-10 producing regulatory T cells following stimulation with *Schistosoma mansoni* antigen-pulsed DCs [42]. In a mouse model of enteropathogenic/enterohemorrhagic bacterial infection with *Citrobacter rodentium*, RELMα-mediated suppression of Th2 cytokines led instead to increased Th17 cytokine-driven inflammation in the colon. Surprisingly, RELMα immunostimulatory effect had no significant effect on bacterial clearance suggesting that RELMα expression in *Citrobacter rodentium* infection was solely detrimental to the host [55, 56].

Inflammatory and fibrotic disease

As in infection, the role for RELM proteins in influencing the immune response is recognized in several studies on inflammatory and fibrotic diseases. However, whether they play a pathogenic function in stimulating inflammation, or instead protect against excessive inflammatory responses is controversial. Some of this conflicting evidence may be caused by discrepancies between correlative and functional studies, while another contributor may be the use of endotoxin-contaminated bacterially-derived recombinant proteins. In addition to these caveats, it is becoming increasingly clear that the disease context and RELM protein level and expression pattern may be critical for their beneficial or pathologic outcomes.

RELMα is highly expressed in lung injury and allergic airway inflammation models, where several studies, using recombinant RELMα administration or RELMα-expressing transgenic mice, confirmed a function in promoting chemotaxis for eosinophils and DCs, and vascular inflammation [48, 57-59]. On the other hand, RELMα$^{-/-}$ mice exhibited similar airway and lung inflammation compared to wild-type mice following ovalbumin or *Aspergillus*-induced allergic airway inflammation [60]. In another study using RELMα-overexpressing transgenic mice, RELMα significantly suppressed ovalbumin-induced Th2 lung immune responses, correlated with reduced pERK signaling [35]. This is consistent with the original studies reporting RELMα$^{-/-}$ mice, where RELMα dampened the Th2 lung inflammatory response to sensitization and challenge with helminth *Schistosoma mansoni* egg antigen [45, 54].

In several studies investigating dextran sodium sulfate-induced intestinal inflammation as a mouse model of ulcerative colitis, RELMα$^{-/-}$ mice exhibited reduced intestinal pathology and Th17 and TNFα cytokine responses compared to wild-type mice [55, 61-63].

RELMα function in tissue repair and fibrosis is better understood with several studies showing that RELMα promotes these processes. Both tissue repair and fibrosis share similar

pathways, such as stimulation by Th2 cytokines [64]. However, tissue repair is the desired outcome to injury while fibrosis, or scarring, occurs when tissue repair is not kept in check. Given that RELMα is stimulated by Th2 cytokines following both lung and skin injury, it was posited that RELMα maybe the downstream mediator of Th2 cytokine-induced tissue repair. Supportive of this, RELMα promoted myofibroblast differentiation and increased expression of type 1 collagen and α-SMA expression, leading to thickened fibrotic dermis and extracellular matrix deposition in bleomycin-induced dermal fibrosis [65]. Another study using skin biopsy-induced injury showed that IL-4 activated RELMα mediated skin healing by controlling collagen fibril assembly [50]. RELMα was profibrotic in bleomycin-induced pulmonary fibrosis through several proposed mechanisms: bone marrow cell recruitment, increased expression of VEGF, fibroblast and myofibroblast activation [66, 67].

Metabolic function

RELMα expression is observed within white adipose tissue of high fat diet-fed mice [53]. RELMα deficiency in hyperlipidemic and atherosclerotic mice resulted in significant cholesterol increase, while overexpression of RELMα resulted in the reverse effect [53]. Mechanistically, RELMα overexpression upregulated the liver cholesterol catabolic enzymes, Cyp7a1 and Cyp8b1, which are responsible for breaking down cholesterol and converting it to bile acid. Consistent with this, RELMα overexpressing mice had increased fecal bile acid content and fecal cholesterol indicating a RELMα-mediated mechanism for cholesterol breakdown and clearance. RELMα thus induces depletion and clearance of cholesterol, and further implies that RELMα has beneficial functions in metabolism. However, in another study, RELMα expressed by $CD301b^+$ mononuclear phagocytes within the white adipose tissue was important in maintaining healthy body weight and glucose levels [68]. When $CD301b^+$ mononuclear

phagocytes were depleted, there was a significant downregulation of metabolic genes in the liver, associated with hyperglycemia. This effect was reversed when the mice were exogenously treated with recombinant RELMα. In contrast, another study reported that RELMα$^{-/-}$ mice were protected from hyperglycemia [69]. It is possible that these discrepancies reflect differences in cell-specific deletion of CD301b^{+} cells compared to whole body RELMα$^{-/-}$ mice.

It is now well recognized that the immune environment, particularly the Th1/Th2 cytokine balance, is an important contributor to metabolic homeostasis or disease [70]. Given that RELMα is expressed by M2 macrophages, and regulates Th2 cytokines, it is possible that RELMα's effect in metabolism is partly mediated through its immunoregulatory function. For example, brown adipose tissue in lean mice is more heavily populated with cells such as M2 Macs and Tregs as well as IL-4, IL-13 and IL-10 cytokines resulting in an overall Th2 immune state that maintains a noninflammatory milieu [71]. In contrast, chronically inflamed white adipose tissue associated with obesity and insulin resistance is populated with effector M1 macrophages that primarily contribute to a proinflammatory IL-1β, TNF-α and IL-6-rich environment [71]. In contrast to RELMα, however, resistin is associated with proinflammatory macrophage activation in obesity, but recent studies suggest that resistin can be anti-inflammatory in certain disease contexts [72, 73]. More specific studies investigating the immune effects of the specific RELM proteins in obesity and diabetes are necessary, however, the current data may support a therapeutic benefit in employing RELM proteins to modulate the Th1/Th2 balance to treat metabolic dysfunction.

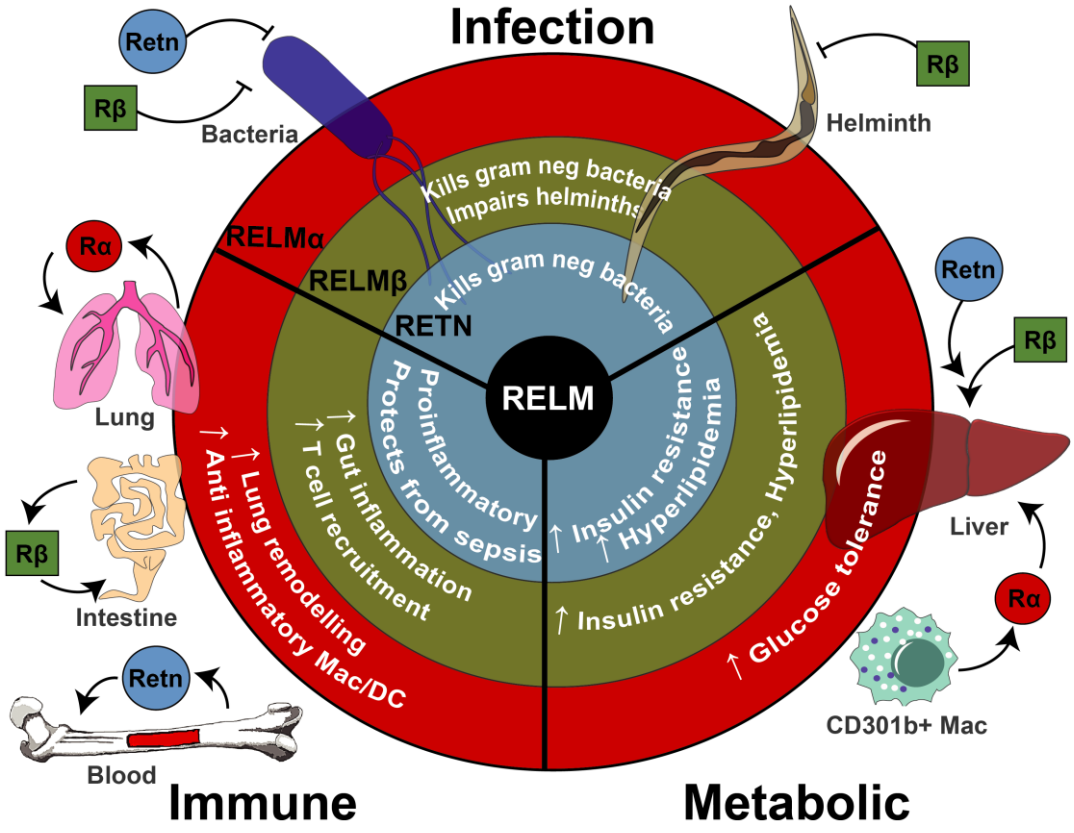

Figure 4. The diverse roles of RELMs in infection, inflammation and metabolism.

Endocannabinoids

Endocannabinoids are endogenous cannabis-like lipids that signal through cannabinoid receptors in animals. The endocannabinoid system is ubiquitous in humans and mice and play a variety of roles with consequences to the host physiology. The discovery of Δ^9-tetrahydrocannabinol (THC), the primary psychoactive component of cannabis, in the 1960's led to the discovery of synthetic cannabinoids, endogenous cannabinoid receptors, then finally to the endogenous cannabinoids by the 1990s and 2000s [74]. Studies on each of these components of the endocannabinoid system together with the development of cannabinoid receptor agonistic and antagonistic compounds exhibited the extensive physiological functions of the endocannabinoid system in the central and peripheral nervous systems and in peripheral organs. To date, the endocannabinoid system has been implicated to have therapeutic potential in disease conditions such as inflammation, obesity, metabolic disorders, anxiety, atherosclerosis, cancer and many more.

Endocannabinoid biosynthesis and degradation

The most widely studied endocannabinoids are N-arachidonoylethanolamine (Anandamide/AEA) and 2-arachidonoylglycerol (2-AG) [75]. Biosynthesis of AEA first involves the *N*-acyltransferase enzymatic conversion of either phosphatidylethanolamide or *sn*-1-arachidonate-containing phospholipid to *N*-arachidonoyl-phosphatidylethanolamine. This *N*-arachidonoyl-phosphatidylethanolamine will then be transformed into AEA by four possible pathways. 1/ Through direct conversion by N-acyl-phosphatidylethanolamine-selective phosphodiesterase, 2/ by first conversion to glycerophosphoAEA by αβ-hydrolase enzyme, 3/ first conversion to phosphoAEA by phospholipase and finally, 4/ by conversion to 1-lyso-N-arachidonoyl-phosphatidyl-ethanolamide by soluble phospholipase A2 enzyme [76, 77].

During 2-AG biosynthesis, first membrane phospholipids and phosphatic acids are converted to 2-arachidonate-containing diacylglycerol by either, phosphatic acid hydrolase or phospholipase Cβ enzymes. The diacylclycerols are then converted to 2-AG by one of the two known isotypes of diacylglycerol lipase [77, 78].

AEA is metabolized and degraded via fatty acid amide hydrolase (FAAH) and 2-AG by monoacylclycerol lipase (MGL). Although AEA and 2-AG are primarily degraded via either FAAH or MGL respectively, other enzymes have also been shown to metabolize the two endocannabinoids. Palmitoylethanolamide-preferring-acid amidase (PAA), cyclooxygenase-2, lipoxygenases and cytochrome P450 can degrade AEA. Similarly, 2-AG can be degraded by FAAH and other lipases such as αβ-hydrolase 6 and 12 (Figure 5) [77, 78].

Endocannabinoid receptor signaling

There are two known cannabinoid receptors, CB1 and CB2. Both CB1 and CB2 belong to class A (rhodopsin/Rho family) of G protein-coupled receptors (GPCRs) [77, 79]. CB1 receptors are the most abundant receptors in mammalian brains and are also found on peripheral tissues and cells. CB2 receptors in contrast are found mainly on cells belonging to the immune system and found less abundantly in the brain and peripheral tissues. Both AEA and 2-AG have the potential to signal via CB1 and CB2, however, AEA has been proven to have higher affinity for CB1 whereas 2-AG has equal affinity for CB1 and CB2 (Figure 5) [77].

CB receptor signaling has many clinically significant outcomes including analgesic, antiemetic and anxyolitic effects. How signaling through two possible receptors could have multifarious physiological functions is debatable. However, it has been shown that CB1 signaling can both stimulate and inhibit forskolin-stimulated adenylyl cyclase, by pertussis toxin-insensitive G_s proteins and by activation of a pertussis toxin-sensitive $G_{i/o}$ protein, respectively.

The effects on adenylyl cyclase by endocannabinoid-receptor interactions leads to changes in calcium levels, cAMP and activation of mitogen-activated protein kinase (MAPK) leading to modulated activity of intracellular transduction pathways [80]. MAPK signaling by CBs affect synaptic plasticity, cell migration, and possibly neuronal growth [81]. Studies conducted on CHO cells testing various cannabinoid ligands of CB1 receptor discovered that specific ligands can activate various adenylyl cyclase leading to activation of either G_s or G_i coupled pathways [82]. Dissimilar to CB1, CB2 receptor signaling has not been found to couple to G_s pathways, rather only to modulate adenylyl cyclase by coupling to $G_{i/o}$ proteins. These studies suggest that various cannabinoid receptors and agonists can confer distinct signaling pathways ultimately leading to distinct phenotypes.

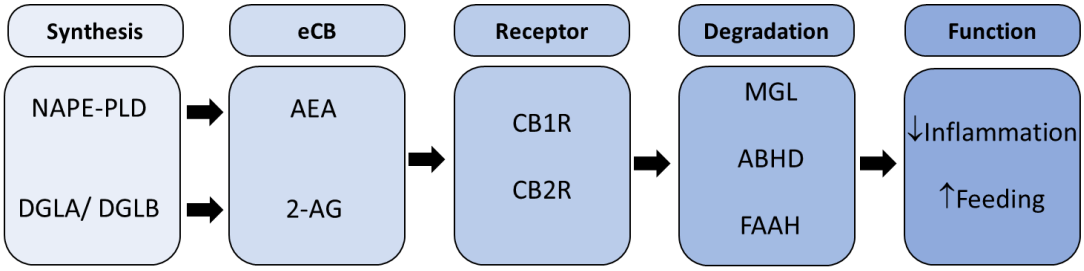

Figure 5. Endocannabinoid biosynthesis, degradation and signaling pathways.

Endocannabinoid function in the brain

The CB1 receptor was first discovered in the brain, therefore, how endocannabinoids function in the brain and central nervous system has been the topic of many studies. Endocannabinoids have been implicated in neurological conditions such as Parkinson's disease, Alzheimer's disease and multiple sclerosis. Further, endocannabinoids have also been implicated in neuropsychological disorders such as anxiety, depression, and eating disorders. In neurodegenerative disorders such as Parkinson's disease, increased CB1 and CB2 signaling in regions of the brain that control motor activity such as the basal ganglia counter acts the characteristic loss of dopaminergic neurons and dopamine signaling leading to impaired locomotion [83]. In anxiety and depression studies, $CB1^{-/-}$ mice showed to have increased anxiety-like readouts in behavioral studies [84]. Rats fed chow or high fat diet were given varying doses of THC and found that THC shifted thermogenesis and lipid metabolism parameters towards reduced energy expenditure and lipolysis [85]. When this was tested in conjunction with high-fat diet, THC promoted increased food intake and reduced energy expenditure. These studies implicated the importance of endocannabinoid signaling in eating disorders such as anorexia nervosa [86].

Endocannabinoid function in the gut

In keeping with how endocannabinoids influence eating disorders, it is increasingly clear that the endocannabinoid system is active in brain-gut signaling via the vagus nerve [87]. In support of this, studies conducted on food deprived rats showed an increase in endocannabinoid production in the small intestine [88]. Further, inhibiting eCB signaling with CB1R antagonistic drug AM6545 reduced hyperphagia in diet-induced obese mice [89].

In the gut, the role of eCB has been discovered to be multifold. One study on obesity tested high-fat diet on rats and found the resulting change in microbiota was associated with

changes in intestinal endocannabinoid signaling. With the use of CB1 agonistic and antagonistic drugs, eCB signaling was found to increase lipopolysaccharides (LPS) which increased gut permeability and adipogenesis [75]. Additionally, eCB have been implicated in gut motility and contraction through inhibition of release of acetylcholine, an excitatory neurotransmitter. In this study (+) WIN-55,212-2 CB agonist was found to impair gut motility by inhibiting the excitatory neurotransmitter acetylcholine. Upon administering a CB1R antagonist, the effect was reversed [90]. These studies display the dynamic functions of eCB in the gastrointestinal tract.

Endocannabinoid function in the immune system

CB receptors are expressed on many immune cell types with CB2R being the most abundant in the immune system. Depending on the cell type through which it signals, eCBs can play various opposing roles by both stimulating and inhibiting immune responses. The immunosuppressive effect of eCB happens through inhibition of the cAMP/protein kinase A (PKA) pathway. Also, eCB can cause apoptosis of cells by phosphorylating IκB-α which then upregulates transcription of apoptotic genes [91].

In innate cells, AEA described to be anti-inflammatory by inhibiting alveolar macrophage effector functions and cytokine expression. The first study found that AEA inhibited macrophage killing of TNF-sensitive fibroblast cells [92]. This finding has since been confirmed by others who showed that AEA inhibited macrophage LPS-induced nitric oxide production and expression of Th1 cytokines IL-6, IL-12, IL-23 [93-95]. Similar results were discovered in DCs where AEA inhibited DC expression of IL-6, IL-12p40 and TNFα [96]. Further studies on $CB1R^{-/-}$ and $CB2R^{-/-}$ mice found upregulation of DC MHC II, CD80 and CD86, receptors important for DC-T cell communication [97]. CBs mainly impair neutrophil function by decreasing neutrophil migration and inhibiting neutrophil degranulation, although these results were CB specific [98].

The effect of 2-AG on innate immune cells is less clear. Similar to AEA, some studies have reported 2-AG to have immunosuppressive effects on macrophages by inhibiting Th1 cytokines IL-6 and TNFα production and by shifting macrophage activation from classically activated to alternatively activated [99]. Contradicting this, studies have shown 2-AG to stimulate nitric oxide and inflammatory cytokine production and enhance cell migration and adhesion of monocytes and neutrophils [99]. One proposed explanation for discrepancies in 2-AG functions has been that 2-AG conversion to cyclooxygenase-2 metabolites could have varied bioactive properties [100].

AEA was also reported as immunosuppressive to adaptive cells such as T and B lymphocytes [99]. It is believed that AEA functions this way by signaling via CB2 receptor, PPAR-γ and by inhibiting NFκB [101]. Similar to innate cells, AEA inhibits lymphoid cell proliferation, Th1 cytokine production and enhances Th2 responses by increasing expression of IL-4 and IL-10 [102, 103]. Similarly, 2-AG (more precisely a 2-AG metabolite) was immunosuppressive towards T cells by impairing pro-inflammatory IL-2 cytokine expression.

Although eCBs at times play controversial roles in immune responses, in general, eCBs are immunosuppressive, with AEA being the most potent. Interestingly, the Th1 response inhibition by eCB is coupled with enhancement of Th2 response in many immune cells types. Moreover, Th1 cytokine production was associated with reduced FAAH (AEA degrading enzyme) activity suggesting that a self-sustaining anti-inflammatory mechanism of eCBs [104]. Therefore, eCBs can be exploited for their anti-inflammatory therapeutic potential.

Conclusion

Helminth infections are a global health burden and the lack of immunity makes re-infections common. For this reason, it is critical that we understand host factors that are involved in the immune response against helminths. In this thesis, we propose two systems that might be of importance to further explore, RELM and endocannabinoid signaling. RELMα is a secreted protein, well studied to be immunomodulatory during Th2 immune settings. Even though this protein has been studies for its immunosuppressive properties, the cell-type specific role of RELMα has yet to be explored. Endocannabinoids are lipid signaling molecules that have functions in dampening Th1 immune responses and driving Th2 immunity. Endocannabinoids have been the subject of many studies for their role in the brain, gut and immune system. However, to date no one has investigated the importance of endocannabinoid signaling in immune responses against parasitic worms. The work presented in this thesis will independently investigate RELMα and endocannabinoid signaling in the *Nb* model of hookworm infection to delineate the contribution of each of these systems to host immunity during helminth infection.

References

1. Hotez, P. J., Brindley, P. J., Bethony, J. M., King, C. H., Pearce, E. J., Jacobson, J. (2008) Helminth infections: the great neglected tropical diseases. J Clin Invest 118, 1311-21.

2. Bethony, J., Brooker, S., Albonico, M., Geiger, S. M., Loukas, A., Diemert, D., Hotez, P. J. (2006) Soil-transmitted helminth infections: ascariasis, trichuriasis, and hookworm. Lancet 367, 1521-32.

3. WHO in World Health Report. (World Health Organization, G., Switzerland, 1999).

4. Hotez, P. J., Brooker, S., Bethony, J. M., Bottazzi, M. E., Loukas, A., Xiao, S. (2004) Hookworm infection. N Engl J Med 351, 799-807.

5. Craig, J. M. and Scott, A. L. (2014) Helminths in the lungs. Parasite Immunol 36, 463-74.

6. Croll, N. A. and Ghadirian, E. (1981) Wormy persons: contributions to the nature and patterns of overdispersion with Ascaris lumbricoides, Ancylosotma duodenale, Necator americanus and Trichuris trichiura. Trop Geogr Med 33, 241-8.

7. Harvie, M., Camberis, M., Tang, S. C., Delahunt, B., Paul, W., Le Gros, G. (2010) The lung is an important site for priming CD4 T-cell-mediated protective immunity against gastrointestinal helminth parasites. Infect Immun 78, 3753-62.

8. Camberis, M., Le Gros, G., Urban, J. (2003) Animal model of Nippostrongylus brasiliensis and Heligmosomoides polygyrus. Curr Protoc Immunol Chapter 19, Unit 19.12.

9. Nair, M. G. and Herbert, D. R. (2016) Immune polarization by hookworms: taking cues from T helper type 2, type 2 innate lymphoid cells and alternatively activated macrophages. Immunology 148, 115-24.

10. Wills-Karp, M., Rani, R., Dienger, K., Lewkowich, I., Fox, J. G., Perkins, C., Lewis, L., Finkelman, F. D., Smith, D. E., Bryce, P. J., Kurt-Jones, E. A., Wang, T. C., Sivaprasad, U., Hershey, G. K., Herbert, D. R. (2012) Trefoil factor 2 rapidly induces interleukin 33 to promote type 2 immunity during allergic asthma and hookworm infection. J Exp Med 209, 607-22.

11. Oboki, K., Nakae, S., Matsumoto, K., Saito, H. (2011) IL-33 and Airway Inflammation. Allergy Asthma Immunol Res 3, 81-8.

12. Stone, K. D., Prussin, C., Metcalfe, D. D. (2010) IgE, mast cells, basophils, and eosinophils. J Allergy Clin Immunol 125, S73-80.

13. Jang, J. C. and Nair, M. G. (2013) Alternatively Activated Macrophages Revisited: New Insights into the Regulation of Immunity, Inflammation and Metabolic Function following Parasite Infection. Curr Immunol Rev 9, 147-156.

14. Gause, W. C., and David Artis, eds. (2015) The Th2 Type Immune Response in Health and Disease: From Host Defense and Allergy to Metabolic Homeostasis and Beyond. Springer.

15. Lucas, T., Waisman, A., Ranjan, R., Roes, J., Krieg, T., Müller, W., Roers, A., Eming, S. A. (2010) Differential roles of macrophages in diverse phases of skin repair. J Immunol 184, 3964-77.

16. Mirza, R., DiPietro, L. A., Koh, T. J. (2009) Selective and specific macrophage ablation is detrimental to wound healing in mice. Am J Pathol 175, 2454-62.

17. Reece, J. J., Siracusa, M. C., Southard, T. L., Brayton, C. F., Urban, J. F., Scott, A. L. (2008) Hookworm-induced persistent changes to the immunological environment of the lung. Infect Immun 76, 3511-24.

18. Marsland, B. J., Kurrer, M., Reissmann, R., Harris, N. L., Kopf, M. (2008) Nippostrongylus brasiliensis infection leads to the development of emphysema associated with the induction of alternatively activated macrophages. Eur J Immunol 38, 479-88.

19. Reese, T. A., Liang, H. E., Tager, A. M., Luster, A. D., Van Rooijen, N., Voehringer, D., Locksley, R. M. (2007) Chitin induces accumulation in tissue of innate immune cells associated with allergy. Nature 447, 92-6.

20. Anthony, R. M., Rutitzky, L. I., Urban, J. F., Stadecker, M. J., Gause, W. C. (2007) Protective immune mechanisms in helminth infection. Nat Rev Immunol 7, 975-87.

21. Zhao, A., Urban, J. F., Anthony, R. M., Sun, R., Stiltz, J., van Rooijen, N., Wynn, T. A., Gause, W. C., Shea-Donohue, T. (2008) Th2 cytokine-induced alterations in intestinal smooth muscle function depend on alternatively activated macrophages. Gastroenterology 135, 217-225.e1.

22. Teng, X., Li, D., Champion, H. C., Johns, R. A. (2003) FIZZ1/RELMα, a Novel Hypoxia-Induced Mitogenic Factor in Lung With Vasoconstrictive and Angiogenic Properties. Circulation Research 92, 1065.

23. Horsnell, W. G. C. and Dewals, B. G. (2016) RELMs in the Realm of Helminths. Trends in Parasitology 32, 512-514.

24. Gerstmayer, B., Küsters, D., Gebel, S., Müller, T., Van Miert, E., Hofmann, K., Bosio, A. (2003) Identification of RELMγ, a novel resistin-like molecule with a distinct expression pattern☆. Genomics 81, 588-595.

25. Johns, R. A., Gao, L., Rafaels, N. M., Grant, A. V., Stockton-Porter, M. L., Watson, H. R., Beaty, T. H., C. Barnes, K. (2009) Polymorphisms in Resistin and Resistin-like Beta Predict Bronchial Hyperreactivity in Human Asthma. Proceedings of the American Thoracic Society 6, 329-329.

26. Ghosh, S., Singh, A. K., Aruna, B., Mukhopadhyay, S., Ehtesham, N. Z. (2003) The genomic organization of mouse resistin reveals major differences from the human resistin: functional implications. Gene 305, 27-34.

27. Steppan, C. M., Brown, E. J., Wright, C. M., Bhat, S., Banerjee, R. R., Dai, C. Y., Enders, G. H., Silberg, D. G., Wen, X. M., Wu, G. D., Lazar, M. A. (2001) A family of tissue-specific resistin-like molecules. Proceedings of the National Academy of Sciences of the United States of America 98, 502-506.

28. Schinke, T., Haberland, M., Jamshidi, A., Nollau, P., Rueger, J. M., Amling, M. (2004) Cloning and functional characterization of resistin-like molecule γ. Biochemical and Biophysical Research Communications 314, 356-362.

29. Patel, S. D., Rajala, M. W., Rossetti, L., Scherer, P. E., Shapiro, L. (2004) Disulfide-Dependent Multimeric Assembly of Resistin Family Hormones. Science 304, 1154.

30. He, W., Wang, M.-L., Jiang, H.-Q., Steppan, C. M., Shin, M. E., Thurnheer, M. C., Cebra, J. J., Lazar, M. A., Wu, G. D. (2003) Bacterial colonization leads to the colonic secretion of RELMβ/FIZZ2, a novel goblet cell-specific protein. Gastroenterology 125, 1388-1397.

31. Banerjee, R. R. and Lazar, M. A. (2001) Dimerization of Resistin and Resistin-like Molecules Is Determined by a Single Cysteine. Journal of Biological Chemistry 276, 25970-25973.

32. Chen, G., Wang, S. H., Jang, J. C., Odegaard, J. I., Nair, M. G. (2016) Comparison of RELM alpha and RELM beta Single- and Double-Gene-Deficient Mice Reveals that RELM alpha Expression Dictates Inflammation and Worm Expulsion in Hookworm Infection2. Infection and Immunity 84, 1100-1111.

33. Shojima, N., Ogihara, T., Inukai, K., Fujishiro, M., Sakoda, H., Kushiyama, A., Katagiri, H., Anai, M., Ono, H., Fukushima, Y., Horike, N., Viana, A. Y. I., Uchijima, Y., Kurihara, H., Asano, T. (2005) Serum concentrations of resistin-like molecules β and γ are elevated in high-fat-fed and obese db/db mice, with increased production in the intestinal tract and bone marrow. Diabetologia 48, 984-992.

34. Jang, J. C., Chen, G., Wang, S. H., Barnes, M. A., Chung, J. I., Camberis, M., Le Gros, G., Cooper, P. J., Steel, C., Nutman, T. B., Lazar, M. A., Nair, M. G. (2015) Macrophage-Derived Human Resistin Is Induced in Multiple Helminth Infections and Promotes Inflammatory Monocytes and Increased Parasite Burden. PLoS Pathogens 11, e1004579.

35. Lee, M.-R., Shim, D., Yoon, J., Jang, H. S., Oh, S.-W., Suh, S. H., Choi, J.-H., Oh, G. T. (2014) Retnla Overexpression Attenuates Allergic Inflammation of the Airway. PLOS ONE 9, e112666.

36. Holcomb, I. N., Kabakoff, R. C., Chan, B., Baker, T. W., Gurney, A., Henzel, W., Nelson, C., Lowman, H. B., Wright, B. D., Skelton, N. J., Frantz, G. D., Tumas, D. B.,

Peale, F. V., Shelton, D. L., Hébert, C. C. (2000) FIZZ1, a novel cysteine-rich secreted protein associated with pulmonary inflammation, defines a new gene family. EMBO J 19, 4046-55.

37. Stütz, A. M., Pickart, L. A., Trifilieff, A., Baumruker, T., Prieschl-Strassmayr, E., Woisetschläger, M. (2003) The Th2 Cell Cytokines IL-4 and IL-13 Regulate Found in Inflammatory Zone 1/Resistin-Like Molecule α Gene Expression by a STAT6 and CCAAT/Enhancer-Binding Protein-Dependent Mechanism. The Journal of Immunology 170, 1789.

38. Loke, P., Nair, M. G., Parkinson, J., Guiliano, D., Blaxter, M., Allen, J. E. (2002) IL-4 dependent alternatively-activated macrophages have a distinctive in vivo gene expression phenotype. BMC Immunol 3, 7.

39. Nair, M. G., Gallagher, I. J., Taylor, M. D., Loke, P., Coulson, P. S., Wilson, R. A., Maizels, R. M., Allen, J. E. (2005) Chitinase and Fizz family members are a generalized feature of nematode infection with selective upregulation of Ym1 and Fizz1 by antigen-presenting cells. Infect Immun 73, 385-94.

40. Raes, G., De Baetselier, P., Noël, W., Beschin, A., Brombacher, F., Hassanzadeh Gh, G. (2002) Differential expression of FIZZ1 and Ym1 in alternatively versus classically activated macrophages. J Leukoc Biol 71, 597-602.

41. Jenkins, S. J., Ruckerl, D., Cook, P. C., Jones, L. H., Finkelman, F. D., van Rooijen, N., MacDonald, A. S., Allen, J. E. (2011) Local macrophage proliferation, rather than recruitment from the blood, is a signature of TH2 inflammation. Science 332, 1284-8.

42. Cook, P. C., Jones, L. H., Jenkins, S. J., Wynn, T. A., Allen, J. E., MacDonald, A. S. (2012) Alternatively activated dendritic cells regulate CD4+ T-cell polarization in vitro and in vivo. Proc Natl Acad Sci U S A 109, 9977-82.

43. Liu, T., Dhanasekaran, S. M., Jin, H., Hu, B., Tomlins, S. A., Chinnaiyan, A. M., Phan, S. H. (2004) FIZZ1 stimulation of myofibroblast differentiation. Am J Pathol 164, 1315-26.

44. Loke, P., Gallagher, I., Nair, M. G., Zang, X., Brombacher, F., Mohrs, M., Allison, J. P., Allen, J. E. (2007) Alternative activation is an innate response to injury that requires CD4+ T cells to be sustained during chronic infection. J Immunol 179, 3926-36.

45. Nair, M. G., Du, Y., Perrigoue, J. G., Zaph, C., Taylor, J. J., Goldschmidt, M., Swain, G. P., Yancopoulos, G. D., Valenzuela, D. M., Murphy, A., Karow, M., Stevens, S., Pearce, E. J., Artis, D. (2009) Alternatively activated macrophage-derived RELM-α is a negative regulator of type 2 inflammation in the lung. The Journal of Experimental Medicine 206, 937-952.

46. Su, Q., Zhou, Y., Johns, R. A. (2007) Bruton's tyrosine kinase (BTK) is a binding partner for hypoxia induced mitogenic factor (HIMF/FIZZ1) and mediates myeloid cell chemotaxis. The FASEB Journal 21, 1376-1382.

47. Fan, C., Su, Q., Li, Y., Liang, L., Angelini, D. J., Guggino, W. B., Johns, R. A. (2009) Hypoxia-induced mitogenic factor/FIZZ1 induces intracellular calcium release through the PLC-IP3 pathway. American Journal of Physiology - Lung Cellular and Molecular Physiology 297, L263.

48. Yamaji-Kegan, K., Su, Q., Angelini, D. J., Champion, H. C., Johns, R. A. (2006) Hypoxia-induced mitogenic factor has proangiogenic and proinflammatory effects in the lung via VEGF and VEGF receptor-2. Am J Physiol Lung Cell Mol Physiol 291, L1159-68.

49. Liu, T., Hu, B., Choi, Y. Y., Chung, M., Ullenbruch, M., Yu, H., Lowe, J. B., Phan, S. H. (2009) Notch1 signaling in FIZZ1 induction of myofibroblast differentiation. Am J Pathol 174, 1745-55.

50. Knipper, J. A., Willenborg, S., Brinckmann, J., Bloch, W., Maaß, T., Wagener, R., Krieg, T., Sutherland, T., Munitz, A., Rothenberg, M. E., Niehoff, A., Richardson, R., Hammerschmidt, M., Allen, J. E., Eming, S. A. (2015) Interleukin-4 Receptor α Signaling in Myeloid Cells Controls Collagen Fibril Assembly in Skin Repair. Immunity 43, 803-16.

51. Minutti, C. M., Jackson-Jones, L. H., García-Fojeda, B., Knipper, J. A., Sutherland, T. E., Logan, N., Ringqvist, E., Guillamat-Prats, R., Ferenbach, D. A., Artigas, A., Stamme, C., Chroneos, Z. C., Zaiss, D. M., Casals, C., Allen, J. E. (2017) Local amplifiers of IL-4Rα-mediated macrophage activation promote repair in lung and liver. Science 356, 1076-1080.

52. Bosurgi, L., Cao, Y. G., Cabeza-Cabrerizo, M., Tucci, A., Hughes, L. D., Kong, Y., Weinstein, J. S., Licona-Limon, P., Schmid, E. T., Pelorosso, F., Gagliani, N., Craft, J. E., Flavell, R. A., Ghosh, S., Rothlin, C. V. (2017) Macrophage function in tissue repair and remodeling requires IL-4 or IL-13 with apoptotic cells. Science 356, 1072-1076.

53. Lee, M.-R., Lim, C.-j., Lee, Y.-H., Park, J.-G., Sonn, S. K., Lee, M.-N., Jung, I.-H., Jeong, S.-J., Jeon, S., Lee, M., Oh, K. S., Yang, Y., Kim, J. B., Choi, H.-S., Jeong, W., Jeong, T.-S., Yoon, W. K., Kim, H. C., Choi, J.-H., Oh, G. T. (2014) The adipokine Retnla modulates cholesterol homeostasis in hyperlipidemic mice. Nature Communications 5, 4410.

54. Pesce, J. T., Ramalingam, T. R., Wilson, M. S., Mentink-Kane, M. M., Thompson, R. W., Cheever, A. W., Urban, J. F., Wynn, T. A. (2009) Retnla (relmalpha/fizz1) suppresses helminth-induced Th2-type immunity. PLoS Pathog 5, e1000393.

55. Osborne, L. C., Joyce, K. L., Alenghat, T., Sonnenberg, G. F., Giacomin, P. R., Du, Y., Bergstrom, K. S., Vallance, B. A., Nair, M. G. (2013) Resistin-like molecule (RELM) α promotes pathogenic Th17 cell responses and bacterial-induced intestinal inflammation. Journal of immunology (Baltimore, Md. : 1950) 190, 2292-2300.

56. Chen, G., Chan, A. J., Chung, J. I., Jang, J. C., Osborne, L. C., Nair, M. G. (2014) Polarizing the T helper 17 response in Citrobacter rodentium infection via expression of resistin-like molecule α. Gut Microbes 5, 363-368.

57. Doherty, T. A., Khorram, N., Sugimoto, K., Sheppard, D., Rosenthal, P., Cho, J. Y., Pham, A., Miller, M., Croft, M., Broide, D. H. (2012) Alternaria induces STAT6-dependent acute airway eosinophilia and epithelial FIZZ1 expression that promotes airway fibrosis and epithelial thickness. J Immunol 188, 2622-9.

58. Madala, S. K., Edukulla, R., Davis, K. R., Schmidt, S., Davidson, C., Kitzmiller, J. A., Hardie, W. D., Korfhagen, T. R. (2012) Resistin-like molecule α1 (Fizz1) recruits lung dendritic cells without causing pulmonary fibrosis. Respir Res 13, 51.

59. Yamaji-Kegan, K., Takimoto, E., Zhang, A., Weiner, N. C., Meuchel, L. W., Berger, A. E., Cheadle, C., Johns, R. A. (2014) Hypoxia-induced mitogenic factor (FIZZ1/RELMα) induces endothelial cell apoptosis and subsequent interleukin-4-dependent pulmonary hypertension. Am J Physiol Lung Cell Mol Physiol 306, L1090-103.

60. Munitz, A., Cole, E. T., Karo-Atar, D., Finkelman, F. D., Rothenberg, M. E. (2012) Resistin-like molecule-α regulates IL-13-induced chemokine production but not allergen-induced airway responses. Am J Respir Cell Mol Biol 46, 703-13.

61. Munitz, A., Waddell, A., Seidu, L., Cole, E. T., Ahrens, R., Hogan, S. P., Rothenberg, M. E. (2008) Resistin-like molecule alpha enhances myeloid cell activation and promotes colitis. J Allergy Clin Immunol 122, 1200-1207.e1.

62. Chellappa, K., Deol, P., Evans, J. R., Vuong, L. M., Chen, G., Briançon, N., Bolotin, E., Lytle, C., Nair, M. G., Sladek, F. M. (2016) Opposing roles of nuclear receptor HNF4α isoforms in colitis and colitis-associated colon cancer. eLife 5, e10903.

63. Hogan, S. P., Seidu, L., Blanchard, C., Groschwitz, K., Mishra, A., Karow, M. L., Ahrens, R., Artis, D., Murphy, A. J., Valenzuela, D. M., Yancopoulos, G. D., Rothenberg, M. E. (2006) Resistin-like molecule beta regulates innate colonic function: barrier integrity and inflammation susceptibility. J Allergy Clin Immunol 118, 257-68.

64. Gieseck, R. L., Wilson, M. S., Wynn, T. A. (2018) Type 2 immunity in tissue repair and fibrosis. Nat Rev Immunol 18, 62-76.

65. Martins, V., De Los Santos, F. G., Wu, Z., Capetozzi, V., Phan, S. H., Liu, T. J. (2015) FIZZ1-Induced Myofibroblast Transdifferentiation from Adipocytes and Its Potential Rote in Dermal Fibrosis and Lipoatrophy. American Journal of Pathology 185, 2768-2776.

66. Liu, T., Yu, H., Ullenbruch, M., Jin, H., Ito, T., Wu, Z., Liu, J., Phan, S. H. (2014) The in vivo fibrotic role of FIZZ1 in pulmonary fibrosis. PLoS One 9, e88362.

67. Yamaji-Kegan, K., Su, Q., Angelini, D. J., Myers, A. C., Cheadle, C., Johns, R. A. (2010) Hypoxia-induced mitogenic factor (HIMF/FIZZ1/RELMalpha) increases lung

inflammation and activates pulmonary microvascular endothelial cells via an IL-4-dependent mechanism. J Immunol 185, 5539-48.

68. Kumamoto, Y., Camporez, J. P. G., Jurczak, M. J., Shanabrough, M., Horvath, T., Shulman, G. I., Iwasaki, A. (2016) CD301b(+) Mononuclear Phagocytes Maintain Positive Energy Balance through Secretion of Resistin-like Molecule Alpha. Immunity 45, 583-596.

69. Munitz, A., Seidu, L., Cole, E. T., Ahrens, R., Hogan, S. P., Rothenberg, M. E. (2009) Resistin-Like Molecule a Decreases Glucose Tolerance during Intestinal Inflammation. Journal of Immunology 182, 2357-2363.

70. Odegaard, J. I. and Chawla, A. (2015) Type 2 responses at the interface between immunity and fat metabolism. Curr Opin Immunol 36, 67-72.

71. Shu, C. J., Benoist, C., Mathis, D. (2012) The immune system's involvement in obesity-driven type 2 diabetes. Semin Immunol 24, 436-42.

72. Schwartz, D. R. and Lazar, M. A. (2011) Human resistin: found in translation from mouse to man. Trends in Endocrinology and Metabolism 22, 259-265.

73. Jang, J. C., Li, J., Gambini, L., Batugedara, H. M., Sati, S., Lazar, M. A., Fan, L., Pellecchia, M., Nair, M. G. (2017) Human resistin protects against endotoxic shock by blocking LPS–TLR4 interaction. Proceedings of the National Academy of Sciences.

74. Pacher, P., Bátkai, S., Kunos, G. (2006) The endocannabinoid system as an emerging target of pharmacotherapy. Pharmacol Rev 58, 389-462.

75. Muccioli, G. G. (2010) Endocannabinoid biosynthesis and inactivation, from simple to complex. Drug Discov Today 15, 474-83.

76. Marzo, V. D. (2008) Targeting the endocannabinoid system: to enhance or reduce? , Volume 7, Nature Reviews Drug Discovery 14.

77. Bakali, E. T. D. G. (2013) Cannabinoids and the Urinary Bladder. Volume 3, Gynecology & Obstetrics 7.

78. Di Marzo, V. (2008) Targeting the endocannabinoid system: to enhance or reduce? , Volume 7, Nature Reviews Drug Discovery 14.

79. Dhopeshwarkar, A. and Mackie, K. (2014) CB2 Cannabinoid receptors as a therapeutic target-what does the future hold? Mol Pharmacol 86, 430-7.

80. Bonhaus, D. W., Chang, L. K., Kwan, J., Martin, G. R. (1998) Dual activation and inhibition of adenylyl cyclase by cannabinoid receptor agonists: evidence for agonist-specific trafficking of intracellular responses. J Pharmacol Exp Ther 287, 884-8.

81. Mechoulam, R. and Parker, L. A. (2013) The endocannabinoid system and the brain. Annu Rev Psychol 64, 21-47.

82. Pacheco, M. A., Ward, S. J., Childers, S. R. (1994) Differential requirements of sodium for coupling of cannabinoid receptors to adenylyl cyclase in rat brain membranes. J Neurochem 62, 1773-82.

83. More, S. V. and Choi, D. K. (2015) Promising cannabinoid-based therapies for Parkinson's disease: motor symptoms to neuroprotection. Mol Neurodegener 10, 17.

84. Patel, S. and Hillard, C. J. (2009) Role of endocannabinoid signaling in anxiety and depression. Curr Top Behav Neurosci 1, 347-71.

85. Verty, A. N., Evetts, M. J., Crouch, G. J., McGregor, I. S., Stefanidis, A., Oldfield, B. J. (2011) The cannabinoid receptor agonist THC attenuates weight loss in a rodent model of activity-based anorexia. Neuropsychopharmacology 36, 1349-58.

86. Marco, E. M., Romero-Zerbo, S. Y., Viveros, M. P., Bermudez-Silva, F. J. (2012) The role of the endocannabinoid system in eating disorders: pharmacological implications. Behav Pharmacol 23, 526-36.

87. DiPatrizio, N. V. (2016) Endocannabinoids in the Gut. Cannabis Cannabinoid Res 1, 67-77.

88. Gómez, R., Navarro, M., Ferrer, B., Trigo, J. M., Bilbao, A., Del Arco, I., Cippitelli, A., Nava, F., Piomelli, D., Rodríguez de Fonseca, F. (2002) A peripheral mechanism for CB1 cannabinoid receptor-dependent modulation of feeding. J Neurosci 22, 9612-7.

89. Argueta, D. A. and DiPatrizio, N. V. (2017) Peripheral endocannabinoid signaling controls hyperphagia in western diet-induced obesity. Physiol Behav 171, 32-39.

90. Croci, T., Manara, L., Aureggi, G., Guagnini, F., Rinaldi-Carmona, M., Maffrand, J. P., Le Fur, G., Mukenge, S., Ferla, G. (1998) In vitro functional evidence of neuronal cannabinoid CB1 receptors in human ileum. Br J Pharmacol 125, 1393-5.

91. Malfitano, A. M., Matarese, G., Pisanti, S., Grimaldi, C., Laezza, C., Bisogno, T., Di Marzo, V., Lechler, R. I., Bifulco, M. (2006) Arvanil inhibits T lymphocyte activation and ameliorates autoimmune encephalomyelitis. J Neuroimmunol 171, 110-9.

92. Cabral, G. A., Toney, D. M., Fischer-Stenger, K., Harrison, M. P., Marciano-Cabral, F. (1995) Anandamide inhibits macrophage-mediated killing of tumor necrosis factor-sensitive cells. Life Sci 56, 2065-72.

93. Chang, Y. H., Lee, S. T., Lin, W. W. (2001) Effects of cannabinoids on LPS-stimulated inflammatory mediator release from macrophages: involvement of eicosanoids. J Cell Biochem 81, 715-23.

94. Correa, F., Hernangómez-Herrero, M., Mestre, L., Loría, F., Docagne, F., Guaza, C. (2011) The endocannabinoid anandamide downregulates IL-23 and IL-12 subunits in a

viral model of multiple sclerosis: evidence for a cross-talk between IL-12p70/IL-23 axis and IL-10 in microglial cells. Brain Behav Immun 25, 736-49.

95. Correa, F., Docagne, F., Clemente, D., Mestre, L., Becker, C., Guaza, C. (2008) Anandamide inhibits IL-12p40 production by acting on the promoter repressor element GA-12: possible involvement of the COX-2 metabolite prostamide E(2). Biochem J 409, 761-70.

96. Chiurchiù, V., Cencioni, M. T., Bisicchia, E., De Bardi, M., Gasperini, C., Borsellino, G., Centonze, D., Battistini, L., Maccarrone, M. (2013) Distinct modulation of human myeloid and plasmacytoid dendritic cells by anandamide in multiple sclerosis. Ann Neurol 73, 626-36.

97. Karmaus, P. W., Chen, W., Crawford, R. B., Harkema, J. R., Kaplan, B. L., Kaminski, N. E. (2011) Deletion of cannabinoid receptors 1 and 2 exacerbates APC function to increase inflammation and cellular immunity during influenza infection. J Leukoc Biol 90, 983-95.

98. Tanasescu, R. and Constantinescu, C. S. (2010) Cannabinoids and the immune system: an overview. Immunobiology 215, 588-97.

99. Chiurchiù, V., Battistini, L., Maccarrone, M. (2015) Endocannabinoid signalling in innate and adaptive immunity. Immunology 144, 352-364.

100. Alhouayek, M., Masquelier, J., Muccioli, G. G. (2014) Controlling 2-arachidonoylglycerol metabolism as an anti-inflammatory strategy. Drug Discov Today 19, 295-304.

101. Sancho, R., Calzado, M. A., Di Marzo, V., Appendino, G., Muñoz, E. (2003) Anandamide inhibits nuclear factor-kappaB activation through a cannabinoid receptor-independent pathway. Mol Pharmacol 63, 429-38.

102. Jackson, A. R., Nagarkatti, P., Nagarkatti, M. (2014) Anandamide attenuates Th-17 cell-mediated delayed-type hypersensitivity response by triggering IL-10 production and consequent microRNA induction. PLoS One 9, e93954.

103. Newton, C. A., Klein, T. W., Friedman, H. (1994) Secondary immunity to Legionella pneumophila and Th1 activity are suppressed by delta-9-tetrahydrocannabinol injection. Infect Immun 62, 4015-20.

104. Chiurchiù, V., Rapino, C., Talamonti, E., Leuti, A., Lanuti, M., Gueniche, A., Jourdain, R., Breton, L., Maccarrone, M. (2016) Anandamide Suppresses Proinflammatory T Cell Responses In Vitro through Type-1 Cannabinoid Receptor-Mediated mTOR Inhibition in Human Keratinocytes. J Immunol 197, 3545-3553.

CHAPTER TWO – Hematopoietic Cell-Derived RELMα Regulates Hookworm Immunity Through Effects on Macrophages

Hashini M. Batugedara[1], Gang Chen[2], Dihong Lu[3], Jay J. Patel[2], Jessica C. Jang[1], Kelly C. Radecki[2], Abigail C. Burr[2], David D. Lo[2], Adler R. Dillman[3], Meera G. Nair[2]

[1]Department of Microbiology, University of California Riverside, Riverside, CA, USA.

[2]Division of Biomedical Sciences, School of Medicine, University of California Riverside, Riverside, CA, USA.

[3]Department of Nematology, University of California Riverside, Riverside, CA, USA.

A version of this chapter was published in the *Journal of Leukocyte Biology*, 2018.

Abstract

Resistin-like molecule α (RELMα) is a highly-secreted protein in type 2 (Th2) cytokine-induced inflammation including helminth infection and allergy. In infection with *Nippostrongylus brasiliensis* (*Nb*), RELMα dampens Th2 inflammatory responses. RELMα is expressed by immune cells, and by epithelial cells (EC), however, the functional impact of immune versus EC-derived RELMα is unknown. We generated bone marrow (BM) chimeras that were RELMα deficient (RELMα$^{-/-}$) in BM or non BM cells and infected them with *Nb*. Non BM RELMα$^{-/-}$ chimeras had comparable inflammatory responses and parasite burdens to RELMα$^{+/+}$ mice. In contrast, both RELMα$^{-/-}$ and BM RELMα$^{-/-}$ mice exhibited increased *Nb*-induced lung and intestinal inflammation, correlated with elevated Th2 cytokines and *Nb* killing. CD11c^{+} lung macrophages were the dominant BM-derived source of RELMα and can mediate *Nb* killing. Therefore, we employed a macrophage-worm co-culture system to investigate whether RELMα regulates macrophage-mediated *Nb* killing. Compared to RELMα$^{+/+}$ macrophages, RELMα$^{-/-}$ macrophages exhibited increased binding to *Nb* and functionally impaired *Nb* development. Supplementation with recombinant RELMα partially reversed this phenotype. Gene expression analysis revealed that RELMα decreased cell adhesion and Fc receptor signaling pathways, which are associated with macrophage-mediated helminth killing. Collectively, these studies demonstrate that BM-derived RELMα is necessary and sufficient to dampen *Nb* immune responses, and identify that one mechanism of action of RELMα is through inhibiting macrophage recruitment and interaction with *Nb*. Our findings suggest that RELMα acts as an immune brake that provides mutually beneficial effects for the host and parasite by limiting tissue damage and delaying parasite expulsion.

Introduction

Infections with parasitic worms induce a T helper type 2 (Th2) immune response that is important for controlling parasite burdens during primary infection and for immunity to subsequent secondary infections [1-4]. Additionally, Th2 immune responses have evolved to rapidly repair tissue damage caused by parasitic worms, and to restore tissue integrity and homeostasis following parasite killing [5-7]. However, excessive Th2 immune responses are detrimental to the host where they can contribute to allergic inflammatory responses and tissue fibrosis [8-10]. Therefore, Th2 immune responses must be carefully balanced for optimal anti-parasitic immunity and tissue repair while limiting excessive inflammation and fibrosis. Investigation of host factors that regulate such immune responses could have broad implications for the treatment of these pathologies. Here we investigated the contribution of Resistin-like molecule α (RELMα/Rα) to this host regulatory pathway in helminth infection.

RELMα is a host-derived protein that is highly expressed in several disease conditions including helminth infection, colitis, diabetes, allergy and asthma [11-16]. In mouse models of asthma, RELMα expression is elevated in the lung following allergen challenge, where it was postulated to promote to airway hyperresponsiveness [11, 17, 18]. Other studies using genetic deletion of RELMα or RELMα overexpression have suggested instead a beneficial function for RELMα in limiting Th2 cytokine-induced inflammation in mouse models of asthma and mouse helminth infection [19-21]. Although protective in dampening lung inflammatory responses, RELMα paradoxically impaired optimal parasite expulsion in infection with the hookworm *Nippostrongylus brasiliensis* (*Nb*) [19, 21].

The mechanism of RELMα-induced immunoregulation has been investigated in *in vitro* activated bone marrow-(BM) derived macrophages and dendritic cells [13, 22-24]. These studies

showed that RELMα expressed by alternatively activated macrophages (AAMac) dampened $CD4^+$ Th2 cell responses while RELMα derived from dendritic cells promoted $CD4^+$ IL-10 production. However, whether *in vivo* derived RELMα from these immune cells functionally impacts helminth infection-induced inflammatory response or helminth expulsion is unclear. Indeed, RELMα is also expressed by non-immune cells such as airway epithelial cells (EC), although the function of non-immune cell-derived RELMα is less well understood. In contrast to immune cells which can traffic to various sites in the body, EC cells are stationary and provide a barrier against pathogens. Nevertheless, EC contribute to host protective immunity by secreting chemokines and other proteins, such as trefoil factors, that mediate lung tissue repair following hookworm infection [25].

In this study, we investigated the functional contribution of RELMα derived from immune and non-immune cells and explored the mechanism of RELMα inhibition of helminth expulsion. Employing RELMα deficient BM chimeras, we show that immune cell-derived RELMα**,** and not EC-derived RELMα**,** downregulates the Th2 inflammatory response against hookworms and impairs clearance of worms by the host. Further, we identify $CD11c^+F4/80^+$ macrophages as the primary source of immune cell-derived RELMα in the lungs. We utilize $CD11c^+$ macrophage-worm co-culture assays to demonstrate that RELMα impairs macrophage-worm interaction and killing. Last, to identify potential downstream mechanisms of RELMα signaling on macrophages, we utilized Nanostring technology to measure RELMα-induced changes in expression of over 700 myeloid specific genes in purified lung macrophages. Functional enrichment pathway analysis revealed that RELMα treatment downregulated genes associated with macrophage-mediated helminth killing, such as cell adhesion and Fc receptor signaling, but upregulated genes associated with cell cycle and apoptosis and Th1 activation. Collectively, our data implicate immune cell-derived RELMα as an important regulatory factor in hookworm infection through two mechanisms:

1/ inhibiting Th2 inflammatory responses and 2/ directly acting on macrophages to impair adhesion to the worm.

Materials and Methods

Mice

C57BL/6 and CD45.1 mice purchased from the Jackson Laboratory were bred in-house. RELMα$^{-/-}$ (*Retnla*$^{-/-}$) mice were generated and genotyped as previously described [19]. Mice were age matched (6 to 14 weeks old), gender matched, and housed five per cage under an ambient temperature with a 12 hr light/12 hr dark cycle. All protocols for animal use and euthanasia were approved by the University of California Riverside Institutional Animal Care and Use Committee (protocols A-20150028B and A-20150027E) and were in accordance with National Institutes of Health guidelines, the Animal Welfare Act, and Public Health Service Policy on Humane Care and Use of Laboratory Animals.

Bone marrow (BM) transfer

C57BL/6 (CD45.2), CD45.1 and RELMα$^{-/-}$ CD45.2 mice were used in BM chimera generation. Age and sex-matched animals were used as recipients of BM isolated from wild-type (WT) or RELMα$^{-/-}$ mice. Recipients were sub lethally irradiated twice with 600 rad and reconstituted with 3×10^6 total BM cells administered via retroorbital injection. Donor chimerism was evaluated 8 weeks later via flow cytometry using blood stained with allotype-specific antibodies that recognized CD45.1 or CD45.2 (eBioscience). Mice that showed <75% donor chimerism were excluded from further experimental analysis.

Infection

Nippostrongylus brasiliensis (Nb) hookworms were obtained from the laboratory of Graham Le Gros (Malaghan Institute, New Zealand). *Nb* life cycle was maintained in Sprague-Dawley rats purchased from Harlan Laboratories. Mice were injected subcutaneously with 500 *Nb* infectious

third-stage larvae (L3) and sacrificed at days 3, 7 or 9 post-infection. The number of parasite eggs in the feces of infected mice were counted using a McMaster counting chamber and saturated salt solution on days 6–9 following infection. To quantify the number of adult worms within the small intestine, the small intestines of infected mice were cut longitudinally and incubated in phosphate buffered saline (PBS) at 37°C for 2 hr to allow worms to migrate out of the tissue. The number of worms in the intestines were then manually quantified. To generate *Nb* immune mice, mice were allowed to clear *Nb* infection and re-infected with 500 L3 at 21 days post primary infection. Immune mice were sacrificed at day 4 post-secondary infection.

Sample collection, processing, flow cytometry and cell sorting

Bronchoalveolar lavage (BAL) fluid and cells were recovered through washing twice with 800 ul of ice-cold 1X PBS. Cells were recovered by centrifugation and leukocytes were enumerated by manual counting using a hemocytometer. For flow cytometry, BAL cells were blocked with 0.6 g rat IgG and 0.6 g anti-CD16/32 (2.4G2) and stained for 25 min with antibodies for SiglecF (E50-2440), Ly6G (1A8), MHCII (M5/114.15.2) (all from BD Biosciences); F4/80 (BM8), Ly6C (HK1.4), CD11b (M1/70), CD11c (N418), CD45.1 (A20) and CD45.2 (104) (all from eBioscience, Affymetrix). Cells were then washed and analyzed on an LSRII instrument (BD Bioscience), followed by data analysis using FlowJo v10 (Tree Star Inc.). Florescent activated cell sorting (FACS) was conducted on Moflo Astrios instrument (BD Bioscience). Cell populations were identified as follows; alveolar macrophages ($CD11c^{+}F4/80^{+}$), dendritic cells ($CD11c^{hi}MHCII^{hi}$), eosinophils ($CD11c^{-}SiglecF^{+}$), monocytes ($CD11b^{+}Ly6C^{+}$) and neutrophils ($CD11b^{+}Ly6G^{+}$).

Real Time Polymerase Chain Reaction (RT-PCR)

RNA from lung tissue was extracted with TRIzol (Sigma), and RNA from cells was extracted by using the Aurum total RNA minikit (Bio-rad). iScript reverse transcriptase was used for cDNA synthesis (Bio-Rad). RT-PCR was performed with the Bio-Rad CFX Connect system using Bio-Rad CFX Manager 3.1 software. *Retnla* and glyceraldehyde 3-phosphate dehydrogenase (GAPDH) primers were purchased from Qiagen.

Cytokine Quantification

For sandwich enzyme-linked immunosorbent assay (ELISA), Greiner 96-well medium bind plates were coated with primary antibody to cytokines (RELMα, Peprotech; IL-13 and IL-4, eBioscience) overnight at room temperature. Plates were blocked with 5% newborn calf serum in 1X PBS for 1 hr at 37°C. Sera or tissue homogenates were added at various dilutions and incubated at room temperature for 2 hr. Cytokines were detected by applying biotinylated antibodies (RELMα, Peprotech; IL-13 and IL-4, eBioscience) for 1 hr at 37°C followed by incubation with streptavidin-peroxidase (Jackson Immunobiology) for 1 hr at room temperature. Substrate TMB (BD Bioscience) was added followed by addition of 2N H_2SO_4 as a substrate stop, and the optical density was captured at 450 nm. Samples were compared to a serial-fold dilution of recombinant cytokine.

Histology

Lungs were inflated with 1 ml 1 part 4% paraformaldehyde (PFA)/30% sucrose and 2 parts OCT embedding medium (Fisher Scientific) and stored overnight in 4% PFA/30% sucrose at 4°C. 1 cm of the proximal jejunum were fixed in 4% PFA overnight at 4°C. Lungs and intestines were blocked in OCT and sectioned at 12 µm. For immunofluorescence staining, sections were incubated with rabbit anti-mRELMα (1:400, Peprotech), biotinylated *griffonia simplicifolia* lectin (1:400,

Vector Laboratories), CC10 (1:400, Santa Cruz Biotechnology), F4/80 (1:400, eBioscience) overnight at 4°C. Sections were incubated with appropriate fluorochrome-conjugated secondary antibodies for 2 hr at room temperature and counterstained with DAPI. For pathology, lung sections were stained with hematoxylin and eosin. Sections were visualized under a DM5500B microscope (Leica).

Nippostrongylus-*lung cell co-culture*

Lung tissue of naive or immune WT or RELMα$^{-/-}$ mice were cut finely, incubated in 30 µg/mL DNAse (Sigma) and 1 mg/mL collagenase (Roche) for 25 min in a 37°C shaking incubator and passed through a 70 µm cell strainer to generate single cell suspensions. Cells were washed with Dulbecco's modified Eagle's medium supplemented with 10% fetal bovine serum, 1% L-glutamine, and 1% penicillin-streptomycin (all from Gibco). Red blood cells were lysed by using ammonium chloride-potassium buffer (Gibco). CD11c positive and negative populations were obtained using CD11c positive selection microbeads (Miltenyi). CD11c positive or negative cell fractions were incubated with 50-100 *Nb* L3 that were ex-sheathed with 0.25% NaOCl (Fisher Scientific) and washed in 400 µg/ml neomycin (Fisher Scientific) and 400 U/ml penicillin-streptomycin (Gibco). Where indicated, CD11c^{+} RELMα$^{-/-}$ cell co-cultures were supplemented with 100 ng/ml recombinant RELMα protein. All treatments were supplemented with immune serum from secondary infected RELMα$^{-/-}$ *Nb*-infected mice and incubated at 37°C 5% CO_2. Co-cultures seeded with $0.2x10^6$ cells were analyzed for cell adherence to worms and worm motility. Co-cultures seeded at $1x10^6$ cells were analyzed for RELMα levels in culture supernatant and worm ATP assays. Supernatants were collected and frozen at -20°C for downstream analyses. Cell adherence to worms was measured with bright field images of 5 fields of view in each triplicate well of the co-culture assay. The number of cells attached per worm were manually quantified.

Worm motility was measured by collecting 15 second videos of 5 fields of view of each well of each treatment. Motility was assessed with custom-made Fiji macros as previously described [26]. For worm measurements, larvae from co-culture assays or *Nb*-infected mouse lungs were placed on a thin layer of 2% agarose pad and covered by a coverslip. Images of worms were taken using a camera (Canon EOS T5i) attached to a bright field microscope (Leica DM2500). Worm measurements were done by tracing worm length and width in bright field images. Worm length was determined by tracing the worm lengthwise long the central line. Worm width was measured by tracing the widest region of the midsection.

Adenosine triphosphate (ATP) assay

At the end of the co-culture assay, cells adhered to worms were removed by lysing with water. Larvae from each treatment were individually picked in 1X PBS, mixed with CellTiter-Glo 2.0 luminescent reagent (Promega) and homogenized using a bead beater at 4°C for 5 min. The homogenates were centrifuged at 1,000 x g for 2 min. Supernatants were transferred to a black 96-well clear-bottom plate and luminescence was recorded by using a Glomax Multi detection system (Promega). An ATP standard curve was generated by using ATP disodium salt (Sigma).

Scanning electron microscopy (SEM)

At day 7 of the co-culture assay, worms from each treatment were washed in 1X PBS and fixed in 2.5% glutaraldehyde (Fisher Scientific) for 1 hr on ice. Samples were washed 3-times in 1X PBS and fixed in 1% osmium (Fisher Scientific) at room temperature in the dark for 1 hr. Samples were washed 3-times in 1X PBS and dehydrated in an ethanol gradient; 25% ethanol for 10 min, 50% ethanol for 10 min, 75% ethanol for 10 min and stored in 100% ethanol at 4°C until imaging.

Samples were air dried overnight at room temperature and sputter coated in platinum and palladium. Samples were imaged using the XL30 scanning electron microscope.

Gene expression analysis by Nanostring

$CD11c^+$ macrophages/dendritic cells were sorted from D9 *Nb* infected $RELM\alpha^{-/-}$ mouse lungs using the Moflo Astrios sorter (Beckman). $8x10^4$ sorted $RELM\alpha^{-/-}$ $CD11c^+$ cells were plated overnight in media with 10% fetal bovine (FBS), then serum-starved for 2hr in 1% FBS media. Cells were then stimulated for 4hr with control PBS or recombinant RELMα (200 ng) (n=3 per group). Cell lysates equivalent to $5x10^3$ cells were prepared according to manufacturer's instructions and analyzed with Myeloid Innate Immunity v2 panel (Nanostring). Gene expression analysis was conducted using the Advanced Analysis Nanostring software. The Nanostring Advanced Analysis algorithm generated biological pathway scores by using normalized expression and extracting pathway-level information from a group of genes using the first principal component (PC) of their expression data [27]. Data for each pathway were scaled across samples before taking the first PC by dividing each gene's log2 expression values by the greater of either their standard deviation or 0.05. Pathway scores for PBS *vs*. RELMα treatments were combined from two independent experiments and tested for statistical significance for a total of n=6 per group. Pathway scores are represented as the difference in pathway score between the two treatments and heatmaps of gene expression. Gene expression ratios (mRNA counts of RELMα/PBS) of two independent experiments were separately calculated by the Nanostring analysis software. Of the total 754 genes, differentially expressed genes (DEG) that reached p values of $p<0.06$ were investigated further. These DEG, representative of one experiment, were sorted and graphed by upregulated *vs*. downregulated genes.

Statistical analysis

All statistics were analyzed by Graphpad Prism software. Where appropriate student's t-test (for normal distribution data), Mann-Whitney nonparametric test (for asymmetric distribution data), two-way ANOVA (for analysis of more than one experiment); *, $p \leq 0.05$; **, $p \leq 0.01$; ***, $p \leq 0.0001$.

Results

Nb *infection induces RELMα expression in EC and alveolar macrophages.*

RELMα exhibits a remarkably diverse expression pattern and is expressed by immune and non-immune cells in a variety of Th2 inflammatory diseases, including helminth infection and airway allergic inflammation. We and others previously showed that RELMα dampens *in vivo* Th2 immune responses to helminths, and that macrophage and dendritic cell-derived RELMα regulates $CD4^+$ T cell cytokine expression [13, 19, 21]. However, the contribution of RELMα derived from immune and non-immune cells *in vivo* following *Nb*-infection has not been evaluated. We examined cell-specific RELMα expression in WT C57BL/6 mice, subcutaneously injected with 500 *Nb* L3 (or control 1X PBS) and sacrificed at day 7 post-infection when RELMα protein levels in the infected tissues are highest [19, 28]. In accordance with previous studies, both the lung and small intestine, which are colonized by *Nb*, had significantly increased *Nb*-induced RELMα, however, RELMα mRNA levels were over 400-fold higher in the lung (Figure 6A). RELMα immunofluorescent (IF) staining of the lung and small intestine (Figure 6B) revealed that RELMα was expressed in the EC lining the airway (green arrow) and in lung parenchymal cells (white arrow). In the small intestine, histological assessment of RELMα staining suggested that RELMα was expressed by goblet cells in the basal crypts (green arrow) and by circulating leukocytes in the submucosa (white arrow). Although RELMα expression in non-immune airway EC and intestinal goblet cells was possible to visualize according to cell morphology, identifying the specific immune cells that express RELMα by IF staining was not possible. Instead, we performed cell sorting on dissociated lung tissue of *Nb*-infected mice, where RELMα expression is highest, followed by real time (RT)-PCR analysis of RELMα mRNA levels, normalized to a housekeeping gene. Purity of sorted cells was analyzed by flow cytometry and hematoxylin and eosin (H&E)-stained cytospins,

revealing >90% purity (Figure 6C). $CD11c^{+}F4/80^{+}$ alveolar macrophages were the major immune cellular source of RELMα in the lung followed by $CD11c^{+}MHCII^{+}$ dendritic cells and $CD11c^{-}$ $SiglecF^{+}$ eosinophils, whereas $Ly6C^{+}$ monocytes and $Ly6G^{+}$ neutrophils produce little to no RELMα (Figure 6D). Together these studies reveal that *Nb* infection induces RELMα expression by lung and intestinal EC and by immune cells, specifically macrophages. To date, the contribution of each of these cellular sources of RELMα to the outcome of *Nb* infection has not been explored.

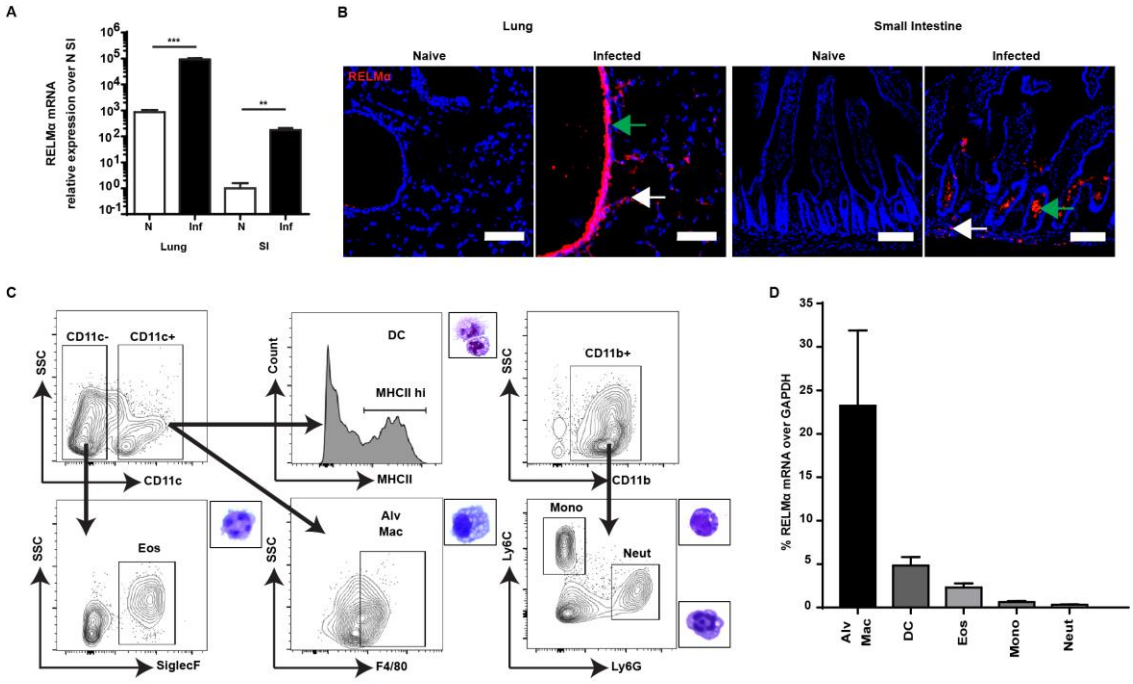

Figure 6: *Nb* infection induces RELMα expression in ECs and alveolar macrophages. C57BL/6 mice were left naïve or infected with *Nb* and evaluated for RELMα expression at day 7 post-infection. (A) RELMα RT-PCR in lung and small intestine (SI) was measured as relative fold induction over naïve SI (n=3 mice per group). (B) IF staining of RELMα (red) and DAPI (blue) was performed in naïve and day 7 *Nb*-infected tissue. Lung; green arrow indicates airway cells and white arrow indicates parenchymal cells. SI; green arrow indicates basal crypts and white arrow indicates circulating leukocytes (scale bar, 100 μm). (C) Gating strategy and confirmatory H&E cytospin for FACS sorted lung cells from *Nb*-infected mice. (D) RELMα mRNA expression was quantified in sorted alveolar macrophages (Alv Mac), dendritic cells (DC), eosinophils (Eos), monocytes (Mono) and neutrophils (Neut) as fold induction over neutrophils (n=4-6 mice per group). Data are represented as mean ± SEM.

Generation of RELMα$^{-/-}$ BM chimeras to determine the contribution of BM and non BM-derived RELMα in Nb *infection.*

Given the lack of available cell-specific RELMα$^{-/-}$ mice, we took advantage of BM chimera technology to delineate the role of non-immune and immune cell-derived RELMα in *Nb* immune responses. Recipient mice were irradiated to deplete BM, followed by retroorbital transfer of donor BM. Successful reconstitution was confirmed 8 weeks later by flow cytometric analysis of the peripheral blood for expression of the congenic markers CD45.1 and CD45.2 (Figure 7A). Specific analysis of alveolar macrophages revealed greater than 96% reconstitution (Figure 7B). BM chimeric mice were infected with *Nb*, and sacrificed at day 9, followed by examination of RELMα expression. Lung IF staining revealed RELMα co-stained with macrophage-binding lectin, *Griffonia simplicifolia* lectin (GSL) in WT and non BM RELMα$^{-/-}$ mice but not BM RELMα$^{-/-}$ or RELMα$^{-/-}$ mice, validating that BM-specific RELMα deletion abrogated macrophage expression of RELMα (Figure 7C). Conversely, RELMα co-stained with airway EC marker CC10 in WT and BM RELMα$^{-/-}$ mice, but was abrogated when recipient mice were RELMα$^{-/-}$ (Figure 7D). Similarly, we examined RELMα expression in the *Nb*-infected small intestine (Figure 7E). All chimeras except RELMα$^{-/-}$ mice had RELMα^{+} cells (red), but only WT and non BM RELMα$^{-/-}$ intestinal tissue sections had co-expression of RELMα with F4/80^{+} macrophages (green).

We next evaluated if deletion of RELMα specifically in the BM or the non-hematopoietic cell compartment affected local or systemic RELMα protein levels. Bronchoalveolar lavage (BAL) fluid RELMα was increased in *Nb*-infected WT mice compared to naïve WT mice (Figure 7F). However, RELMα deletion in the BM (BM RELMα$^{-/-}$) did not affect BAL fluid RELMα levels, suggesting that BM cells contribute little to no RELMα in the airways. In contrast, when RELMα was deleted in airway EC (non BM RELMα$^{-/-}$), BAL fluid RELMα was significantly reduced to

levels observed in naïve mice. We observed the opposite phenotype for systemic RELMα expression (Figure 7G), where BM-specific RELMα deletion significantly abrogated *Nb*-induced circulating RELMα, while non BM RELMα$^{-/-}$ mice still exhibited elevated serum RELMα levels. Together, these data delineate the contribution of immune and non-immune cell-derived RELMα in *Nb* infection, and show that RELMα in the airways is derived uniquely by non-immune cells, while immune cells are the main source of systemic RELMα in the serum. Nonetheless, the functional impact of local versus systemic RELMα in *Nb* immune responses is unknown.

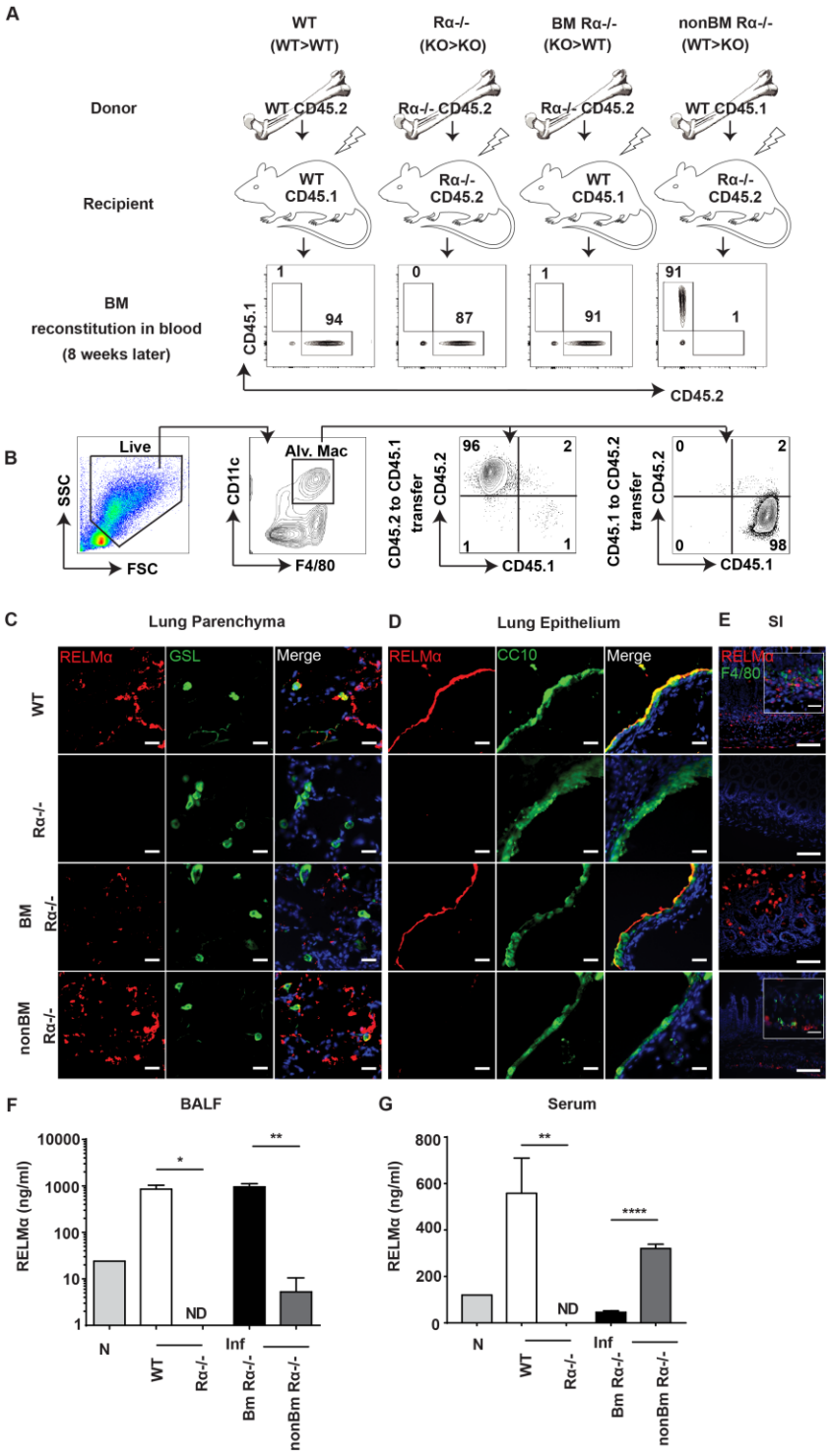
A
WT (WT>WT)
Rα-/- (KO>KO)
BM Rα-/- (KO>WT)
nonBM Rα-/- (WT>KO)
Donor
WT CD45.2
Rα-/- CD45.2
Rα-/- CD45.2
WT CD45.1
Recipient
WT CD45.1
Rα-/- CD45.2
WT CD45.1
Rα-/- CD45.2
BM reconstitution in blood (8 weeks later)
CD45.1
CD45.2
1
94
0
87
1
91
91
1
B
Live
SSC
FSC
CD11c
Alv. Mac
F4/80
CD45.2 to CD45.1 transfer
CD45.2
CD45.1
96
2
1
1
CD45.1 to CD45.2 transfer
CD45.2
CD45.1
0
2
0
98
C
Lung Parenchyma
D
Lung Epithelium
E
SI
RELMα
GSL
Merge
CC10
F4/80
WT
Rα-/-
BM Rα-/-
nonBM Rα-/-
F
BALF
G
Serum
RELMα (ng/ml)
10000
1000
100
10
1
800
600
400
200
0
*
**
**
****
ND
ND
N
Inf
WT
Rα-/-
Bm Rα-/-
nonBm Rα-/-

Figure 7: Generation of RELMα$^{-/-}$ BM chimeras to determine the contribution of BM and non BM-derived RELMα in *Nb* infection. (A) BM chimera design and validation by flow cytometric analysis of peripheral blood. (B) Evaluation of alveolar macrophage reconstitution in bone marrow chimeric mice. (C-E) Day 9 *Nb*-infected BM chimeras were evaluated for RELMα expression by IF staining followed by microscopic examination. (C) Lung parenchyma and (D) lung epithelium stained for RELMα (red), GSL/CC10 (green) and DAPI (blue) (scale bar, 25 μm). (E) Small intestine stained for RELMα (red), F4/80 (green) and DAPI (blue) (scale bar, 200 μm, insert 50 μm). (F-G) RELMα levels in the BAL fluid (F) and serum (G) of day 9 *Nb*-infected BM chimeras were measured by ELISA (ND not detected, n=4 mice per group). Data are presented as mean ± SEM, and representative of 3 separate experiments.

BM-derived RELMα regulates Nb *infection-induced tissue inflammation, Th2 immune responses and parasite expulsion.*

To elucidate the role of BM and non BM RELMα in *Nb*-induced lung and intestinal inflammation, histological examination of lung and intestinal tissue sections from infected BM chimeric mice was performed. RELMα$^{-/-}$ and BM RELMα$^{-/-}$ mice exhibited the most severe lung alveolar destruction (green arrow) and intestinal immune cell infiltration in the submucosa (blue arrow) (Figure 8A). In contrast, non BM RELMα$^{-/-}$ had comparable tissue inflammatory responses to WT mice, suggesting that BM-derived RELMα critically protects from *Nb*-induced tissue damage and inflammation, while non BM-derived RELMα is dispensable. Flow cytometric analysis of the BAL cells revealed that there were no significant differences in immune cell populations, however, RELMα$^{-/-}$ and BM RELMα$^{-/-}$ mice exhibited a trend towards increased Th2 inflammation including elevated eosinophils and macrophages compared to WT and non BM RELMα$^{-/-}$ mice (Figure 8B). Similarly, serum IL-13 levels and BAL fluid IL-4 levels quantified by enzyme linked immunosorbent assay (ELISA) revealed that RELMα$^{-/-}$ and BM RELMα$^{-/-}$ mice had elevated levels of these Th2 cytokines (Figure 8C).

We next determined if the increased infection-induced inflammatory responses functionally impacted *Nb* burdens (Figure 8D). RELMα$^{-/-}$ and BM RELMα$^{-/-}$ mice had significantly reduced intestinal worm and fecal egg burdens, while there were no differences between WT and non BM RELMα$^{-/-}$ mice. Therefore, although RELMα is highly expressed by non BM-derived airway EC and BM-derived immune cells, RELMα from immune cells is necessary and sufficient to downregulate *Nb* immune responses, while non BM-derived RELMα has no obvious effect on *Nb* infection. Functionally, BM-derived RELMα is host-protective by limiting tissue damage and

inflammation, but also leads to higher parasite burdens likely due to impaired Th2 cytokine-mediated mechanisms of *Nb* killing.

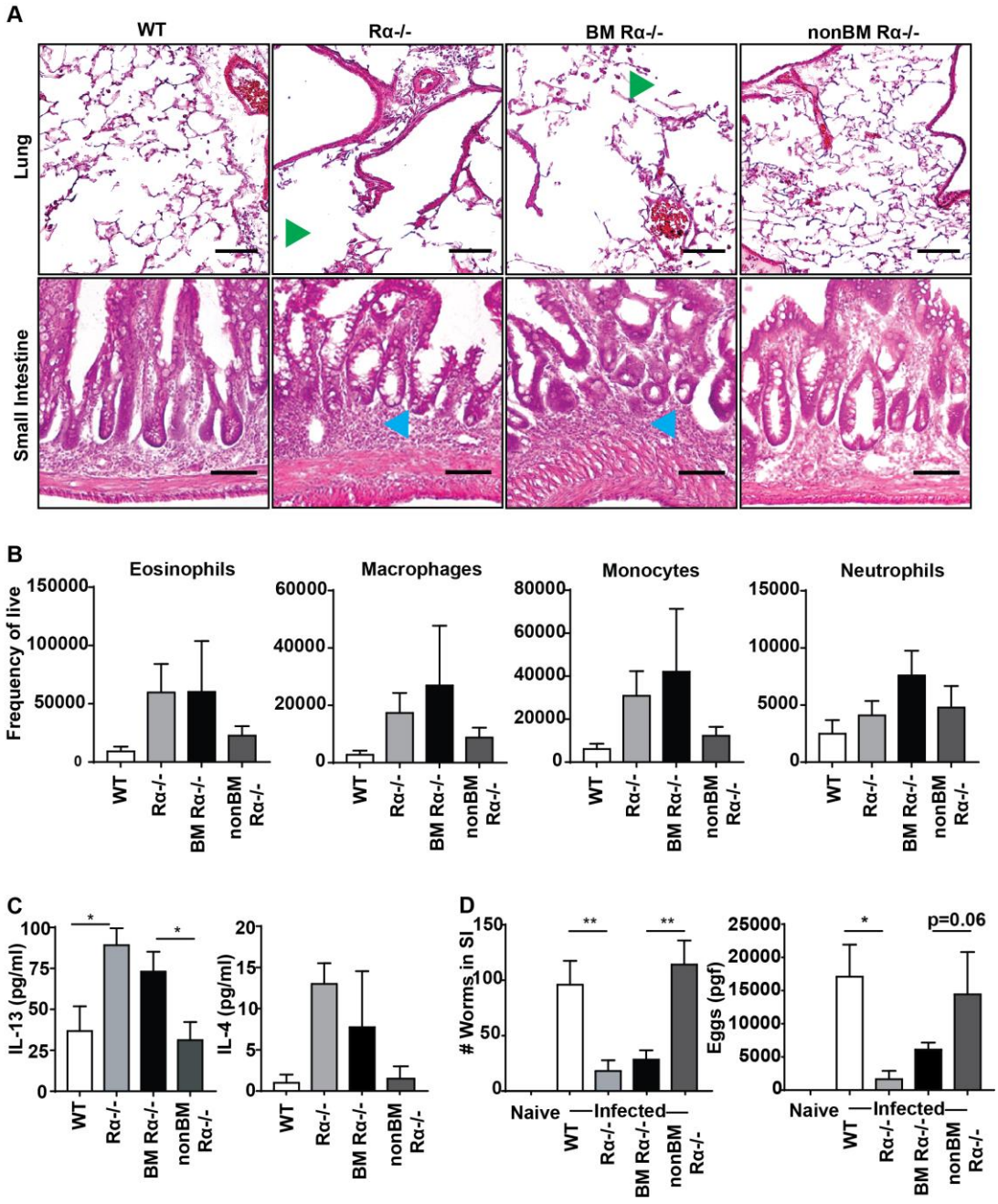
A
WT
Rα-/-
BM Rα-/-
nonBM Rα-/-
Lung
Small Intestine
B
Eosinophils
Macrophages
Monocytes
Neutrophils
Frequency of live
150000
100000
50000
0
60000
40000
20000
80000
15000
10000
5000
WT
Rα-/-
BM Rα-/-
nonBM Rα-/-
C
IL-13 (pg/ml)
IL-4 (pg/ml)
100
75
50
25
20
15
10
*
D
Worms in SI
Eggs (pgf)
150
25000
**
p=0.06
Naive
Infected

Figure 8: BM-derived RELMα regulates *Nb* infection-induced tissue inflammation, Th2 immune responses and parasite expulsion. BM chimeras were infected with *Nb* and sacrificed at day 9 to evaluate *Nb* immune responses and burdens. (A) H&E stained sections of *Nb*-infected lung and SI tissue (Green arrow, airway destruction; Blue arrow, infiltrating leukocytes; scale bar, 200 μm). (B) Flow cytometric analysis of BAL cell populations in infected mice (n=3-4 mice per group. (C) IL-13 and IL-4 protein levels were measured by ELISA in serum and BAL fluid respectively of infected mice (n=3-6 mice per group). (D) Intestinal worm and fecal egg burdens were measured at day 9 post-infection (n=8-21 mice per group). For panel D egg burden, log transformation of the raw data was done prior to statistical analysis. Data are presented as mean ± SEM.

RELMα$^{-/-}$ CD11c^{+} lung macrophages have enhanced ability to bind and impair Nb *fitness.*

Previous studies using a *Nb* vaccination model have shown that alternatively activated macrophages from the lung interact with and mediate *Nb* killing [29]. Together with our findings that RELMα deficiency specifically in immune cells enhanced *Nb* killing, we hypothesized that RELMα$^{-/-}$ macrophages would exhibit enhanced ability to kill *Nb*. We therefore investigated whether RELMα affected lung macrophage interaction and killing of *Nb* L3 in an *in vitro Nb*-lung cell co-culture assay, modified from the *Nb* vaccination studies (Figure 9A). WT and RELMα$^{-/-}$ mice were infected with *Nb* for 21 days, followed by secondary *Nb* challenge to enhance alternatively activated macrophage responses. Four days following re-infection, lungs were recovered for isolation of lung macrophages. Lung alveolar macrophages express CD11c therefore we performed CD11c enrichment by magnetic bead purification. Although lung dendritic cells also express CD11c, the percentage of lung dendritic cells (CD11c^{+}MHC2^{hi}, 20%) is lower than lung macrophages (CD11c^{+}F4/80^{+}, 60%). We first examined RELMα secretion by CD11c positive and negative fraction in response to co-culture with live *Nb* L3 (Figure 9B). Co-culture with *Nb* L3 led to increased RELMα secretion especially in the CD11c^{+} fraction. These results are consistent with the real-time PCR results of sort-purified lung cells and confirm that CD11c^{+} macrophages express more RELMα than other immune cell-types such as eosinophils, which have been previously reported to express high RELMα levels.

We next examined CD11c^{+} lung macrophage interaction with *Nb* L3 over the course of 7 days (Figure 9C). There was equivalent cell adherence to the *Nb* at day 1 post co-culture, however, we observed that RELMα$^{-/-}$ CD11c^{+} cells exhibited increased adherence to worms compared to WT cells starting at day 3 post co-culture, suggesting that RELMα inhibited the ability of CD11c^{+} cells to bind to *Nb*. To determine if cell adherence functionally affected *Nb*, we measured *Nb* motility in

the co-culture using videos. Compared to *Nb* incubated with WT macrophages, *Nb* incubated with RELMα$^{-/-}$ macrophages had significantly decreased motility (Figure 9D). At the end of the *in vitro* co-culture, we recovered *Nb* L3 and measured worm adenosine triphosphate (ATP) levels as a measure of worm viability (Figure 9E). There was a significant decrease in *Nb* ATP levels from RELMα$^{-/-}$ macrophage cultures compared to WT macrophage cultures. Together, these data suggest that RELMα inhibits macrophage adherence to *Nb,* and subsequent functional effects decrease *Nb* viability.

It is possible that the enhanced phenotype of RELMα$^{-/-}$ lung macrophages is indirect as a consequence of the elevated *in vivo* Th2 cytokine response, which would promote alternatively activated macrophage activation. Alternatively, since WT macrophages secrete RELMα *in vitro* in response to co-culture with *Nb* L3, RELMα in the supernatant may directly regulate macrophage-*Nb* interaction. To delineate direct versus indirect effects of RELMα, we supplemented RELMα$^{-/-}$ macrophage cultures with recombinant RELMα and examined cell adherence to *Nb* and subsequent effects on *Nb* fitness. The addition of RELMα to RELMα$^{-/-}$ macrophages partially decreased cell adherence, resulting in an intermediate phenotype between RELMα$^{-/-}$ and WT macrophages (Figure 9C). In contrast, RELMα treatment of RELMα$^{-/-}$ cultures completely restored *Nb* motility and ATP levels to those observed in *Nb* cultured with WT macrophages (Figure 9D-E). Together these results suggest that RELMα acts both directly on lung macrophages to suppress interaction with *Nb,* and indirectly, through other cell-types and cytokines to regulate macrophage activation.

We also examined *Nb* co-culture with CD11c^{+} cells from naïve (unvaccinated) WT or RELMα$^{-/-}$ mice in comparison to co-culture with immune (vaccinated) CD11c^{+} mice (above). Naïve WT CD11c^{+} cells cultured with *Nb* produced significantly less RELMα than immune CD11c^{+} cells at days 3, 5 and 7 post co-culture (Figure 9F). Examination of cell adherence to Nb revealed that

both naïve WT and RELMα$^{-/-}$ cells exhibited minimal binding (Figure 9G). This was in contrast to immune cells, where RELMα$^{-/-}$ CD11c^{+} cells adhered the most, consistent with previous findings (see Figure 9C). Finally, immune RELMα$^{-/-}$ CD11c^{+} cells were significantly better able to impair *Nb* motility than WT CD11c^{+} cells (Figure 9H). However, no significant difference was found in unvaccinated WT or RELMα$^{-/-}$ CD11c^{+} cells in their ability to reduce *Nb* motility. These results suggest that RELMα production and worm damage by CD11c^{+} cells require signals from the infection milieu *in vivo*.

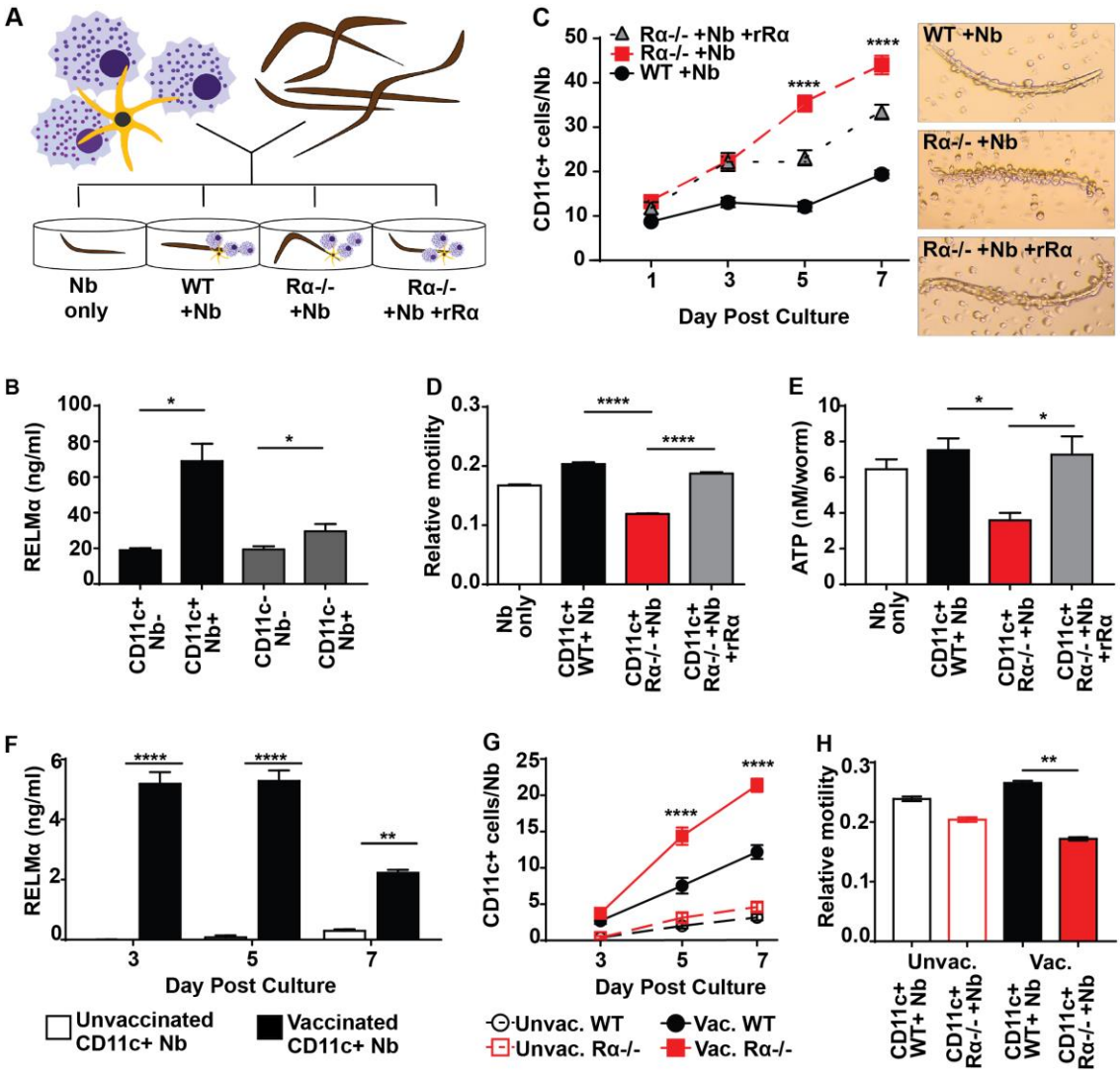
A
Nb only
WT +Nb
Rα-/- +Nb
Rα-/- +Nb +rRα
C
Rα-/- +Nb +rRα
Rα-/- +Nb
WT +Nb
CD11c+ cells/Nb
Day Post Culture
WT +Nb
Rα-/- +Nb
Rα-/- +Nb +rRα
B
RELMα (ng/ml)
CD11c+ Nb-
CD11c+ Nb+
CD11c- Nb-
CD11c- Nb+
D
Relative motility
Nb only
CD11c+ WT+ Nb
CD11c+ Rα-/- +Nb
CD11c+ Rα-/- +Nb +rRα
E
ATP (nM/worm)
Nb only
CD11c+ WT+ Nb
CD11c+ Rα-/- +Nb
CD11c+ Rα-/- +Nb +rRα
F
RELMα (ng/ml)
Day Post Culture
Unvaccinated CD11c+ Nb
Vaccinated CD11c+ Nb
G
CD11c+ cells/Nb
Day Post Culture
Unvac. WT
Vac. WT
Unvac. Rα-/-
Vac. Rα-/-
H
Relative motility
Unvac.
Vac.
CD11c+ WT+ Nb
CD11c+ Rα-/- +Nb
CD11c+ WT+ Nb
CD11c+ Rα-/- +Nb

Figure 9: RELMα$^{-/-}$ CD11c^{+} lung macrophages have enhanced ability to bind and impair *Nb* fitness. (A) Design of co-culture assay of *Nb* L3 with lung cells from day 21 *Nb*-infected WT or RELMα$^{-/-}$ mice. (B) RELMα secretion by WT cells was measured in supernatants from day 3 post culture of CD11c positive and negative fractions from lung cells with or without *Nb*. (C) Microscopic quantification of adherent cells to *Nb* was performed for co-culture with CD11c^{+} cells from WT or RELMα$^{-/-}$ mice and representative bright field images shown. (D) Relative *Nb* motility (E) and ATP levels were measured at day 7 post co-culture. Where indicated, 100 ng/ml recombinant RELMα (rRα) was added to RELMα$^{-/-}$ CD11c^{+} cell-*Nb* co-culture. (F) RELMα secretion by unvaccinated *vs.* vaccinated CD11c^{+} cells were measured at D3, 5 and 7 post-culture (n=3 per group). (G) Microscopic quantification of adherent cells to *Nb* was performed for co-culture with CD11c^{+} cells from unvaccinated *vs.* vaccinated mice and representative bright field images are shown. (H) Relative *Nb* motility was measured at day 7 post co-culture. Data are presented as mean ± SEM (n=3/group), and representative of 2 separate experiments.

To more closely examine the functional impact of RELMα$^{-/-}$ cell interaction with *Nb* worms, we recovered *Nb* L3 from *in vitro* co-culture with WT or RELMα$^{-/-}$ lung cells and measured worm size. *Nb* incubated with RELMα$^{-/-}$ cells were shorter in length and significantly smaller in width compared to *Nb* incubated with WT cells (Figure 10A). To visualize macrophage-*Nb* interaction, we performed scanning electron microscopic (SEM) imaging of *Nb* L3 following co-culture with WT or RELMα$^{-/-}$ macrophages (Figure 10B). SEM images revealed close interaction and adherence of both WT and RELMα$^{-/-}$ macrophages to *Nb* L3. However, WT macrophages were rounder, and the area of focal adhesion to the worm was small and distinct. In contrast, the focal contact point of RELMα$^{-/-}$ macrophages appeared larger in area, resulting in flatter macrophages for a more expansive contact with the worm on a per cell basis. We investigated the physiological relevance of the *in vitro* effects of RELMα$^{-/-}$ cells on *Nb* growth in *in vivo Nb* infection. WT and RELMα$^{-/-}$ mice were infected with *Nb* and sacrificed at day 3, followed by recovery of *Nb* larvae from the lungs. Although numbers of worms recovered from WT mice *vs* RELMα$^{-/-}$ mice were equivalent (Figure 10C), *Nb* recovered from RELMα$^{-/-}$ lungs were shorter in length and significantly smaller in width compared to *Nb* recovered from WT lungs (Figure 10D). While there are important differences in timing between the *in vitro* (7 days) and *in vivo* (3 days), these data both indicate that *Nb*-induced macrophages differentiated in a RELMα deficient environment exhibit an enhanced activation phenotype. We show that RELMα directly inhibits macrophage-*Nb* interaction leading to impaired *Nb* killing. Since RELMα is predominantly expressed by macrophages, these data suggest that RELMα is secreted as an inhibitory cytokine that acts back on macrophages and other cell-types to dampen *Nb*-specific immune responses.

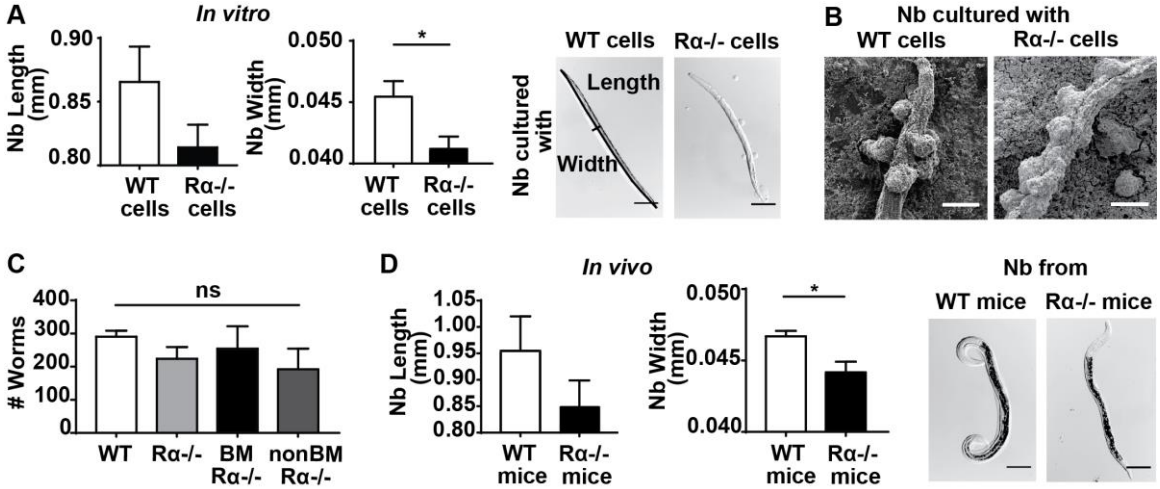

Figure 10. RELMα$^{-/-}$ lung cells impair *Nb* growth. *Nb* from day 7 co-culture assay or day 3 infected lungs of WT and RELMα$^{-/-}$ mice were compared. (A-B) *Nb* L3 worms from day 7 co-culture with total lung cells were measured and visualized for length and width (scale bar, 0.1 mm; n=9-11 worms per group). (B) Scanning Electron Micrograph of *Nb* L3 and CD11c^{+} lung macrophages at end of co-culture (scale bar, 20 μm). (C) *Nb* larvae were collected from day 3 *Nb*-infected WT or RELMα$^{-/-}$ mice, counted, and (D) measured and visualized for length and width (scale bar, 0.1 mm; n=5-6 worms per group). Data are presented as mean ± SEM.

Gene expression analysis reveals that RELMα signaling in lung macrophages downregulates pathways associated with cell adhesion and Fc receptor signaling.

We previously showed that recombinant RELMα treatment of RELMα$^{-/-}$ macrophages could restore the WT macrophage phenotype, notably the reduced ability to bind to the worm and impair its motility and fitness (see Figure 9C). Therefore, we employed this controlled *in vitro* system to delineate potential downstream mechanisms by which RELMα regulates macrophage-*Nb* interaction. We utilized Nanostring technology to screen over 750 myeloid-associated genes in RELMα$^{-/-}$ CD11c^{+} lung macrophages and identify those that were differentially expressed in response to RELMα. CD11c^{+} lung macrophages were sorted from the lungs of RELMα$^{-/-}$ mice at day 9 post *Nb* infection, with ~99% purity (Figure 11A). Macrophages were rested overnight then stimulated with control PBS or recombinant RELMα for 4 hrs, followed by analysis of cell lysate for 750 myeloid associated gene-encoded mRNAs. Nanostring advanced pathway analysis of RELMα *vs.* PBS-treatment revealed a number of biological pathways that were changed in response to RELMα treatment (Figure 11B). Genes associated with Th1 cytokine and chemokine signaling, and cell cycle and apoptosis were upregulated. These results may be consistent with previous studies showing that RELMα promotes chemotaxis and proliferation [30-32]. Given that RELMα downregulates Th2 cytokines [13, 21], it is likely that Th1 cytokine signaling is conversely enhanced. In addition, genes associated with TLR signaling, antigen presentation, Fc receptor signaling, and cell migration and adhesion were significantly downregulated in the RELMα treatment compared to PBS (Figure 11C and 11D). downregulation of cell adhesion pathways is in line with our observation that RELMα treatment impairs cell adhesion to *Nb*. Further, previous studies have shown the importance of Fc receptor-mediated nematode killing [26], therefore,

downregulation of these pathways by RELMα may explain the reduced ability of macrophages to bind and impair *Nb* motility and fitness.

Further, we analyzed the most differentially expressed genes between PBS *vs.* RELMα treatments (Table 2). Of these, RELMα downregulated 14 genes and the remaining 18 were upregulated. Interestingly, some genes associated with alternatively activated or resolving macrophages activation were downregulated, such as *Arg1*, the macrophage inhibitory factor *Mif*, the anti-inflammatory receptors *Fpr-rs5* (member of the lipoxin receptor family N-formyl peptide receptor 1), and *Trem2* [33, 34]. Of the genes that were upregulated by RELMα, we found genes associated with wound healing (*Mmp19* and *Pdgfra*), genes associated with cell survival (*Tm7sf3*, *Bcl2*) and genes associated with macrophage signaling and effector functions (*Rgs1*). These results show that RELMα signaling impacts various biological pathways and we have identified potential candidate genes that might be negatively regulated by RELMα to impair adhesion to the worm and killing.

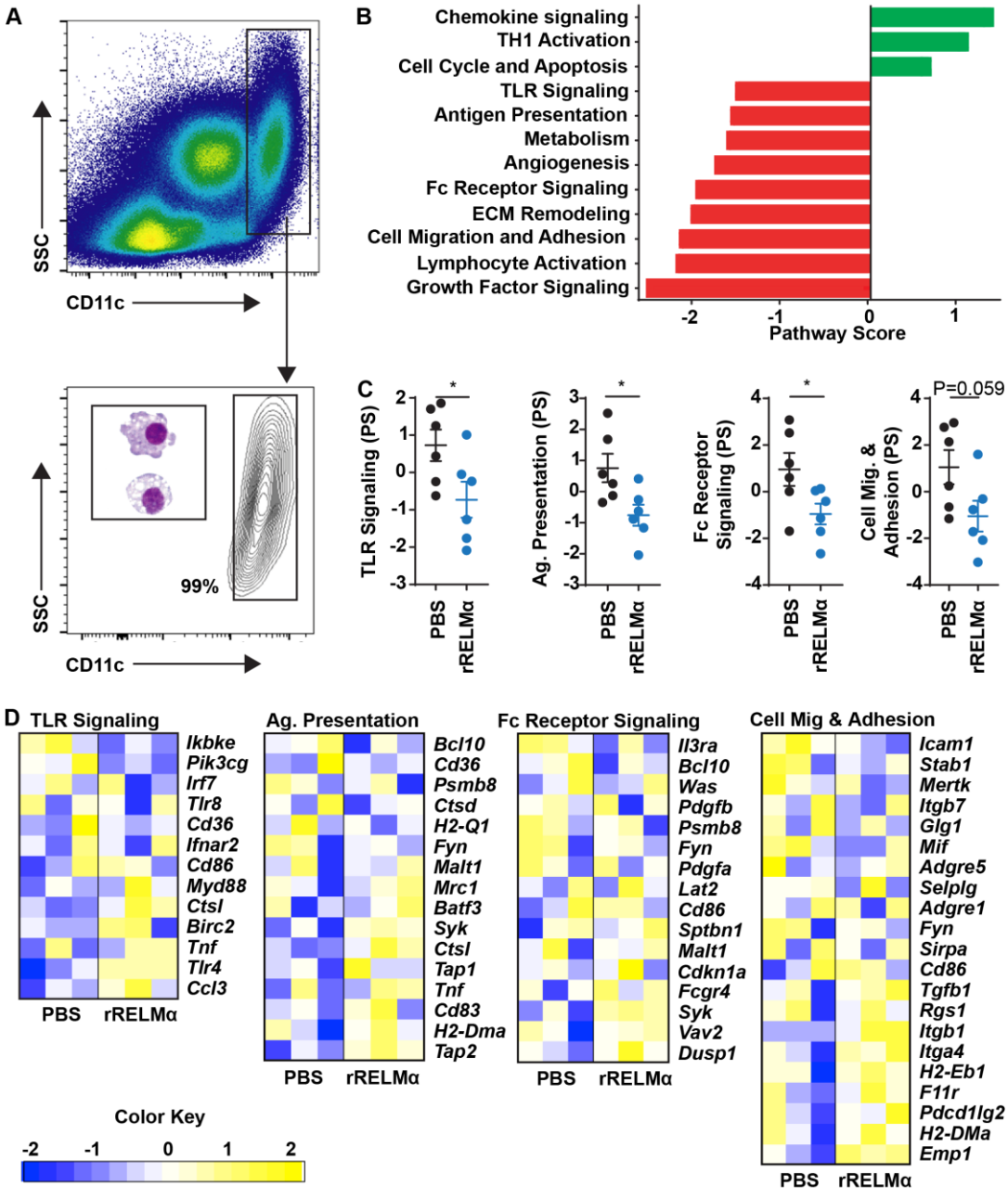
A
SSC
CD11c
99%
B
Chemokine signaling
TH1 Activation
Cell Cycle and Apoptosis
TLR Signaling
Antigen Presentation
Metabolism
Angiogenesis
Fc Receptor Signaling
ECM Remodeling
Cell Migration and Adhesion
Lymphocyte Activation
Growth Factor Signaling
Pathway Score
C
TLR Signaling (PS)
Ag. Presentation (PS)
Fc Receptor Signaling (PS)
Cell Mig. & Adhesion (PS)
P=0.059
PBS
rRELMα
D
TLR Signaling
Ikbke
Pik3cg
Irf7
Tlr8
Cd36
Ifnar2
Cd86
Myd88
Ctsl
Birc2
Tnf
Tlr4
Ccl3
Ag. Presentation
Bcl10
Cd36
Psmb8
Ctsd
H2-Q1
Fyn
Malt1
Mrc1
Batf3
Syk
Ctsl
Tap1
Tnf
Cd83
H2-Dma
Tap2
Fc Receptor Signaling
Il3ra
Bcl10
Was
Pdgfb
Psmb8
Fyn
Pdgfa
Lat2
Cd86
Sptbn1
Malt1
Cdkn1a
Fcgr4
Syk
Vav2
Dusp1
Cell Mig & Adhesion
Icam1
Stab1
Mertk
Itgb7
Glg1
Mif
Adgre5
Selplg
Adgre1
Fyn
Sirpa
Cd86
Tgfb1
Rgs1
Itgb1
Itga4
H2-Eb1
F11r
Pdcd1lg2
H2-DMa
Emp1
Color Key

Figure 11. RELMα downregulates antigen presentation, Fc receptor signaling, TLR signaling, cell migration and adhesion. (A) $CD11c^{+}$ macrophages were sorted from D9 *Nb*-infected $RELM\alpha^{-/-}$ mouse lungs and evaluated for purity. Representative flow cytometry plot and cytospin is presented. (B) Nanostring analysis of biological pathways that were changed by RELMα (n=6 per group). (C) Biological pathways downregulated by RELMα (n=6 per group). (D) Heatmap showing individual gene expression of genes belonging to respective biological pathway (n=3 per group).

Table 2. Differentially expressed genes in PBS versus RELMα treatment. ✦ NanoString nCounter Advanced Analysis; # KEGG pathway.

Putative function	RELMα suppressed	RELMα increased
Cell cycle and apoptosis		*Btg2*✦
Cell migration and adhesion	*Mif*✦, *Amica1*[138], *Ccl19*[139], *Ccr6*[140], *Fgf18*[141], *Fpr-rs5*[142], *Sema5a*[143]	*F11r*✦, *Itgb1*✦, *Rgs1*✦
Chemokine signaling	*Ccl19*#, *Ccr6*#,	*Ccl3*✦, *Ccl6*✦, *Rgs1*✦
Lectin signaling	*Fcnb*[144]	*Irf1*#
Cytokine/IFN signaling		*Tm7sf3*✦, *Il1r2*#, *Irf1*✦, *Tnfrsf14*[145]
Differentiation and maintenance of myeloid cells		*Ikzf1*✦
ECM remodeling	*Adamts3*[146]	*F11r*✦, *Furin*✦, *Itgb1*✦, *Kcnq1ot1*✦, *Mmp19*✦
Growth factor signaling		*Bcl2*✦, *Furin*✦, *Itgb1*✦, *Pdgfra*[147]
Lymphocyte activation	*Trem2*✦	*Golim4*✦, *Itgb1*✦
Metabolism	*Arg1*✦, *Sgpp1*✦, *Hnf1b*[148]	
Pathogen response/TLR signaling	*Rnase2b*[74]	*Bcl2*✦, *Chil3*✦, *Ccl3*✦

Discussion

Although hookworms are intestinal parasites, their development relies on their initial migration through the host lung [35]. As such, the Th2 immune response that occurs in the lung is critical for parasite clearance, especially following secondary challenge, and needs to be considered when investigating protective immunity to hookworms [36, 37]. However, hookworm-induced lung inflammation must also be closely regulated to prevent aberrant worm-induced inflammation. Th2 cytokine-activated AAMacs are critical contributors to this delicate balance between immunity and inflammation. In *Nb* infection, these cells can directly interact with and kill the worm but also are protective in resolving infection-induced lung hemorrhage and reducing neutrophil infiltration [5, 29, 38]. AAMacs also indirectly mediate *Nb* expulsion by promoting Th2 cytokine responses and inducing intestinal smooth muscle contractility [39, 40]. AAMacs secrete factors and upregulate cell surface molecules that may contribute to these functions, however, studies delineating the contribution of these specific factors to AAMac function *in vivo* are lacking. In this study, we focused on the function of RELMα, a secreted protein that is highly expressed by AAMacs in a Th2 cytokine-dependent manner [41].

By utilizing BM chimeric mice, we tested the importance of BM-derived and EC-derived RELMα for the outcome of hookworm infection and hookworm-induced inflammation. BM-derived RELMα was found to downregulate immune cell infiltration in the lungs, IL-13 and IL-4 cytokines. Consequently, mice expressing RELMα only in BM-derived cells had higher worm burdens in the intestine compared to mice expressing RELMα in ECs. Therefore, we discovered that BM or immune cell-sourced RELMα is immunomodulatory whereas EC-sourced RELMα is not. An explanation for this observed phenotype could lie in the addressing of the fundamental differences between immune cells and non-immune cells. Immune cells circulate in the blood between lymph nodes and inflamed tissue but in stark contrast, ECs are stationary cells. During an

infection setting, immune cells such as AAMacs have the capacity to communicate with other immune cells as well as interact with the parasite. These data are supportive of other studies showing immunoregulatory roles of AAMacs during helminth infection. While EC-derived RELMα is not immunomodulatory in *Nb* infection, high quantities of RELMα, presumably derived from EC, is observed in airways following allergen challenge. Whether EC-derived RELMα plays a more significant role in airway inflammation associated with asthma are avenues for future research.

Quantification of RELMα mRNA in sorted lung immune cells showed that alveolar macrophages were the principal source of RELMα in BM-derived cells. To further investigate the function of macrophage-derived RELMα, we performed co-culture assays of *Nb* with WT and RELMα$^{-/-}$ CD11c^{+} lung macrophages. We show that one mechanism by which RELMα impairs *Nb* killing is through impairing macrophage adherence and interaction with the worm. We employ recombinant RELMα to show that RELMα exerts its inhibitory effects directly on the worm or the macrophage. Previous studies investigating RELM protein binding of worms have shown that RELMβ but not RELMα functionally affects helminth suggesting that the effect of RELMα may be on macrophages and not on *Nb* [42, 43]. In these studies, RELMβ inhibited worm chemotaxis. Similarly, it is possible that RELMα inhibits macrophage chemotaxis to the worm. Alternatively, RELMα could regulate macrophage expression of surface integrins that mediate macrophage adherence [26, 29].

To test which potential molecules could be regulated by RELMα, we performed Nanostring gene expression analysis of PBS or rRELMα-treated RELMα$^{-/-}$ lung macrophages sorted from *Nb*-infected mice. Among the RELMα-induced upregulated pathways were chemokine signaling and Th1 activation pathways. Our previous results showed lower Th2 cytokine

expression, therefore, enhanced Th1 pathways in rRELMα-treated macrophages may be consistent with RELMα regulating the balance between Th1/Th2 immune pathways. Within the chemokine pathway, RELMα upregulated *Ccl3* and *Ccl6*, while downregulating *Ccl19* and *Mif*. The differential effects of these chemokines are unclear, but may contribute to inhibiting macrophage migration to *Nb*. Consistent with our functional data showing that RELMα impaired macrophage adhesion to *Nb*, genes associated with cell adhesion were downregulated in RELMα-treated macrophages. Additionally, genes associated with Fc receptor signaling were downregulated, which may suggest RELMα-induced impairment of Fc receptor-mediated *Nb* killing [26].

Interestingly, expression of the AAMac-specific enzyme Arginase 1 was downregulated by RELMα, however, the AAMac-secreted protein Ym1 (*Chil3*) was upregulated. Arginase 1 and its downstream products have previously been implicated in causing physical damage to *Heligmosomoides polygyrus* worms *in vitro* [26], therefore is a potential candidate gene for the reduced *Nb* viability when cultured with RELMα$^{-/-}$ macrophages. Other downregulated genes included *Fpr-rs5*, *Fcnb* and *Amica1*. *Fpr-rs5* is a member of formyl peptide receptor 1 family, which binds anti-inflammatory lipoxins and mediates biological responses such as Ca^{2}+ mobilization, cell attachment and migration [33, 44]. *Fcnb*, ficolin B, is a pattern recognition receptor that activates the complement pathway, which has been shown to mediate helminth killing [45, 46]. *Amica1* encodes a JAM transmembrane adhesion molecule that mediates myeloid cell migration and adhesion [47]. Lastly, *Fgf18* is a fibroblast growth factor that induces macrophage infiltration and M2 polarization [48]. Therefore, given their known functions, *Arg1, Fpr-rs5, Fcnb, Fgf18* and *Amica1* are all RELMα-downregulated candidate genes, which could contribute to macrophage migration and adherence to worms.

For the RELMα-upregulated genes, we observed the matrix metalloproteinase *Mmp19* and the platelet-derived growth factor receptor *Pdgfra*. These genes encode factors associated with

tissue repair, in line with RELMα's proposed role in this process [49], therefore RELMα induction of these *in vivo* may contribute to enhanced lung tissue repair following *Nb*-induced acute injury [50-52]. RELMα also induced genes associated with cell survival, such as the apoptosis inhibitor *Bcl2* and Tm7sf3 [53]. TM7SF3 is a seven-span transmembrane protein that protects from cellular stress and the unfolded protein response. Increased activation of this protein by RELMα may therefore promote cell survival. These findings are consistent with a previous study showing that RELMα inhibits apoptosis [11], and suggest that RELMα preserves macrophage longevity. There are currently no known membrane receptors for RELMα, and future studies could investigate if RELMα binds TM7SF3 or a protein associated with this receptor. RELMα also induced expression of *Btg2*, p53-regulated gene associated with inhibiting proliferation [54]. This is contrary to previous studies showing that RELMα induces proliferation of endothelial and smooth muscle cell lines [55, 56], however, the RELMα effects examined here were specifically in primary macrophages, which may explain these differences. Intriguingly, RELMα upregulated expression of *Rgs1*, a G-protein signaling regulator molecule, which has been demonstrated to reduce chemotaxis and dampen chemokine receptor signaling in macrophages and decrease integrin-dependent adhesion in B cells [57]. Together, our results suggest that RELMα inhibits macrophage proliferation, promotes macrophage survival and desensitizes macrophage effector functions. Further functional studies are needed to confirm these possibilities; however, these gene expression analyses provide a useful foundation and candidate genes for investigation of the RELMα receptor and downstream signaling.

An interesting observation made in the co-culture assay was that *Nb* L3 cultured with WT macrophages were more motile and viable compared to *Nb* L3 alone. The improved fitness and activity of *Nb* L3 when cultured with WT cells could indicate that the worms require cues from the

host for their activity and development. Studies of schistosomes have shown that the flukes require signals from host adaptive cells for their proper development [58-60]. Similarly, it is possible that the hookworms interact with and respond to host cells such as macrophages for their development. We found that *Nb* cultured with RELMα$^{-/-}$ cells are less motile and viable compared to *Nb* with WT cells or *Nb* alone. This result could be due to significantly more immune cell damage to worms in the absence of RELMα. Our work is corroborated by previously published data that highlight the importance of macrophages and not dendritic cells in maintaining immunity to helminths [39]. However, in this study, macrophages were identified as CD11b^{+} cells and dendritic cells were identified as CD11c^{+} cells. In the *Nb*-infected lung, we found that macrophages co-express CD11c^{+} and CD11b^{+}. One caveat of our methodology is that by purifying CD11c^{+} cells, we select for CD11c^{mid} lung macrophages and CD11c^{hi} dendritic cells. However, we find that alveolar macrophages are in higher frequency than dendritic cells in the lung and are the dominant cellular source of RELMα.

Given the results of the co-culture assay, we postulated that *Nb* isolated from RELMα$^{-/-}$ lungs would have decreased fitness compared to WT mice. Length and width measurements of *Nb* confirmed this as worms from RELMα$^{-/-}$ mouse lungs were smaller in size. These data highlight the significance of the lung immune response against the worm in weakening the parasite before it reaches the gut. We and others show that fewer adult *Nb* are recovered from the intestines of RELMα$^{-/-}$ mice compared to WT mice [19, 21]. A recent publication was the first to show that *Nb* L3 feed on host red blood cells when in the lung and suggested that disrupting this feeding would lead to developmental arrest of the worm. Given the level of obstruction we see in co-culture assays where RELMα$^{-/-}$ cells bind to and paralyze *Nb*, it is a possibility, that these L3s are then unable to feed and therefore suffer growth arrest [61]. This is in line with our *ex vivo* observation that L4 recovered from RELMα$^{-/-}$ mice seem developmentally impaired compared to those isolated from

WT mice. Our data suggests that macrophages in the absence of RELMα damage the worm or prevent worm feeding leading to a functional impact on worm fitness and fecundity in the intestine.

In addition to high expression in the lung by hematopoietic and non-hematopoietic, RELMα derived from hematopoietic cells is also significantly increased in the blood of *Nb*-infected mice, and may modulate circulating immune cell function. Previous studies have shown that helminth infection-induced AAMacs can differentiate in the tissue, but also arise from circulating blood monocytes [62]. In addition to the regulatory effects of RELMα on the macrophages in the lung, it is also possible that RELMα may exert regulatory effects on blood monocyte-derived AAMacs that then infiltrate the infected lung and small intestine with potential functional consequences on worm killing or tissue inflammation. Indeed, we observed increased submucosal intestinal inflammation in the BM RELMα$^{-/-}$ and RELMα$^{-/-}$ mice, suggesting a regulatory role for RELMα in the intestine. The tissue-specific localization of macrophages, and the life cycle stage of the worm, may however determine their direct or indirect effects on the worm. *Nb* L3 and L4 are present in the blood and lung respectively, therefore are more likely to interact with macrophages. In contrast *Nb* adults reside in the intestinal lumen, and expulsion is dependent on several non immune cells such as epithelial and smooth muscle cells that are nevertheless instructed by immune cells such as macrophages. Comparing RELMα's functional effects on blood macrophages or intestinal macrophages *vs.* lung macrophages could provide a more comprehensive understanding of the function of this pleiotropic molecule at different *Nb* life cycle stages.

In conclusion, our studies utilize BM chimeras and macrophage-worm co-culture assays to show that RELMα derived from macrophages downregulates *Nb*-induced inflammatory responses and subsequent *Nb* clearance partly by direct inhibition of macrophage-worm interactions. Macrophage-derived RELMα is therefore an immunomodulatory molecule that protects the host from an uncontrolled Th2 inflammatory immune response at the cost of killing parasitic worms.

Delineating the protective versus pathogenic pathways triggered by macrophage-derived RELMα could provide therapeutic insight into tipping the balance towards host protective immunity against hookworms.

References

1. Urban, J. F., Katona, I. M., Paul, W. E., Finkelman, F. D. (1991) Interleukin 4 is important in protective immunity to a gastrointestinal nematode infection in mice. Proc Natl Acad Sci U S A 88, 5513-7.

2. Finkelman, F. D., Shea-Donohue, T., Morris, S. C., Gildea, L., Strait, R., Madden, K. B., Schopf, L., Urban, J. F. (2004) Interleukin-4- and interleukin-13-mediated host protection against intestinal nematode parasites. Immunol Rev 201, 139-55.

3. Grencis, R. K. (2015) Immunity to helminths: resistance, regulation, and susceptibility to gastrointestinal nematodes. Annu Rev Immunol 33, 201-25.

4. Nono, J. K., Ndlovu, H., Abdel Aziz, N., Mpotje, T., Hlaka, L., Brombacher, F. (2017) Interleukin-4 receptor alpha is still required after Th2 polarization for the maintenance and the recall of protective immunity to Nematode infection. PLoS Negl Trop Dis 11, e0005675.

5. Chen, F., Liu, Z., Wu, W., Rozo, C., Bowdridge, S., Millman, A., Van Rooijen, N., Urban, J. F., Wynn, T. A., Gause, W. C. (2012) An essential role for TH2-type responses in limiting acute tissue damage during experimental helminth infection. Nat Med 18, 260-6.

6. Gause, W. C., Wynn, T. A., Allen, J. E. (2013) Type 2 immunity and wound healing: evolutionary refinement of adaptive immunity by helminths. Nat Rev Immunol 13, 607-14.

7. Novak, M. L. and Koh, T. J. (2013) Macrophage phenotypes during tissue repair. J Leukoc Biol 93, 875-81.

8. Chiaramonte, M. G., Cheever, A. W., Malley, J. D., Donaldson, D. D., Wynn, T. A. (2001) Studies of murine schistosomiasis reveal interleukin-13 blockade as a treatment for established and progressive liver fibrosis. Hepatology 34, 273-82.

9. Fallon, P. G., Emson, C. L., Smith, P., McKenzie, A. N. (2001) IL-13 overexpression predisposes to anaphylaxis following antigen sensitization. J Immunol 166, 2712-6.

10. Gause, W. C., and Artis, David, eds. (2015) The Th2 Type Immune Response in Health and Disease: From Host Defense and Allergy to Metabolic Homeostasis and Beyond. Springer.

11. Holcomb, I. N., Kabakoff, R. C., Chan, B., Baker, T. W., Gurney, A., Henzel, W., Nelson, C., Lowman, H. B., Wright, B. D., Skelton, N. J., Frantz, G. D., Tumas, D. B., Peale, F. V., Shelton, D. L., Hébert, C. C. (2000) FIZZ1, a novel cysteine-rich secreted protein associated with pulmonary inflammation, defines a new gene family. EMBO J 19, 4046-55.

12. Steppan, C. M., Brown, E. J., Wright, C. M., Bhat, S., Banerjee, R. R., Dai, C. Y., Enders, G. H., Silberg, D. G., Wen, X., Wu, G. D., Lazar, M. A. (2001) A family of tissue-specific resistin-like molecules. Proc Natl Acad Sci U S A 98, 502-6.

13. Nair, M. G., Du, Y., Perrigoue, J. G., Zaph, C., Taylor, J. J., Goldschmidt, M., Swain, G. P., Yancopoulos, G. D., Valenzuela, D. M., Murphy, A., Karow, M., Stevens, S., Pearce, E. J., Artis, D. (2009) Alternatively activated macrophage-derived RELM-{alpha} is a negative regulator of type 2 inflammation in the lung. J Exp Med 206, 937-52.

14. Munitz, A., Waddell, A., Seidu, L., Cole, E. T., Ahrens, R., Hogan, S. P., Rothenberg, M. E. (2008) Resistin-like molecule alpha enhances myeloid cell activation and promotes colitis. J Allergy Clin Immunol 122, 1200-1207.e1.

15. Munitz, A., Seidu, L., Cole, E. T., Ahrens, R., Hogan, S. P., Rothenberg, M. E. (2009) Resistin-like molecule alpha decreases glucose tolerance during intestinal inflammation. J Immunol 182, 2357-63.

16. Bokarewa, M., Nagaev, I., Dahlberg, L., Smith, U., Tarkowski, A. (2005) Resistin, an adipokine with potent proinflammatory properties. J Immunol 174, 5789-95.

17. Munitz, A., Cole, E. T., Karo-Atar, D., Finkelman, F. D., Rothenberg, M. E. (2012) Resistin-like molecule-α regulates IL-13-induced chemokine production but not allergen-induced airway responses. Am J Respir Cell Mol Biol 46, 703-13.

18. Dong, L., Wang, S. J., Camoretti-Mercado, B., Li, H. J., Chen, M., Bi, W. X. (2008) FIZZ1 plays a crucial role in early stage airway remodeling of OVA-induced asthma. J Asthma 45, 648-53.

19. Chen, G., Wang, S. H., Jang, J. C., Odegaard, J. I., Nair, M. G. (2016) Comparison of RELMα and RELMβ Single- and Double-Gene-Deficient Mice Reveals that RELMα Expression Dictates Inflammation and Worm Expulsion in Hookworm Infection. Infect Immun 84, 1100-11.

20. Lee, M. R., Shim, D., Yoon, J., Jang, H. S., Oh, S. W., Suh, S. H., Choi, J. H., Oh, G. T. (2014) Retnla overexpression attenuates allergic inflammation of the airway. PLoS One 9, e112666.

21. Pesce, J. T., Ramalingam, T. R., Wilson, M. S., Mentink-Kane, M. M., Thompson, R. W., Cheever, A. W., Urban, J. F., Wynn, T. A. (2009) Retnla (relmalpha/fizz1) suppresses helminth-induced Th2-type immunity. PLoS Pathog 5, e1000393.

22. Siracusa, M. C., Reece, J. J., Urban, J. F., Scott, A. L. (2008) Dynamics of lung macrophage activation in response to helminth infection. J Leukoc Biol 84, 1422-33.

23. Cook, P. C., Jones, L. H., Jenkins, S. J., Wynn, T. A., Allen, J. E., MacDonald, A. S. (2012) Alternatively activated dendritic cells regulate CD4+ T-cell polarization in vitro and in vivo. Proc Natl Acad Sci U S A 109, 9977-82.

24. Raes, G., De Baetselier, P., Noël, W., Beschin, A., Brombacher, F., Hassanzadeh Gh, G. (2002) Differential expression of FIZZ1 and Ym1 in alternatively versus classically activated macrophages. J Leukoc Biol 71, 597-602.

25. Wills-Karp, M., Rani, R., Dienger, K., Lewkowich, I., Fox, J. G., Perkins, C., Lewis, L., Finkelman, F. D., Smith, D. E., Bryce, P. J., Kurt-Jones, E. A., Wang, T. C., Sivaprasad, U., Hershey, G. K., Herbert, D. R. (2012) Trefoil factor 2 rapidly induces interleukin 33 to promote type 2 immunity during allergic asthma and hookworm infection. J Exp Med 209, 607-22.

26. Esser-von Bieren, J., Mosconi, I., Guiet, R., Piersgilli, A., Volpe, B., Chen, F., Gause, W. C., Seitz, A., Verbeek, J. S., Harris, N. L. (2013) Antibodies trap tissue migrating helminth larvae and prevent tissue damage by driving IL-4Rα-independent alternative differentiation of macrophages. PLoS Pathog 9, e1003771.

27. Tomfohr, J., Lu, J., Kepler, T. B. Pathway level analysis of gene expression using singular value decomposition. BMC Bioinformatics.

28. Nair, M. G., Gallagher, I. J., Taylor, M. D., Loke, P., Coulson, P. S., Wilson, R. A., Maizels, R. M., Allen, J. E. (2005) Chitinase and Fizz family members are a generalized feature of nematode infection with selective upregulation of Ym1 and Fizz1 by antigen-presenting cells. Infect Immun 73, 385-94.

29. Chen, F., Wu, W., Millman, A., Craft, J. F., Chen, E., Patel, N., Boucher, J. L., Urban, J. F., Kim, C. C., Gause, W. C. (2014) Neutrophils prime a long-lived effector macrophage phenotype that mediates accelerated helminth expulsion. Nat Immunol 15, 938-46.

30. Su, Q., Zhou, Y., Johns, R. A. (2007) Bruton's tyrosine kinase (BTK) is a binding partner for hypoxia induced mitogenic factor (HIMF/FIZZ1) and mediates myeloid cell chemotaxis. FASEB J 21, 1376-82.

31. Li, D., Fernandez, L. G., Dodd-o, J., Langer, J., Wang, D., Laubach, V. E. (2005) Upregulation of hypoxia-induced mitogenic factor in compensatory lung growth after pneumonectomy. Am J Respir Cell Mol Biol 32, 185-91.

32. Teng, X., Li, D., Champion, H. C., Johns, R. A. (2003) FIZZ1/RELMα, a Novel Hypoxia-Induced Mitogenic Factor in Lung With Vasoconstrictive and Angiogenic Properties. Circulation Research 92, 1065.

33. Gao, J. L., Chen, H., Filie, J. D., Kozak, C. A., Murphy, P. M. (1998) Differential expansion of the N-formylpeptide receptor gene cluster in human and mouse. Genomics 51, 270-6.

34. Turnbull, I. R., Gilfillan, S., Cella, M., Aoshi, T., Miller, M., Piccio, L., Hernandez, M., Colonna, M. (2006) Cutting edge: TREM-2 attenuates macrophage activation. J Immunol 177, 3520-4.

35. Harvie, M., Camberis, M., Tang, S. C., Delahunt, B., Paul, W., Le Gros, G. (2010) The lung is an important site for priming CD4 T-cell-mediated protective immunity against gastrointestinal helminth parasites. Infect Immun 78, 3753-62.

36. Thawer, S. G., Horsnell, W. G., Darby, M., Hoving, J. C., Dewals, B., Cutler, A. J., Lang, D., Brombacher, F. (2014) Lung-resident $CD4^+$ T cells are sufficient for IL-4Rα-dependent recall immunity to Nippostrongylus brasiliensis infection. Mucosal Immunol 7, 239-48.

37. Horsnell, W. G., Darby, M. G., Hoving, J. C., Nieuwenhuizen, N., McSorley, H. J., Ndlovu, H., Bobat, S., Kimberg, M., Kirstein, F., Cutler, A. J., Dewals, B., Cunningham, A. F., Brombacher, F. (2013) IL-4Rα-associated antigen processing by B cells promotes immunity in Nippostrongylus brasiliensis infection. PLoS Pathog 9, e1003662.

38. Nair, M. G. and Herbert, D. R. (2016) Immune polarization by hookworms: taking cues from T helper type 2, type 2 innate lymphoid cells and alternatively activated macrophages. Immunology 148, 115-24.

39. Borthwick, L. A., Barron, L., Hart, K. M., Vannella, K. M., Thompson, R. W., Oland, S., Cheever, A., Sciurba, J., Ramalingam, T. R., Fisher, A. J., Wynn, T. A. (2016) Macrophages are critical to the maintenance of IL-13-dependent lung inflammation and fibrosis. Mucosal Immunol 9, 38-55.

40. Zhao, A., Urban, J. F., Anthony, R. M., Sun, R., Stiltz, J., van Rooijen, N., Wynn, T. A., Gause, W. C., Shea-Donohue, T. (2008) Th2 cytokine-induced alterations in intestinal smooth muscle function depend on alternatively activated macrophages. Gastroenterology 135, 217-225.e1.

41. Loke, P., Nair, M. G., Parkinson, J., Guiliano, D., Blaxter, M., Allen, J. E. (2002) IL-4 dependent alternatively-activated macrophages have a distinctive in vivo gene expression phenotype. BMC Immunol 3, 7.

42. Artis, D., Wang, M. L., Keilbaugh, S. A., He, W., Brenes, M., Swain, G. P., Knight, P. A., Donaldson, D. D., Lazar, M. A., Miller, H. R., Schad, G. A., Scott, P., Wu, G. D. (2004) RELMbeta/FIZZ2 is a goblet cell-specific immune-effector molecule in the gastrointestinal tract. Proc Natl Acad Sci U S A 101, 13596-600.

43. Herbert, D. R., Yang, J. Q., Hogan, S. P., Groschwitz, K., Khodoun, M., Munitz, A., Orekov, T., Perkins, C., Wang, Q., Brombacher, F., Urban, J. F., Rothenberg, M. E., Finkelman, F. D. (2009) Intestinal epithelial cell secretion of RELM-beta protects against gastrointestinal worm infection. J Exp Med 206, 2947-57.

44. Le, Y., Murphy, P. M., Wang, J. M. (2002) Formyl-peptide receptors revisited. Trends Immunol 23, 541-8.

45. Endo, Y., Iwaki, D., Ishida, Y., Takahashi, M., Matsushita, M., Fujita, T. (2012) Mouse ficolin B has an ability to form complexes with mannose-binding lectin-associated serine

proteases and activate complement through the lectin pathway. J Biomed Biotechnol 2012, 105891.

46. Bonne-Année, S., Kerepesi, L. A., Hess, J. A., O'Connell, A. E., Lok, J. B., Nolan, T. J., Abraham, D. (2013) Human and mouse macrophages collaborate with neutrophils to kill larval Strongyloides stercoralis. Infect Immun 81, 3346-55.

47. Guo, Y. L., Bai, R., Chen, C. X., Liu, D. Q., Liu, Y., Zhang, C. Y., Zen, K. (2009) Role of junctional adhesion molecule-like protein in mediating monocyte transendothelial migration. Arterioscler Thromb Vasc Biol 29, 75-83.

48. Wei, W., Mok, S. C., Oliva, E., Kim, S. H., Mohapatra, G., Birrer, M. J. (2013) FGF18 as a prognostic and therapeutic biomarker in ovarian cancer. J Clin Invest 123, 4435-48.

49. Knipper, J. A., Willenborg, S., Brinckmann, J., Bloch, W., Maaß, T., Wagener, R., Krieg, T., Sutherland, T., Munitz, A., Rothenberg, M. E., Niehoff, A., Richardson, R., Hammerschmidt, M., Allen, J. E., Eming, S. A. (2015) Interleukin-4 Receptor α Signaling in Myeloid Cells Controls Collagen Fibril Assembly in Skin Repair. Immunity 43, 803-16.

50. Caley, M. P., Martins, V. L., O'Toole, E. A. (2015) Metalloproteinases and Wound Healing. Adv Wound Care (New Rochelle) 4, 225-234.

51. Liu, T., Yu, H., Ullenbruch, M., Jin, H., Ito, T., Wu, Z., Liu, J., Phan, S. H. (2014) The in vivo fibrotic role of FIZZ1 in pulmonary fibrosis. PLoS One 9, e88362.

52. Horikawa, S., Ishii, Y., Hamashima, T., Yamamoto, S., Mori, H., Fujimori, T., Shen, J., Inoue, R., Nishizono, H., Itoh, H., Majima, M., Abraham, D., Miyawaki, T., Sasahara, M. (2015) PDGFRα plays a crucial role in connective tissue remodeling. Sci Rep 5, 17948.

53. Isaac, R., Goldstein, I., Furth, N., Zilber, N., Streim, S., Boura-Halfon, S., Elhanany, E., Rotter, V., Oren, M., Zick, Y. (2017) TM7SF3, a novel p53-regulated homeostatic factor, attenuates cellular stress and the subsequent induction of the unfolded protein response. Cell Death Differ 24, 132-143.

54. Rouault, J. P., Falette, N., Guéhenneux, F., Guillot, C., Rimokh, R., Wang, Q., Berthet, C., Moyret-Lalle, C., Savatier, P., Pain, B., Shaw, P., Berger, R., Samarut, J., Magaud, J. P., Ozturk, M., Samarut, C., Puisieux, A. (1996) Identification of BTG2, an antiproliferative p53-dependent component of the DNA damage cellular response pathway. Nat Genet 14, 482-6.

55. Yamaji-Kegan, K., Takimoto, E., Zhang, A., Weiner, N. C., Meuchel, L. W., Berger, A. E., Cheadle, C., Johns, R. A. (2014) Hypoxia-induced mitogenic factor (FIZZ1/RELMα) induces endothelial cell apoptosis and subsequent interleukin-4-dependent pulmonary hypertension. Am J Physiol Lung Cell Mol Physiol 306, L1090-103.

56. Tong, Q., Zheng, L., Li, B., Wang, D., Huang, C., Matuschak, G. M., Li, D. (2006) Hypoxia-induced mitogenic factor enhances angiogenesis by promoting proliferation and migration of endothelial cells. Exp Cell Res 312, 3559-69.

57. Patel, J., McNeill, E., Douglas, G., Hale, A. B., de Bono, J., Lee, R., Iqbal, A. J., Regan-Komito, D., Stylianou, E., Greaves, D. R., Channon, K. M. (2015) RGS1 regulates myeloid cell accumulation in atherosclerosis and aortic aneurysm rupture through altered chemokine signalling. Nat Commun 6, 6614.

58. Lamb, E. W., Crow, E. T., Lim, K. C., Liang, Y. S., Lewis, F. A., Davies, S. J. (2007) Conservation of CD4+ T cell-dependent developmental mechanisms in the blood fluke pathogens of humans. Int J Parasitol 37, 405-15.

59. Riner, D. K., Ferragine, C. E., Maynard, S. K., Davies, S. J. (2013) Regulation of innate responses during pre-patent schistosome infection provides an immune environment permissive for parasite development. PLoS Pathog 9, e1003708.

60. Lamb, E. W., Walls, C. D., Pesce, J. T., Riner, D. K., Maynard, S. K., Crow, E. T., Wynn, T. A., Schaefer, B. C., Davies, S. J. (2010) Blood fluke exploitation of non-cognate CD4+ T cell help to facilitate parasite development. PLoS Pathog 6, e1000892.

61. Bouchery, T., Filbey, K., Shepherd, A., Chandler, J., Patel, D., Schmidt, A., Camberis, M., Peignier, A., Smith, A. A. T., Johnston, K., Painter, G., Pearson, M., Giacomin, P., Loukas, A., Bottazzi, M. E., Hotez, P., LeGros, G. (2018) A novel blood-feeding detoxification pathway in Nippostrongylus brasiliensis L3 reveals a potential checkpoint for arresting hookworm development. PLoS Pathog 14, e1006931.

62. Harris, N. L. and Loke, P. (2017) Recent Advances in Type-2-Cell-Mediated Immunity: Insights from Helminth Infection. Immunity 47, 1024-1036.

CHAPTER THREE - Host and Helminth-Derived Endocannabinoids are Generated During Infection with Effects on Host Immunity.

Hashini M. Batugedara[1], Donovan Argueta[2], Jessica C. Jang2, Dihong Lu[3], Marissa Macchietto[4], Jaspreet Kaur[2], Shaokui Ge[2], Adler R. Dillman[3], Nicholas V. DiPatrizio[2] and Meera G. Nair[2]

[1]Department of Microbiology, University of California Riverside, Riverside, CA, USA

[2]Division of Biomedical Sciences, University of California Riverside, Riverside, CA USA

[3]Department of Nematology, University of California Riverside, Riverside, CA USA

[4]Institute of Health Informatics, University of Minnesota Twin Cities, MN, USA

A version of this chapter was published in *Infection and Immunity*, 2018.

Abstract

Helminths have co-evolved with their hosts resulting in the development of specialized host immune mechanisms and parasite-specific regulatory products. Identification of new pathways that regulate helminth infection could provide a better understanding of host-helminth interaction and may identify new therapeutic targets for helminth infection. Here we identify the endocannabinoid system as a new mechanism that influences host immunity to helminths. Endocannabinoids are lipid-derived signaling molecules that control important physiologic processes such as feeding behavior and metabolism. Following murine infection with *Nippostrongylus brasiliensis* (*Nb*), an intestinal nematode with a similar life cycle to hookworms, we observed increased levels of endocannabinoids (2-AG, AEA) and the endocannabinoid-like molecule OEA in the infected lung and intestine. To investigate endocannabinoid function in helminth infection, we employed pharmacological inhibitors of cannabinoid subtype receptor 1 and 2 (CB_1R and CB_2R). Compared to vehicle-treated mice, inhibition of CB_1R but not CB_2R resulted in increased *Nb* worm burden and egg output, associated with significantly decreased expression of T helper type 2 cytokine IL-5 in intestinal tissue and splenocyte cultures. Strikingly, bioinformatic analysis of genomic and RNA-seq datasets identified putative genes encoding endocannabinoid biosynthetic and degradative enzymes in many parasitic nematodes. To test the novel hypothesis that helminth parasites produce their own endocannabinoids, we measured endocannabinoid levels in *Nb* by mass spectrometry and quantitative PCR and found that *Nb* parasites produced endocannabinoids, especially at the infectious larval stage. To our knowledge, this is the first report of helminth and host-derived endocannabinoids that promote host immune responses and reduce parasite burden.

Introduction

Parasitic helminths infect an estimated two billion individuals worldwide [1]. Although helminth infection is not typically fatal, it is associated with a multitude of pathologic conditions including malnutrition and growth retardation. A majority of soil-transmitted helminths reside in the gastrointestinal tract, where they can negatively impact the host's nutritional status by stealing nutrients, or prevent nutrient absorption by damaging or causing inflammation of the intestinal tissue [2]. Additionally, recent studies have identified new mechanisms by which helminths impact host feeding and metabolism [3]. Gastrointestinal helminth infection was reported to decrease food intake [4], and was beneficial in high fat diet-fed mice, where it improves glucose metabolism and reduces adiposity [5, 6]. This effect was partly mediated through T helper type 2 (Th2) cytokine-activated M2 macrophages in the adipose tissue, which have a known beneficial effect in metabolic homeostasis [7]. In the intestine, helminth infection induced a Th2 cytokine-dependent expansion of tuft cells, which express taste receptors, and cholecystokinin (CCK)-positive enteroendocrine cells, which secrete hormones that regulate feeding behavior [8]. Overall, these findings support a multifactorial relationship between helminth and host immune response that affects host feeding behavior and metabolism. Identification of new helminth or host-derived factors that regulate this process, and how they affect host health and helminth killing, could provide a better understanding of the pathologic or beneficial effects of helminth infection that could be exploited therapeutically.

Among the many host-derived molecules that affect feeding and metabolism, endocannabinoids are an important class of lipid molecules that regulate these physiologic processes [9, 10]. Endocannabinoids are the body's natural cannabis-like molecules that signal through cannabinoid receptors, which are highly expressed on neurons [11]. Unsurprisingly, a highly recognized function of endocannabinoids is promoting neural-mediated behaviors such as food intake and reward [9]. Endocannabinoids, however, are generated throughout the body, and

cannabinoid receptors are present on extra-neuronal cells, including intestinal epithelial cells and immune cells [12-14]. Signaling by the endocannabinoids, 2-arachidonoylglycerol (2-AG) or anandamide (AEA), through cannabinoid receptors on intestinal cells impacts feeding behavior [15, 16], while signaling on immune cells can promote anti-inflammatory pathways [17]. Despite functional effects on intestinal physiology and immune responses, no studies reported to date have investigated the role of endocannabinoids in parasite infection.

In this study, we investigated the expression and function of endocannabinoids in murine infection with *Nippostrongylus brasiliensis* (*Nb*), a rodent nematode parasite that shares a similar life cycle to human hookworms [18]. We show that *Nb* infection significantly induces the biosynthesis of endocannabinoids and endocannabinoid-like molecules in the infected lung and intestine. We also performed functional assays to measure endocannabinoid biosynthetic and degradative enzyme activity in the infected jejunal tissue, and observed significantly increased endocannabinoid synthetic but not degradative enzyme activity. Endocannabinoid levels were negatively correlated with early infection-induced weight loss, associated with reduced food intake, and *Nb* egg output, suggesting that endocannabinoids are associated with improved host immunity. To test this hypothesis, we employed validated peripheral pharmacologic inhibitors of the cannabinoid subtype 1 receptor (CB_1R) and CB_2R, AM6545 and AM630 respectively, which act peripherally and do not cross the blood-brain barrier [16, 19]. Pharmacologic inhibition of CB_1R, but not CB_2R, significantly increased *Nb* worm burdens and fecal egg output. Increased parasite burden was associated with reduced Th2 cytokines (IL-5 and IL-4), but not Th1 cytokine IFNγ, suggesting that *Nb*-induced endocannabinoid signaling through CB_1R was important for optimal host Th2 immune responses. Strikingly, bioinformatic analyses of the genomes and RNA-seq datasets from *Nb* and other parasitic nematodes, including hookworms *Ancylostoma ceylanicum* and *Necator americanus*, revealed putative genes encoding endocannabinoid synthetic and

degradative enzymes. We validated the bioinformatic predictions in *Nb* by quantitative real-time PCR and mass spectrometry, and showed that *Nb* produces endocannabinoids at all life cycle stages. Taken together, these studies report for the first time the production of endocannabinoids by parasitic helminths, and suggest that helminth infection-induced endocannabinoids functionally influence the host immune response and parasite burden. These findings support a new area of investigation into the function of the endocannabinoid system in infectious diseases.

Materials and Methods

Parasite

Nippostrongylus brasiliensis life cycle was maintained in Sprague-Dawley rats, as previously described [20, 21]. Hatched infectious L3 larvae were recovered from 1-2-week-old fecal egg cultures by a Baermann apparatus. L4 larvae were recovered from lung tissue of day 2-infected rats by manual picking from coarsely minced lung tissue in media after 2h incubation at 37°C. Adult *Nb* parasites were recovered from day 6-8 *Nb* infected rat by dissection and slitting of the whole small intestine, followed by 2h incubation in warm PBS and manual picking of the worms from the intestinal tissue or supernatant. Eggs in the feces of infected mice and rats were counted using a McMaster counting chamber. For endocannabinoid quantification, parasites were washed 3x in excess PBS, counted and weighed.

Mice and tissue recovery

C57BL/6 mice were purchased from the Jackson Laboratory or bred in-house. All mice in the experiment were age-matched (6-8 week old) males and females housed in a specific pathogen free facility. Mice were anesthetized with isoflurane and injected subcutaneously with 500 *Nb* L3 larvae. Behavior was assessed using single-housing units (TSE Systems, Chesterfield, MO, USA). Mice were placed into units 3 days prior to recording for acclimation and daily feeding was monitored using Phenomaster software (TSE Systems). Where indicated, mice were treated intraperitoneally with vehicle control (7.5% DMSO, 7.5% Tween80, 85% Saline), CB_1R antagonist AM6545 (10mg/kg), or CB_2R antagonist AM630 (10mg/kg). Blood recovery was done by cardiac puncture into tubes containing 7.2 mg EDTA. Following excision of the small intestine, mucosa was stripped and recovered for endocannabinoid quantification. 1cm jejunal tissues were weighed and homogenized in 0.5mL PBS with Mini-Beadbeater-96 (BioSpec Products) at 4^{o}C, and supernatants

was collected after centrifugation (4000*g* for 15min at 4ºC) for cytokine quantification. All protocols for animal use and euthanasia were approved by the University of California, Riverside Institutional Animal Care and Use Committee (https://or.ucr.edu/ori/committees/iacuc.aspx; protocol A-20150028E and A-20170036) and were in accordance with the National Institutes of Health Guidelines. Animal studies are in accordance with the provisions established by the Animal Welfare Act and the Public Health Servies (PHS) Policy on the Humane Care and Use of Laboratory Animals.

Lipid extraction and FAEs and MAGs analysis

Lipid extraction and analysis were performed as previously described [16, 22]. Briefly, frozen tissue or worms (2,000 L3/sample; 400 L4/sample; 100 Adults/sample) were homogenized in 1.0mL of methanol solution containing the internal standards, [$^2H_5$] 2-AG, [$^2H_4$]-AEA, [$^2H_4$]-OEA (Cayman Chemical, Ann Arbor, MI, USA). Lipids were extracted with chloroform (2mL) and washed with water (1mL). Lipids were similarly extracted from plasma samples, with the exception of a 0.9 % saline wash replacing water (0.1mL plasma at the expense of saline). Organic phases were collected and separated by open-bed silica gel column chromatography as previously described [15]. Eluate was gently dried under N_2 stream (99.998% pure) and resuspended in 0.1mL of methanol:chloroform (9:1), with 1µL injection for ultra-performance liquid chromatography/tandem mass spectrometry (UPLC/MS/MS) analysis.

Data was acquired using an Acquity I Class UPLC with in-line connection to a Xevo TQ-S Micro Triple Quadrapole Mass Spectrometer (Waters Corporation, Milford, MA, USA) with electrospray ionization (ESI) sample delivery. Lipids were quantified using a stable isotope dilution method detecting proton or sodium adducts of the molecular ions $[M + H/Na]^+$ in multiple reaction monitoring (MRM) mode. Extracted ion chromatograms for MRM transitions were used to quantify

analytes: 2-AG (*m/z* = 379.3 > 287.3), 2-DG (*m/z* = 403.3 > 311.2), AEA (*m/z* = 348.3 > 62.0), OEA (*m/z* = 326.4 > 62.1), DHEA, (*m/z* = 372.3 > 62.0), 19:2 MAG (*m/z* = 386.4 > 277.2), with [$^2H_5$]-2-AG (*m/z* = 384.3 > 93.4), [$^2H_4$]-AEA (*m/z* = 352.4 > 66.1), and [$^2H_4$]-OEA (*m/z* = 330.4 > 66.0) as internal standards. Controls included one "blank" sample that was processed and analyzed in the same manner as all samples, except no tissue was included. This control revealed no detectable endocannabinoids and related lipids included in our analysis.

Functional enzyme assays of DGL and MGL activity

Free-fatty acid measurements: Data for free fatty acids (19:2 FFA, product of MGL assay) were measured using the UPLC/MS/MS instrument as described above. Mobile phase compositions for 19:2 FFA were the same as above, but the flow gradient began at flow rate 0.4 mL/min: 90% Methanol 0.1 min, 90% to 100% methanol 0.1 to 2.0 mins, 100% methanol 2.0 to 2.1 mins, 100% to 90% methanol 2.1 to 2.2 mins, and 90% methanol 2.2 to 2.5 mins. 19:2 MAG, product of DGL assay, was analyzed exactly as described above as for other MAGs. MS detection of fatty acids was in negative ion mode with capillary voltage maintained at 1.10 kV. Cone voltages for respective analytes: 19:2 FFA = 48v; 17:1 FFA = 64v. Lipids were quantified using a dilution series detecting deprotonated molecular ions $[23]^-$ in selected ion recording (SIR) mode. Extracted ion chromatograms for SIR masses were used to quantify the analytes: 19:2 FFA (*m/z* = 293.3) and the internal standard 17:1 FFA (*m/z* = 267.2).

Tissue Preparation: Intestinal epithelium was collected as described above and approximately 100 mg of frozen tissue was homogenized in 2 mL of ice-cold 50mM Tris-HCl, 320mM sucrose (pH 7.5) buffer. Homogenates were centrifuged at 800*g* for 10 min while kept at 4^{o}C and supernatant collected. Protein supernatants were sonicated twice for 10s and then freeze-thawed in liquid

nitrogen twice. Samples were spun again, as described above, and supernatant was quantified with BCA assay and diluted with Tris-HCl/sucrose buffer.

DGL activity assay: 25 µg tissue homogenates, in 0.1mL Tris-HCl/sucrose (pH7.5), were incubated with 0.3 µM JZL184 [MGL inhibitor; Cayman Chemical, Ann Arbor, Michigan [24]] and accompanying treatments for 10min at room temperature. Homogenates were incubated with 0.1mL solution of Tris-HCL with 0.2% Triton X-100 (pH 7.0) containing 20 nmol dinonadecadienoin (Nu-Chek Prep, Waterville, MN; final volume 0.2mL/reaction) at 37°C for 30 min. Reaction was stopped by adding 1 mL of MeOH containing 25 pmol [$^2H_5$]-2-AG. Lipids were extracted as described above an analyzed via UPLC/MS/MS.

MGL activity assay: 10 µg tissue homogenates, in 0.1 mL Tris-HCl/sucrose (pH 7.5) were incubated with 0.4mL solution of Tris-HCL with 0.1% BSA (pH 8.0) containing 50 nmol nonadecadienoin (Nu-Chek Prep; final volume 0.5mL/reaction) at 37°C for 10 min. Reaction was stopped by adding 1 mL of MeOH containing 10 nmol heptadecanoic acid (Nu-Chek Prep). Lipids were extracted as described above and analyzed via UPLC/MS/MS.

Cytokine quantification

ELISA: IL-5 cytokine quantification of intestinal homogenate and spleen supernatants was performed by standard sandwich ELISA according to previously described protocols [20].

Cytokine Bead Array: IL-4, IFNγ and IL-10 cytokine quantification was performed on intestinal homogenate and supernatants from 72h-stimulated splenocytes ($5x10^6$/well, 0.5µg/mL αCD3 and αCD28) using the TH1/TH2 CBA assay (BD Biosciences) according to manufacturer's instructions.

RNA quantification

Mouse tissue recovered for RNA extraction was first incubated overnight in RNAlater (Qiagen) at 4˚C then extracted by TRIzol (Life Technologies). iScript Reverse Transcriptase (Biorad) was used for cDNA synthesis. Real-time PCR was performed using iTaq Universal SYBR Green Supermix (Bio-Rad) and the Biorad CFX Connect. 18S primers were purchased from Qiagen, and *Cnr1* and *Cnr2* primers were purchased from Biorad.

L3 infective juveniles (3 replicates of 500~1000 L3) were collected from cultured rat fecal plates. L4 worms (3 replicates of 100-500 L4) were collected from dissected lungs of infected rats 2 days post infection. Adult worms (3 replicates of 100-200 adult worms) were collected from dissected intestines of infected rats. Worms were washed in ddH20, flash-frozen, then homogenized in RiboZol (VWR) using pellet pestles and pestle motor (Fisher Scientific and VWR). RNA was extracted according to RiboZol manufacturer instructions. Reverse transcription was done using ProtoScript II Reverse Transcriptase (NEB), followed by real-time PCR as above. Primer sequences were as follows: *Nb Actin* (F-ACGACGTGGCAGCTCTCGTTGTGG, R-GGTGCTTCGGTCAGCAGCACGGGA), *Nb-Faah*-(F-TCGGAGCAGGTGTTGTGAAGA, R-AGCCGGTACCACGGATCTGA), *Nape* (F-GGCGTACAGTCCACGATGGTT, R-GGTGCTTCGGCTCGAGGTAG).

Gene orthology analysis and protein alignment

To identify enzymes and regulatory proteins involved in lipolysis and endocannabinoid signaling we leveraged previously identified orthologs in *C. elegans* [49-52]. WormBase ParaSite (version WBPS9) was consulted to identify putative orthologs of these genes in several parasitic nematodes. To validate the putative parasitic nematode orthologs, we performed an orthology analysis using available predicted protein datasets from WormBase release WSPS9 — *Ancylostoma ceylanicum*,

Ancylostoma duodenale, *Ascaris lumbricoides*, *Ascaris suum*, *C. elegans*, *Necator americanus*, *N. brasiliensis*, *Steinernema carpocapsae*, *Strongyloides ratti*, *Strongyloides stercoralis*, and *Toxocara canis*. Version 1.4 of the OrthoMCL pipeline was used to cluster proteins into families of orthologous genes, with default settings and the BLAST parameters recommended in the OrthoMCL documentation [25].

The NAPE-PLD gene was further explored by aligning the sequence of mouse NAPE-PLD and the putative homolog from *N. brasiliensis*. Protein sequences were aligned using MUSCLE [26] and visualized using Mesquite (version 3.2). The accession numbers of the proteins used are NP_848843 for the mouse NAPE-PLD from GenBank and NBR_0001270801-mRNA-1 for the Nb NAPE-PLD from WormBase ParaSite. The B_2 lactamase domain in the alignment was identified using Smart protein database [27].

Gene expression analysis

To determine if genes for the endocannabinoid system are expressed in other parasitic nematodes, we downloaded the RNA-seq data for *T. canis* [28] (SRR1707010, SRR1707031-6), *S. ratti* [29] (ERR299168-79, ERR225783-4), *S. stercoralis* [30] (ERR146945-6, ERR146948-9), *A. suum* [31] (SRR851186-95), *N. americanus* [32] (SRR609895, SRR609951), *N. brasiliensis* [33]; PRJEB16076, and *A. ceylanicum* [34] (SRR1124912-4, SRR1124985-6) from NCBI. The published RNA-seq data for *N. brasiliensis* was downloaded from European Nucleotide Archive (http://www.ebi.ac.uk/). The reads were mapped to each species' indexed transcriptome (downloaded from WormBase ParaSite, WSPS9) with bowtie 1.0.0 in paired-end mode with the following settings: bowtie –X 800 -m 200 -S --seedlen 25 –trim3 [50 or 100] -n 2 --offrate 1 [35]. Gene expression was quantified with RSEM version 1.2.31 [36].

Statistical Analysis

Graphpad Prism software was used for statistical analyses. Where appropriate, student's t-test (for normal distribution data), one-way ANOVA (for analysis of of more than two groups), two-way ANOVA (for analysis of more than one experiment), linear regression and nonparametric spearman correlation (for correlation analysis) was performed *, $p \leq 0.05$; **, $p \leq 0.01$; ***, $p \leq 0.0001$. To evaluate CB_1R inhibitor effect on *Nb* burdens across experimental repeats, we employed linear mixed models. Here, the inhibitor was tested as the main effect, which was adjusted by baseline weight and the weight on day 3, the experimental cooperation was the random effect. On basis of the distribution types for egg, and worm, the corresponding distribution families were Gamma, and Poisson respectively.

Results

Nippostrongylus brasiliensis *infection induces lung and intestinal endocannabinoid production.*

Endocannabinoids are lipid signaling mediators that affect a variety of behaviors (e.g. feeding and memory) and metabolic processes (e.g. glucose homeostasis) (Figure 12) [9]. Additionally, endocannabinoids can regulate the immune response and dampen inflammation [37]. Despite reported immunoregulatory function, however, whether endocannabinoids are generated in parasite infection and the functional consequence for the host or pathogen are unknown. *Nb* infects the small intestine of mice and has been shown to affect food intake and metabolism [3-5]. Given that endocannabinoids and endocannabinoid receptors are expressed in the intestine, we hypothesized that *Nb* infection may affect endocannabinoid signaling. Similar to the hookworm lifecycle, *Nb* infects both the lung and the intestine as part of its life cycle and feeds on host blood [38]. We therefore measured tissue and circulating endocannabinoid levels in naïve and *Nb*-infected mice at days 2 and 7 post-infection, when the parasites have infected the lung and jejunum respectively. We observed a modest but significant increase in 2-AG and AEA in *Nb*-infected lung tissue, and a trend towards increased levels of endocannabinoid-like molecule oleoylethanolamine (OEA) (Fig 13A). Strikingly, 2-AG levels in jejunal tissue were almost 10-fold higher than in the lung, and we observed a more than two-fold increase following *Nb* infection (Fig 13B). AEA and OEA, both of which regulate feeding and are anti-inflammatory [39], were also significantly elevated in the jejunum in response to *Nb* infection (Fig 13B). In contrast, circulating endocannabinoid levels in the plasma were unchanged following *Nb* infection (Fig 13C), suggesting that *Nb*-induced endocannabinoids were restricted to the tissue infection site. Given that the 2-AG levels were highest in the infected jejunum, we next evaluated activity of the biosynthetic and degradative enzymes responsible for 2-AG metabolism in jejunal epithelium of infected versus naïve mice. Specifically, we measured the enzymatic activities of diacylglycerol lipase (DGL,

biosynthetic) and monoacylglycerol lipase (MGL, degradative) by functional enzyme assays [15]. We found significant increases in the activity of DGL in the jejunal tissue of infected mice when compared to non-infected mice (Fig 13D, left), which suggests that levels of 2-AG in jejunum are elevated in infected mice by a mechanism that includes increases in jejunal DGL-mediated 2-AG biosynthesis. In contrast, we did not observe any changes in enzymatic activity of MGL (Fig 13D, right). Endocannabinoids signal through the G protein-coupled cannabinoid receptors subtype 1 and 2, therefore, we measured the cannabinoid receptor coding genes *Cnr1* and *Cnr2* mRNA by quantitative PCR of the jejunal tissue. *Nb* infection induced significant increases in both *Cnr1* and *Cnr2* (Fig 13E). Collectively, these data demonstrate that *Nb* infection increases endocannabinoid levels locally in the infected lung and intestinal tissue, and promotes intestinal endocannabinoid receptor expression, suggesting that the endocannabinoid system is induced in helminth infection.

.

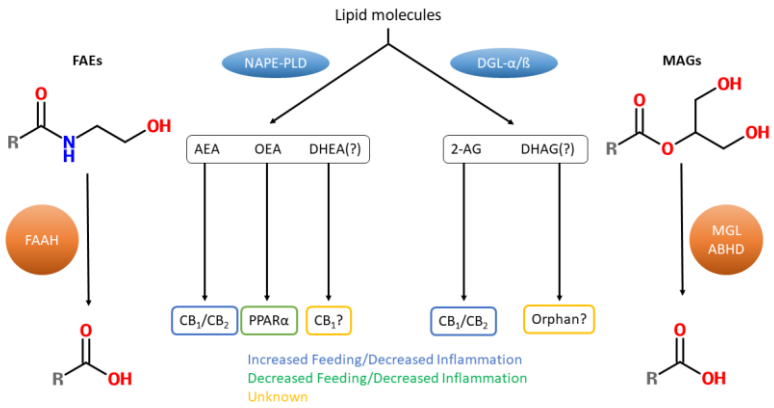

Figure 12. Endocannabinoid metabolism and signaling pathways. Endocannabinoids are lipid-derived signaling molecules that belong to two lipid classes: fatty acid ethanolamides (FAEs) and monoacylglycerols (MAGs). FAEs include the endocannabinoid, anandamide (AEA), and the endocannabinoid-related molecules, oleoylethanolamide (OEA) and docosahexaenoylethanolamide (DHEA), as well as others. FAEs are generated by the activity of N-acyl phosphatidylethanolamie-specific phospholipase D (NAPE-PLD), and are degraded by fatty acid amide hydrolase (FAAH). The MAG endocannabinoid, 2-AG, on the other hand, is synthesized primarily by the activities of diacylglycerol lipase α or β (DGLα/β), and is degraded primarily by monoacylglycerol lipase (MGL) or to a lesser extent by several alpha beta hydrolase domain enzymes (ABHD). Both, AEA and 2-AG, bind and activate cannabinoid type-1 (CB_1) and type-2 receptors (CB_2), and activation of CB_1 receptor is known to generally increase feeding and is associated with decreased inflammation. OEA is known to act through peroxisome proliferator-activated receptor α (PPARα) to decrease feeding and possibly inflammation. The physiological relevance and cognate receptors of DHEA and the MAG, docosahexaenoyl glycerol (DHAG), are unclear.

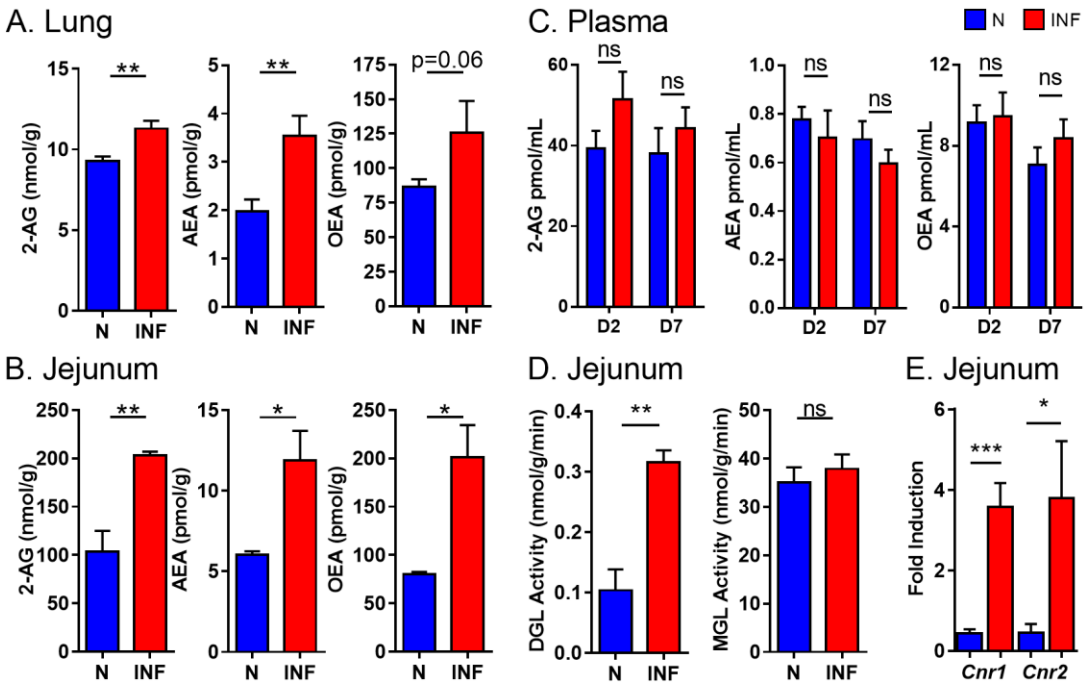

Figure 13. *Nb* infection induces endocannabinoid production and cannabinoid receptor expression. C57BL/6 mice were left naïve or infected for 2 or 7 days with 500 *Nb* L3. 2-AG, AEA and OEA levels in the (A) lung at day 2, (B) jejunum at day 7 and (C) plasma at day 2 and day 7. (D) 2-AG biosynthetic (DGL, left) and degradative (MGL, right) enzyme activity was measured in jejunal tissue from naïve or day 7 infected mice. (E) *Nb* infection-induced *Cnr1* and *Cnr2* mRNA in the jejunal tissue at day 7 was quantified as fold induction over naïve after normalization with 18S housekeeping gene. Data is presented as mean ± S.E.M (n-4-6/group) and are representative of four experiments.

Intestinal endocannabinoids are negatively correlated with Nippostrongylus brasiliensis *infection-induced weight loss and parasite egg burdens*

We examined if *Nb*-induced endocannabinoids were associated with health outcomes for the host or parasite by correlative analyses between endocannabinoid levels and infection-induced weight loss or parasite egg burdens. *Nb* infectious larval stage 3 (L3) migrate to the lung, where they develop into L4 followed by infection of the small intestine, where they develop into adults and produce eggs (Fig 14A, B). At the infectious dose of 500 L3, *Nb* infection of the lung, which occurs between day 1 and 3 post-infection, causes lung hemorrhaging and inflammation likely due to the physical damage of the worm burrowing through the lung tissue. During this acute infection of the lung, we observe significant weight loss that is remarkably resolved once the *Nb* parasites are established in the intestine at day 6 (Fig 14A). Consistent with this weight loss, analysis of feeding patterns in naïve and infected mice revealed reduced food intake ($p<0.05$) and motor activity ($p=0.05$) at day 1 post-infection, when the *Nb* parasites have reached the lung, that was also resolved by day 6 post-infection (Fig 14C). We also observed a significant positive correlation between *Nb*-induced acute weight loss at day 3 and *Nb* egg burdens at day 7 post infection (Fig 14D, left). This correlation suggests that acute infection-induced weight loss at day 3 may be a good predictor of subsequent parasite establishment in the intestine. The effect of *Nb* infection on mouse weight changes may be due to lung tissue inflammation or changes in mouse feeding behavior.

Given that endocannabinoids can regulate both these processes, we investigated correlations between endocannabinoids and *Nb* parasite burdens. We observed that 2-AG intestinal levels from day 7-infected mice were negatively correlated with early infection-induced weight loss (day 3) and day 7 parasite egg burden (Fig 14D, right). To comprehensively define the relationship between endocannabinoids versus host and parasite fitness, we performed Spearman

correlation analyses across all experiments (Table 5). We observed a negative correlation between day 7-infected jejunum 2-AG and OEA and (i) early (day 3) infection-induced weight changes; (ii) day 7 parasite egg burden. In contrast, we observed a positive correlation between plasma 2-AG and OEA, weight loss, and parasite egg burden. These data indicate that high endocannabinoid levels locally in the intestine are associated with reduced early infection-induced weight loss and decreased parasite egg burden.

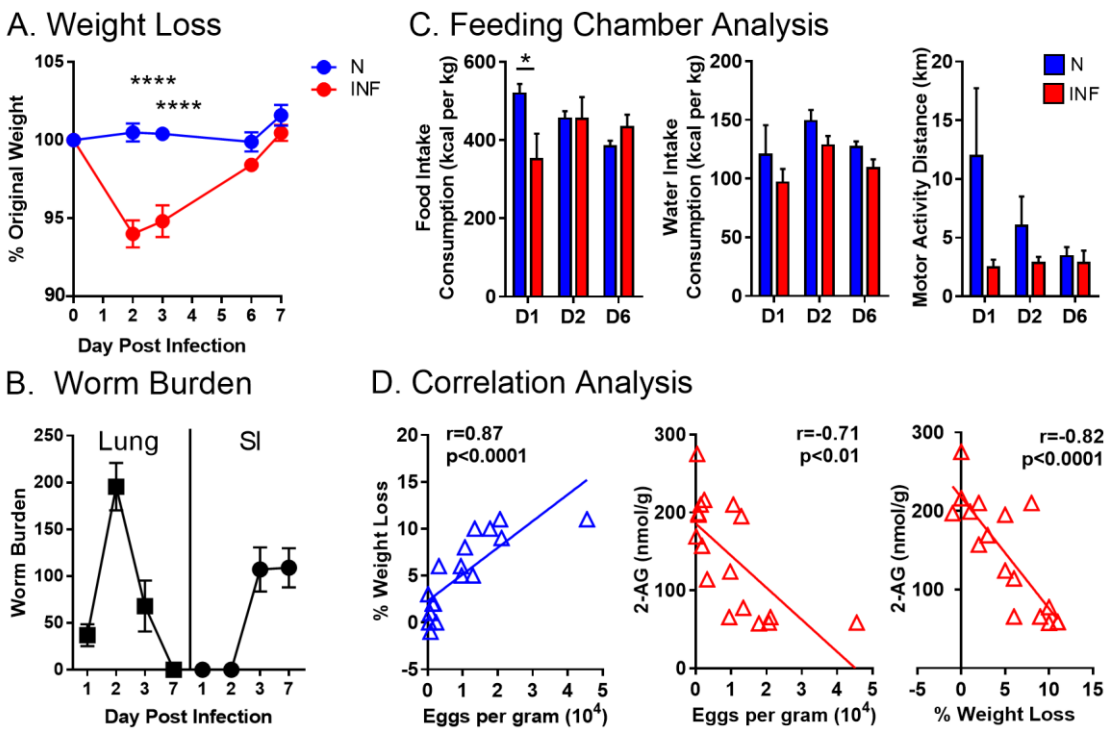

Figure 14: Intestinal endocannabinoid levels are negatively correlated with infection-induced weight loss and fecal egg burdens. (A) Time course of *Nb* infection-induced weight loss. (B) Compiled data of *Nb* parasite burdens in lung and small intestine. (C) Food, water intake and motor activity of naïve or *Nb*-infected mice were evaluated in a feeding chamber. (D) Correlation analysis was performed between parasite egg burden and weight loss (left) and jejunal 2-AG (right). Data is presented as mean ± S.E.M and are representative of two to four experiments (n-4-6/group).

Table 3. Correlation analysis between endocannabinoids from day 7 *Nb*-infected mice, day 3 infection-induced weight loss and day 7 parasite egg burden.

	Jejunum eCB			Plasma eCB		
Weight Loss	**2-AG**	**AEA**	**OEA**	**2-AG**	**AEA**	**OEA**
Spearman r	-0.8154	-0.3678	-0.7159	0.7688	0.3617	0.7269
p value	***	ns	**	***	ns	**
Egg Burden	**2-AG**	**AEA**	**OEA**	**2-AG**	**AEA**	**OEA**
Spearman r	-0.7137	-0.4265	-0.6593	0.7279	0.1878	0.6127
p value	**	ns	**	**	ns	*

Disruption of CB_1 receptor but not CB_2 receptor signaling increases Nippostrongylus brasiliensis *egg burden and impairs intestinal IL-5 responses.*

The endocannabinoids, 2-AG and AEA, both of which were upregulated following *Nb* infection (see Fig 13), signal through CB_1R and CB_2R [12]. We investigated the function of endocannabinoid signaling in *Nb* infection by treatment with the peripherally-restricted neutral CB_1R antagonist AM6545 [40, 41], CB_2R antagonist AM630 [19], and DMSO as a vehicle control. To rule out potential confounding effects on the parasite establishment in the intestine, mice were treated daily with antagonists or vehicle starting at day 4 post-infection when all *Nb* parasites have reached the intestine. At this timepoint, CB_1R or CB_2R inhibition had no effect on mouse weight (Fig 15A). Interestingly, CB_1R but not CB_2R inhibition led to increased fecal *Nb* egg output and intestinal *Nb* worm counts (Fig 15B), suggesting that CB_1R signaling is necessary for optimal *Nb* explusion. We validated these CB_1R inhibitor-mediated differences in *Nb* burdens across three experimental repeats, using generalized linear models, and found that CB_1R inhibitor treatment led to 2.21 fold higher egg burden (p=0.01) and 1.46 fold higher worm burdens (p<0.01) (Table 4). CB_1R inhibition resulted in significantly decreased intestinal levels of the Th2 cytokine IL-5, but not IL-4, IFNγ or IL-10 (Fig 15C). Further, *in vitro* CD3/CD28-activated splenocytes from CB_1R inhibitor-treated mice secreted significantly less IL-5, IL-4 and IL-10 compared to vehicle-treated mice, but exhibited no defect in IFNγ secretion (Fig 15D). This cytokine effect was specific to CB_1R signaling as inhibition of CB_2R signaling had no significant effect. Given that host immunity to *Nb* is dependent on Th2 cytokines, the CB_1R inhibitor-induced decrease in IL-5 and IL-4 may explain the increase in parasite egg burden. Additionally, the significant reduction in IL-10 secretion is consistent with an anti-inflammatory function for CBR signaling [39]. These data support the functional link between the endocannabinoid system and immunity to *Nb*, and suggest

that CB_1R signaling has a beneficial impact for the host following *Nb* infection by promoting Th2 cytokine expression and reducing parasite burdens.

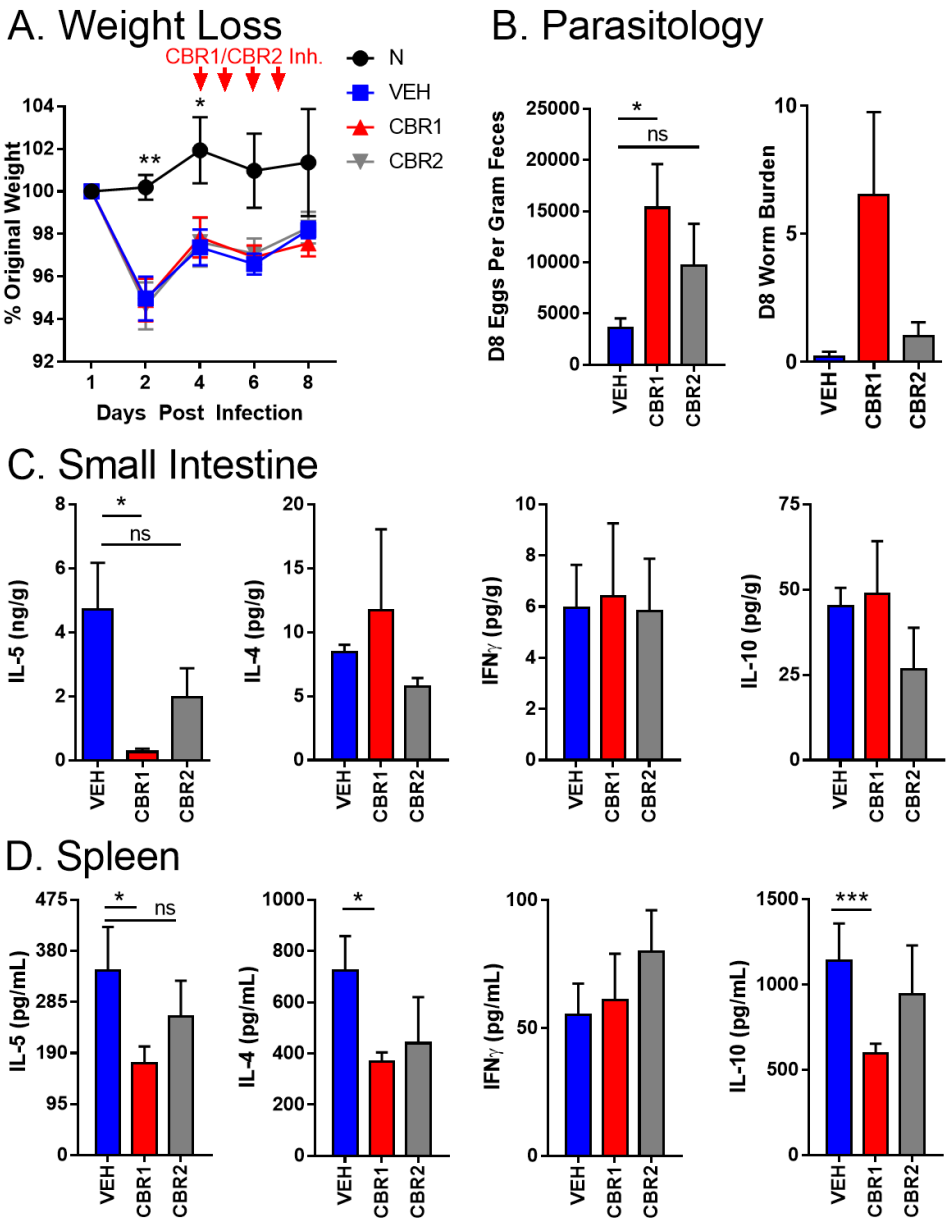
A. Weight Loss
CBR1/CBR2 Inh.
N
VEH
CBR1
CBR2
% Original Weight
Days Post Infection
B. Parasitology
D8 Eggs Per Gram Feces
D8 Worm Burden
C. Small Intestine
IL-5 (ng/g)
IL-4 (pg/g)
IFNγ (pg/g)
IL-10 (pg/g)
D. Spleen
IL-5 (pg/mL)
IL-4 (pg/mL)
IFNγ (pg/mL)
IL-10 (pg/mL)
VEH
CBR1
CBR2
ns

Figure 15. Pharmacologic inhibition of cannabinoid receptor 1 but not cannabinoid receptor 2 increases helminth burdens associated with decreased IL-5 expression. C57BL/6 mice were left naïve (black) or infected with *Nb*. At days 4-7 post-infection, mice were treated intraperitoneally with AM6545 (CB1 inh; red), AM630 (CB2 inh; grey), or DMSO (Veh; blue). (A) Infection-induced weight loss was monitored and compared to naïve mice. (B) Fecal egg burdens (left) and intestinal worm counts (right) were quantified in *Nb*-infected mice. (C-D) IL-5, IL-4, IFNγ and IL-10 cytokines were quantified in day 8 infected (C) intestinal tissue homogenate and (D) supernatant from 72 hr anti-CD3/anti-CD28 stimulated splenocytes. Data is presented as mean ± S.E.M (n=4-6/group) and representative of three separate experiments.

Table 4. Effect of CBR1 inhibitor on *Nb* egg and worm burden estimated by linear regression models.

CB1 inh. effect	Effect Estimation	95% Confidence Interval	p value
Egg burden	2.21	1.25 ~ 3.91	0.01
Worm count	1.46	1.29 ~ 1.64	<0.001

The endocannabinoid system is present in Nippostrongylus brasiliensis *and other parasitic helminths.*

The endocannabinoid system is conserved in vertebrates and some invertebrates [42], and endocannabinoid biosynthetic and degradative enzymes are expressed in *Caenorhabditis elegans* [43]. However, whether the endocannabinoid system exists in parasitic helminths is unknown. We conducted bioinformatic analyses of available parasitic nematode genomes for genes involved in the endocannabinoid synthetic and signaling pathway (Table 5). Within the *Nb* genome, genes encoding synthetic enzymes for the monoacylglycerols, 2-AG and DHAG (*dagl*), and the fatty acid ethanolamides, AEA, OEA, and DHEA (*nape*) were identified. We also found orthologs of the fatty acid ethanolamide degradative enzyme, fatty acid amide hydrolase (*faah-1*), the proposed monoacylglycerol degradative enzymes, alpha beta hydroxylases *abhd-12* and *abhd-5*. Although nematodes did not have obvious orthologs of monoacylglycerol lipase (*magl*), the major degradative enzyme for 2-AG found in mammals, we identified a putative nematode gene encoding the minor 2-AG degradative enzyme *abhd-6* [44]. Moreover, the synthetic and degradative endocannabinoid genes were conserved in other nematodes including human hookworms *Ancylostoma duodenale* and *Necator americanus*, and human roundworm *Ascaris lumbricoides*.

Analysis of available RNA-seq datasets revealed the expression of putative genes for the endocannabinoid pathway in parasitic nematodes of man (*A. ceylanicum*, *A. suum*, *N. americanus*, *Toxocara canis, Strongyloides stercoralis*), rodents (*Nb*, *Strongyloides ratti*) and even insects (*Steinernema carpocapsae*) (Fig 16 and Fig 17). Further, these genes were expressed in a tissue- or stage-specific manner in some of these parasites. For example, the hookworm *A. ceylanicum*, which infects humans and other mammals, showed expression of *abhd-5* in all stages sampled, but showed highest expression of *abhd-5* in the infective L3 stage. In the human hookworm *N. americanus*, both *nape-1* and *abhd-12* were more highly expressed in L3 larvae than in adult nematodes.

Although it was previously thought that no obvious orthologs of CB_1 and CB_2 receptors were present in nematodes, a recent study identified the neuropeptide receptor NPR-19 as a cannabinoid-like receptor in *C. elegans* [45-49]. We were able to find putative orthologs of the cannabinoid-like receptor NPR-19 in other nematodes including *A. ceylanicum*, *N. americanus* and *Wuchereria bancrofti* (Table 5). However, we were not able to find an obvious ortholog of NPR-19 in *Nb*, though this may be due to the incomplete state of the available *Nb* genome (N50 = 33.5 kb; ie. nearly 30% of the predicted protein-coding genes are on contigs smaller than 10 kb), rather than the absence of an NPR-19 ortholog [50, 51].

Table 5. Putative genes in endocannabinoid signaling and degradation identified in the genome of *Nb*, human hookworms and other parasitic nematodes.

	Nbra	*Aduo*	*Acey*	*Name*	*Scar*	*Alum*	*Srat*	*Sste*	*Tcan*
npr-19	X	√	√	√	√	√	√	√	√
nape-1	√	√	√	√	√	√	X	X	√
faah-1	√	√	√	√	√	√	√	√	√
dagl-2	√	√	√	√	√	√	√	√	√
magl	X	X	X	X	X	X	X	X	X
abhd-6	√	√	√	√	√	√	√	√	√
abhd-12	√	√	√	√	√	√	√	√	√
abhd-5	√	√	√	√	√	√	√	√	√

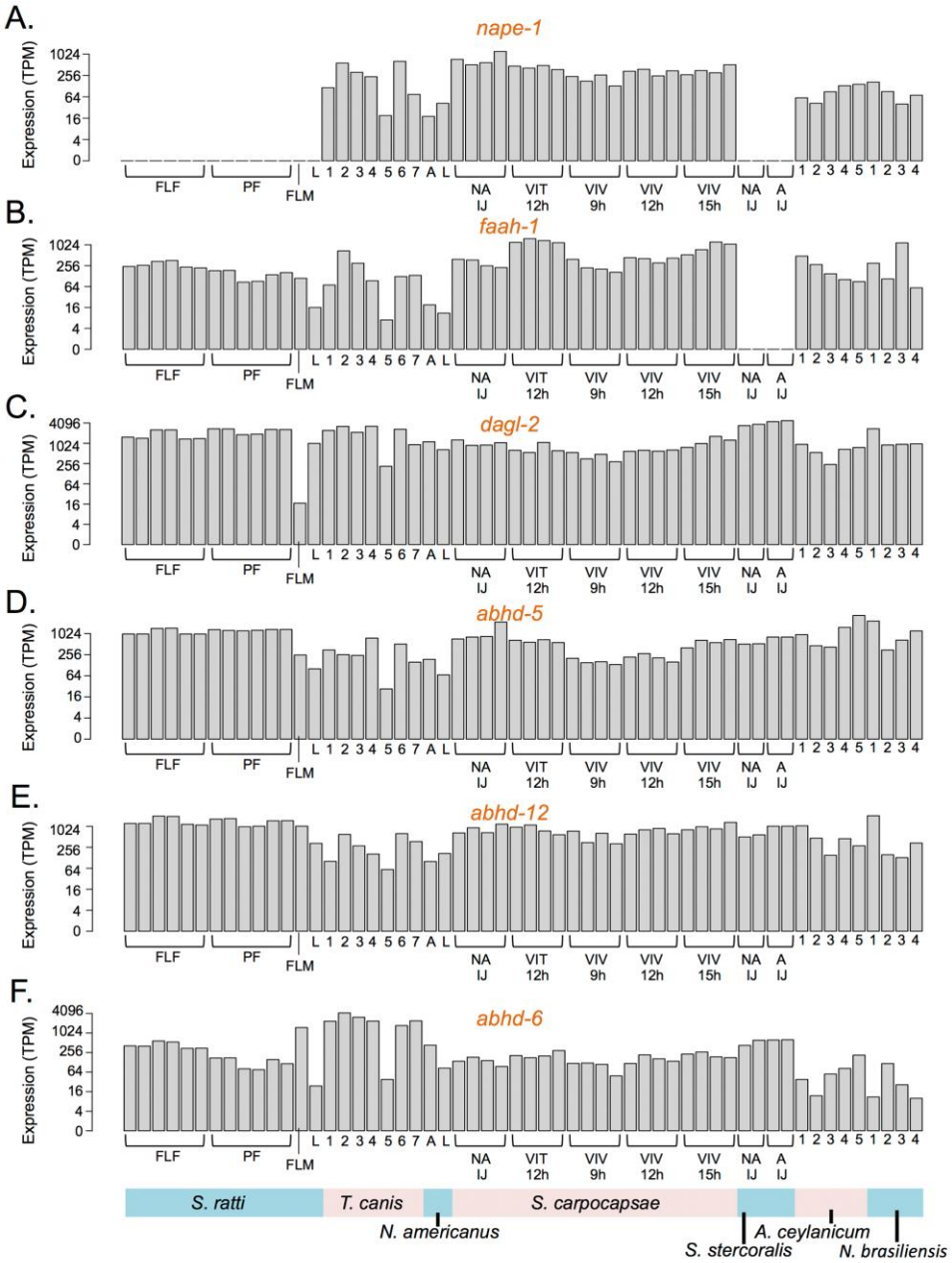
A.
nape-1
B.
faah-1
C.
dagl-2
D.
abhd-5
E.
abhd-12
F.
abhd-6
Expression (TPM)
1024
256
64
16
4
0
4096
FLF
PF
FLM
L 1 2 3 4 5 6 7 A L
NA IJ
VIT 12h
VIV 9h
VIV 12h
VIV 15h
NA IJ
A IJ
1 2 3 4 5 1 2 3 4
S. ratti
T. canis
S. carpocapsae
N. americanus
S. stercoralis
A. ceylanicum
N. brasiliensis

Figure 16: Expression of genes encoding endocannabinoid biosynthetic and degradative enzymes in parasitic nematodes. Nematode expression data for endocannabinoid biosynthetic enzyme *nape-1* (A) and degradative enzyme *faah-1* (B), the monoacylglycerol biosynthetic enzyme *dagl-2* (C) and the potential degradative enzymes alpha beta hydrolases (*abhd-5*, D) and (*abhd-12*, E), and the minor 2-AG degradative enzyme (*abhd-6*, F) are shown in transcripts per million (TPM). The life stages for *S. ratti* expression are: Free-living female (FLF), parasitic female (PF), free-living male (FLM), and infective L3 (L). The expression data shown for *T. canis* expression are: Female gut (1), female reproductive tract (2), female anterior body (3), male gut (4), male reproductive tract (5), male anterior body (6), and L3 (7). The life stages for *N. americanus* expression are: Adult (A) and infectious L3 (L). The life stages for *S. carpocapsae* expression are: Non-activated infective juveniles (IJs) (NA IJ), 12 hr *in vitro* activated IJs (VIT 12h), 9 hr *in vivo* activated IJs (VIV 9h), 12 hr *in vivo* activated IJs (VIV 12h), and 15 hr *in vivo* activated IJs (VIV 15h). The life stages for *S. stercoralis* expression are: Non-activated IJ (NA IJ) and activated IJ (A IJ). The life stages for *A. ceylanicum* expression are: 17 days postinfection (1), 12 days postinfection (2), 5 days postinfection (3), 24 hr incubation in hookworm culture media (4), and infective L3 (5). The life stages for *N. brasiliensis* expression are adult (1), L4 from mouse lung (2), infectious L3 (3), and eggs (4).

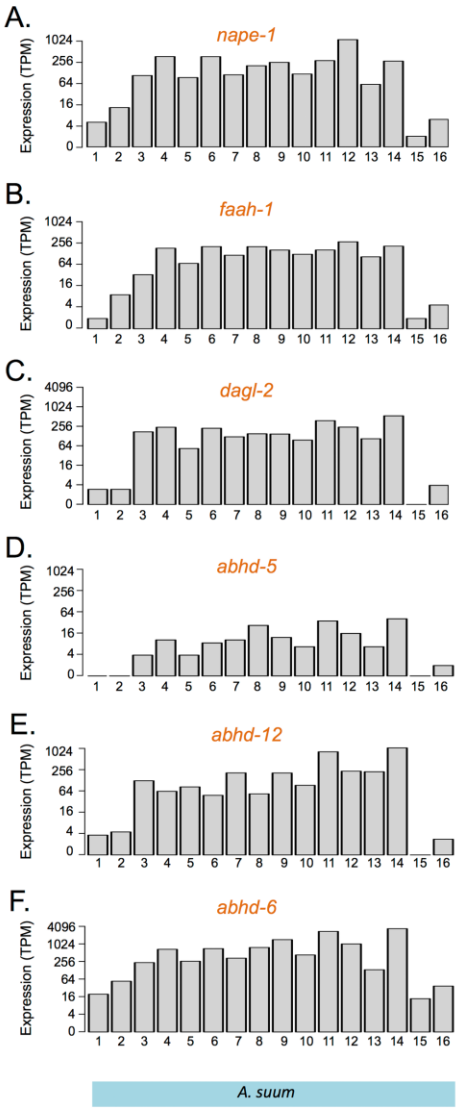

Figure 17. RNA-seq expression of *Ascaris suum*. The life stages for *A. suum* expression were not clearly identified in the RNA-seq data available in the public database and are therefore not defined in the figure.

Nippostrongylus brasiliensis *produces endocannabinoids*

Given the presence of genes encoding endocannabinoid synthetic and degradative enzymes in the *Nb* genome, we investigated if *Nb* could produce endocannabinoids at any stage of its life cycle. We isolated infectious *Nb* L3 from hatched fecal cultures, *Nb* L4 from day 2-infected lungs, and *Nb* adults from day 7-infected jejunum, performed thorough washes in PBS, and measured endocannabinoid levels. Although there were no endocannabinoids in the control washes, we measured detectable levels of endocannabinoids and endocannabinoid-like molecules in worm extracts from all life cycle stages (Fig 18A). These exhibited identical chromatogram patterns to reference endocannabinoids, AEA (Fig 18B) and 2-AG (Fig 18C), and endocannabinoid-like molecules (Figure 19 A-C). On a per-weight basis, adult *Nb* produced the most 2-AG and DHAG, whereas L4s produced OEA. Strikingly, infectious L3 produced over 100-fold more AEA than the other life cycle stages or the host (see Fig 13B). *Nb* L4 and adults feed on host tissue and blood, therefore, it may be possible that some endocannabinoids detected may be host-derived. However, the infectious L3 were isolated from culture and concentrations of AEA reached 1000 pmol per gram worm, which is 100-200 times the level found in upper intestinal mucosal scrapings (5-10 pmol per g tissue) and 300-1000 times found in circulation (1-3 pmol per mL) (Fig 13 and [16]). Thus, the endocannabinoids measured in L3s are likely generated by the parasite. Consistent with the presence of a functional endocannabinoid system in *Nb*, sequence alignment of the predicted *Nb* gene encoding NAPE-PLD, the dominant enzyme catalyzing the biosynthesis of fatty acids ethanolamides, including AEA, OEA, and DHEA, revealed 43% identity and sequence conservation in the functional lactamase domain (Fig 18D). To validate that the predicted *Nb* genes encoding endocannabinoid biosynthetic and degradative enzymes were expressed, we performed quantitative PCR for predicted *Nb-Nape*, *Nb-Faah* and *Nb-Actin* as a housekeeping gene control (Fig 18E). *Nb-Nape* and *Nb-Faah* mRNA were present in all *Nb* life cycle stages, with highest

expression in the infectious L3 stage. Overall, these data show for the first time that endocannabinoids are produced by *Nb* and suggest that the endocannabinoid system is also present in parasitic nematodes that infect humans.

A. Parasite Endocannabinoid Analysis

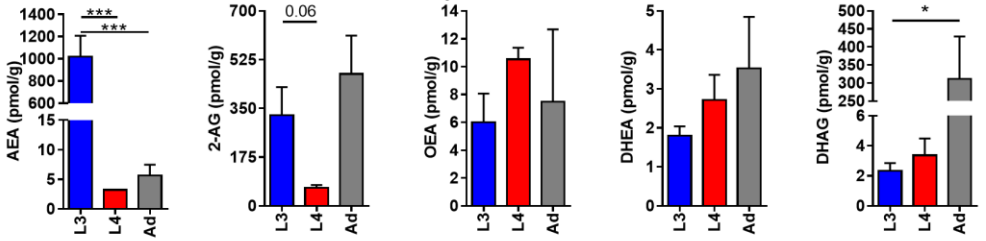

B. AEA

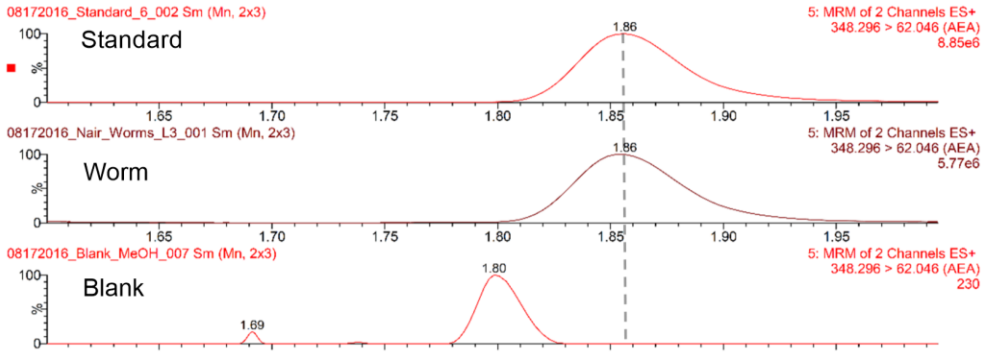

C. 2-AG

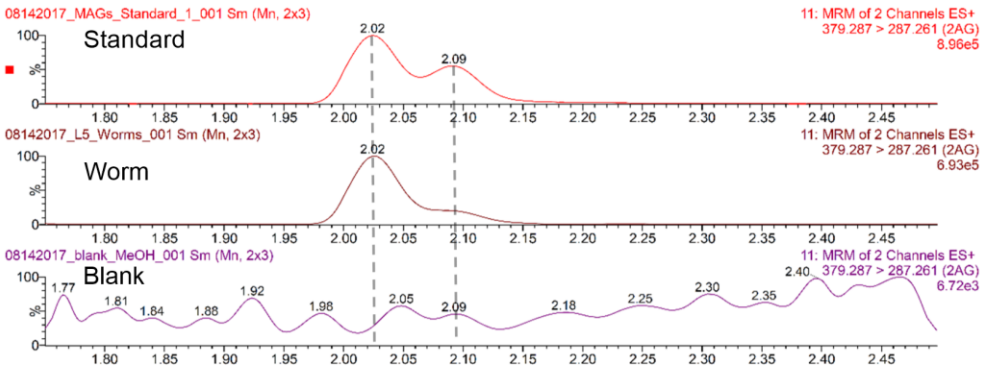

D. NAPE-PLD

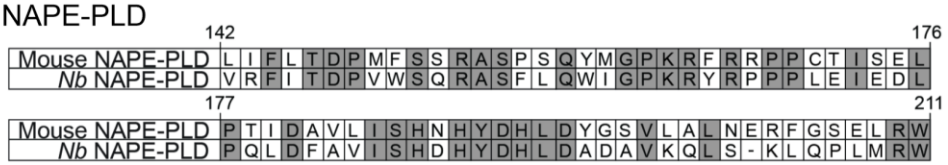

E. Parasite Endocannabinoid Synth./Degrad. Genes

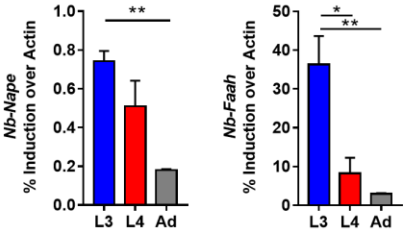

Figure 18. *Nb* produce endocannabinoids and cannabinoid-like molecules. *Nb* parasites from life cycle stages were isolated, washed and assessed for levels of endocannabinoids and endocannabinoid-like molecules by UPLC/MS/MS. (A) Levels of analytes at various life stages: anandamide (AEA), 2-arachidonoyl-*sn*-glycerol (2-AG), oleoylethanolamide (OEA), docosahexaenoylethanolamide (DHEA), and docosahexaenoylglycerol (DHAG). Representative chromatograms of AEA and 2-AG. (D) Legend for the alignment: a 68-amino acid (AA) region of an alignment of mouse and *Nb* NAPE-PLD (43% shared identity). The alignment region shown is the first 68 AAs in a 202 AA lactamase (B_2) domain identified in mouse NAPE-PLD. (E) Quantitative reverse transcription PCR of *Nippostrongylus* life cycle stages for predicted *Nb-Nape* and *Nb-Faah*.

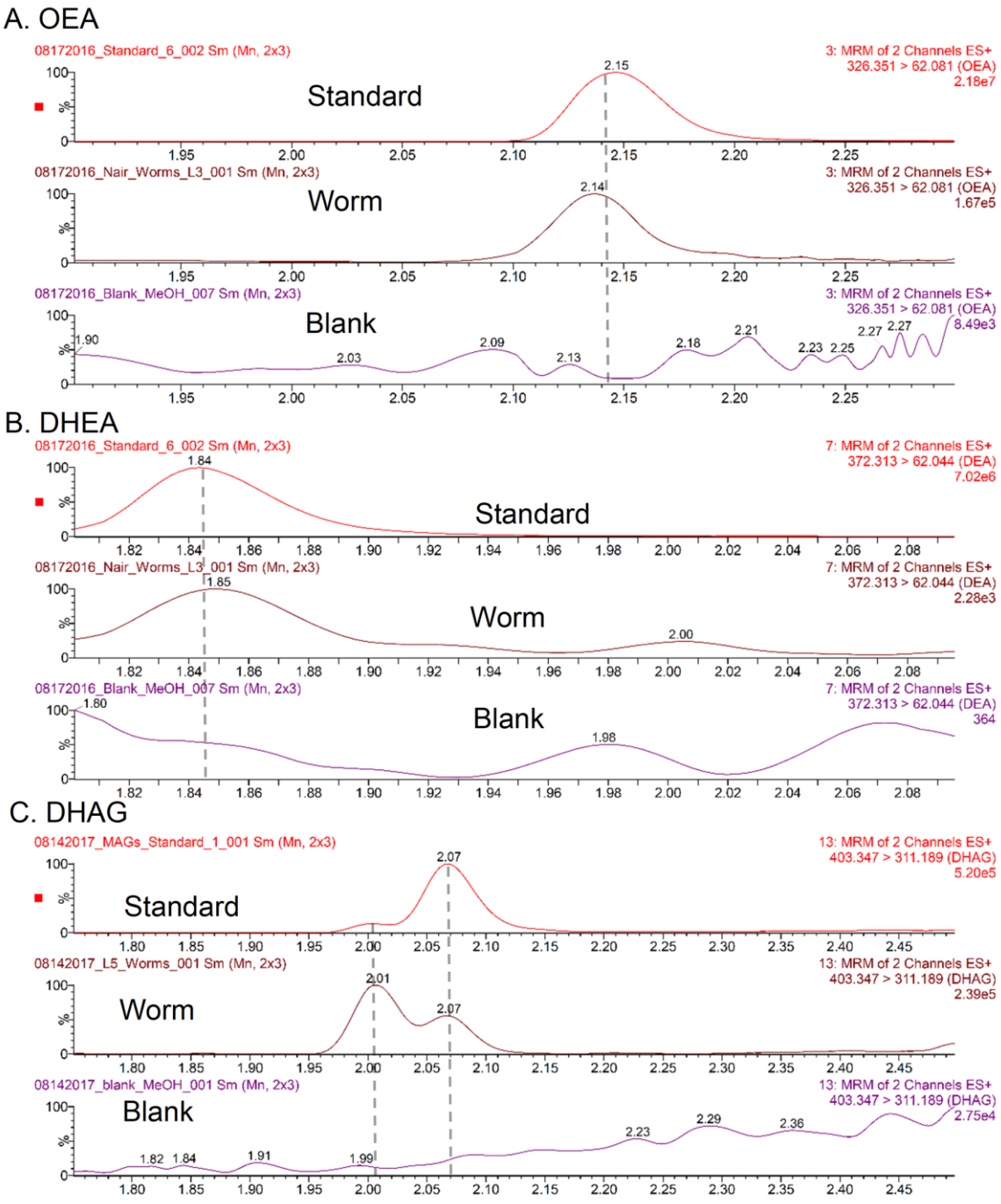

Figure 19. Chromatograms for endocannabinoid-like molecules in *Nb*. Representative chromatograms of (A) OEA, (B) DHEA, and (C) DHAG.

Discussion

In this study, we investigated the endocannabinoid signaling system following infection with *Nb*. While recognized for its critical function in the central and enteric nervous system, the endocannabinoid system is also activated by and can influence inflammatory immune responses [22, 37, 52]. For example, 2-AG and AEA are anti-inflammatory, which has provided the basis for the potential therapeutic use of synthetic cannabinoids, or cannabis, in autoimmune or inflammatory diseases [53]. Oral treatment of mice with AEA promoted a tolerogenic immune response and regulatory macrophages in the intestine that was protective in a non-obese diabetic model [54]. Despite an immune function in the intestine, the functional significance of endocannabinoids in intestinal parasite infection has not been examined. Our finding that helminth infection triggers significant endocannabinoid synthesis that is correlated with both host health outcomes and parasite fecundity suggests that endocannabinoids may be an important player in host-helminth dynamics.

Inhibition of CB_1R led to decreased expression of the Th2 cytokine IL-5 in the intestine and IL-4, IL-5 and IL-10 in the spleen, but no difference in Th1 cytokine IFNγ. This was associated with increased parasite egg and worm burdens, suggesting that CB_1R signaling may be important for the optimal host immune response to keep helminth burdens in check. Endocannabinoids also signal through CB_2R [37], however, CB_2R antagonist treatment did not significantly change cytokine responses or helminth burdens. CB_1R and CB_2R inhibition was conducted during a short time frame of days 4-6 post-infection, and we cannot confirm complete abrogation of CB_1R or CB_2R signaling in the intestine with this treatment regime. Future studies with earlier treatment regimes or CB_1R/CB_2R deficient mice may delineate functional differences between these signaling pathways in helminth infection. Cannabinoid CB_1Rs are expressed in cholecystokinin

(CCK)-positive enteroendocrine cells in the duodenum of mice [55] and ghrelin-expressing cells of the stomach of rats [56], and *Nb* infection in rats is associated with elevations in circulating levels of CCK [4]. Thus, it is possible that helminth infection may induce changes in feeding behavior, as seen in Fig 14, by a mechanism that includes endocannabinoid-mediated changes in the production and/or release of peptides important for feeding behavior, including CCK. We observed significant correlations between endocannabinoid levels, infection-induced weight loss and parasite burdens. However, further functional studies are necessary to determine causal relationships between these multiple parameters and the contribution, if any, of infection-induced endocannabinoids on feeding behavior.

In addition to host endocannabinoid expression, we show for the first time that *Nb* produces endocannabinoids and that genes encoding endocannabinoid biosynthetic and degradative enzymes are present in the genomes of multiple parasitic nematode including some of the most common helminth parasites of man. One proposed strategy by which parasites modulate host immunity is by releasing molecules that are already native within the host, or at least native-like molecules [57]. For example, *A. suum* and *T. canis* have been shown to synthesize morphine or morphine-like substrates, and morphine is a known immunomodulator [58, 59]. It is well recognized that the endocannabinoid system is conserved in a diverse variety of vertebrates, including pythons [60] and goldfish [61]; however, whether it evolved earlier and is functional in more primitive eukaryotic organisms is less well understood [45]. We observed that *Nb* has predicted genes encoding the NAPE-PLD and FAAH enzyme that catalyze endocannabinoid synthesis and breakdown. Quantitative PCR analysis confirmed *Nb* expression of both these predicted genes. Moreover, mass spectrometry analysis revealed that infectious L3 *Nb* produced extremely high levels of AEA, reaching 100-1000 times that found in tissue or blood of mice. A recent study showed that truffles, the fruiting body of fungi produce AEA potentially as an

attractant and feeding stimulant for animals to ensure its dissemination [62]. Given that AEA is anti-inflammatory, high level synthesis at the infectious stage may also function to dampen the host immune response. It is possible that in addition to endocannabinoids, *Nb* may produce and release other signaling molecules endogenous to the host, such as morphine, and that there is overlap in the biological effects of these molecules on host immunity or behavior. Given the difference in mass between *Nb* and the host, the endocannabinoids detected in the infected mice are likely host-derived. However, it is possible that *Nb*-derived endocannabinoids may functionally impact the host at the cellular level. Future studies are necessary to test these hypotheses.

Inhibition of CB_1R signaling significantly increased *Nb* egg burden, however, whether the functional effect was through influencing the host or alteration of the endocannabinoid system in *Nb* is unclear. In the host, the increased *Nb* burdens when CB_1R signaling is inhibited could be due to the altered immune response, or through reducing intestinal motility. Indeed, immune cells express both CB_1 and CB_2 receptors [63] (ie. macrophages, dendritic cells, T cells) and intestinal epithelial cells express CB_1R [14]. Whether CB_1R inhibitor-mediated increase in *Nb* burden was through direct effects on immune cells, through effects on the intestinal epithelial cells, or a combination of both, is unclear and would require further studies. In addition to regulating immune responses, the endocannabinoid system throughout the gastrointestinal tract serves a variety of physiological roles including the control of motility, immune function, mucosal barrier function, and feeding behavior [64-66]. Although outside of the scope of the present study, future studies should include an evaluation of the impact that endocannabinoid-induced changes in intestinal motility has on egg burden. Furthermore, it is possible that endocannabinoid metabolism and/or release may be secondarily affected by perturbations in physiological responses governed by endocannabinoids themselves. It is also possible that CB_1R inhibition could directly affect *Nb.* Although the *Nb* genome does not have canonical cannabinoid receptor genes, genes encoding

endocannabinoid degradative enzymes are present in the *Nb* genome, suggesting that *Nb* may also respond to the endocannabinoids it produces through an as yet unidentified receptor. Consistent with this, *C. elegans* produces and responds to cannabinoids through NPR-19 [47-49]. Inhibiting CB_1R signaling was ultimately beneficial to *Nb* leading to improved parasite fertility. Why *Nb* would produce endocannabinoids that adversely affect its fertility is unclear at present. Our data, however, support a functional impact of the host and parasite endocannabinoid system, and suggest that further studies delineating the beneficial or detrimental function of endocannabinoids in the host versus the helminth are warranted. For example, the timing of cannabinoid receptor signaling inhibition may be critical. In our studies, we inhibited CB_1R signaling after adult parasite establishment in the intestine; however, *Nb* produces highest AEA during the initial infection, possibly as an anti-inflammatory mechanism to downregulate the host immune response. *Nb*-derived AEA may also prevent excessive host inflammation that could lead to host mortality, which would be an equally adverse outcome for the helminth. Notwithstanding this, our discovery of parasite-derived endocannabinoids implicates the endocannabinoid system as a primitive pathway that contributes to host-pathogen interaction and suggests that investigation of the existence of the endocannabinoid system in other pathogens is warranted.

The complexity of host-helminth interaction and the numerous factors that influence the health outcomes for the parasite and the host are increasingly recognized. In addition to an optimized Th2 response for parasite expulsion, parasitic helminths trigger a multitude of non-immune pathways that affect physiologic processes such as feeding and metabolism, but can also influence the immune response [67-69]. Our findings suggest that the endocannabinoid system is a previously unrecognized contributor to this dynamic process and may therefore have a significant impact on the host's health outcome beyond parasite expulsion.

References

1. Hotez, P. J., Brindley, P. J., Bethony, J. M., King, C. H., Pearce, E. J., Jacobson, J. (2008) Helminth infections: the great neglected tropical diseases. J Clin Invest 118, 1311-21.

2. Stephensen, C. B. (1999) Burden of infection on growth failure. J Nutr 129, 534S-538S.

3. Shea-Donohue, T., Qin, B., Smith, A. (2017) Parasites, nutrition, immune responses and biology of metabolic tissues. Parasite Immunol 39.

4. Ovington, K. S. (1986) Physiological responses of rats to primary infection with Nippostrongylus brasiliensis. J Helminthol 60, 307-12.

5. Wu, D., Molofsky, A. B., Liang, H. E., Ricardo-Gonzalez, R. R., Jouihan, H. A., Bando, J. K., Chawla, A., Locksley, R. M. (2011) Eosinophils sustain adipose alternatively activated macrophages associated with glucose homeostasis. Science 332, 243-7.

6. Yang, Z., Grinchuk, V., Smith, A., Qin, B., Bohl, J. A., Sun, R., Notari, L., Zhang, Z., Sesaki, H., Urban, J. F., Shea-Donohue, T., Zhao, A. (2013) Parasitic nematode-induced modulation of body weight and associated metabolic dysfunction in mouse models of obesity. Infect Immun 81, 1905-14.

7. Barnes, M. A., Carson, M. J., Nair, M. G. (2015) Non-traditional cytokines: How catecholamines and adipokines influence macrophages in immunity, metabolism and the central nervous system. Cytokine 72, 210-9.

8. Howitt, M. R., Lavoie, S., Michaud, M., Blum, A. M., Tran, S. V., Weinstock, J. V., Gallini, C. A., Redding, K., Margolskee, R. F., Osborne, L. C., Artis, D., Garrett, W. S. (2016) Tuft cells, taste-chemosensory cells, orchestrate parasite type 2 immunity in the gut. Science 351, 1329-33.

9. DiPatrizio, N. V. and Piomelli, D. (2012) The thrifty lipids: endocannabinoids and the neural control of energy conservation. Trends Neurosci 35, 403-11.

10. Simon, V. and Cota, D. (2017) MECHANISMS IN ENDOCRINOLOGY: Endocannabinoids and metabolism: past, present and future. Eur J Endocrinol 176, R309-R324.

11. Di Marzo, V., Melck, D., Bisogno, T., De Petrocellis, L. (1998) Endocannabinoids: endogenous cannabinoid receptor ligands with neuromodulatory action. Trends Neurosci 21, 521-8.

12. Munro, S., Thomas, K. L., Abu-Shaar, M. (1993) Molecular characterization of a peripheral receptor for cannabinoids. Nature 365, 61-5.

13. Galiègue, S., Mary, S., Marchand, J., Dussossoy, D., Carrière, D., Carayon, P., Bouaboula, M., Shire, D., Le Fur, G., Casellas, P. (1995) Expression of central and

peripheral cannabinoid receptors in human immune tissues and leukocyte subpopulations. Eur J Biochem 232, 54-61.

14. DiPatrizio, N. V., Igarashi, M., Narayanaswami, V., Murray, C., Gancayco, J., Russell, A., Jung, K. M., Piomelli, D. (2015) Fasting stimulates 2-AG biosynthesis in the small intestine: role of cholinergic pathways. Am J Physiol Regul Integr Comp Physiol 309, R805-13.

15. DiPatrizio, N. V., Astarita, G., Schwartz, G., Li, X., Piomelli, D. (2011) Endocannabinoid signal in the gut controls dietary fat intake. Proc Natl Acad Sci U S A 108, 12904-8.

16. Argueta, D. A. and DiPatrizio, N. V. (2017) Peripheral endocannabinoid signaling controls hyperphagia in western diet-induced obesity. Physiol Behav 171, 32-39.

17. Correa, F., Hernangómez, M., Mestre, L., Loría, F., Spagnolo, A., Docagne, F., Di Marzo, V., Guaza, C. (2010) Anandamide enhances IL-10 production in activated microglia by targeting CB(2) receptors: roles of ERK1/2, JNK, and NF-kappaB. Glia 58, 135-47.

18. Nair, M. G. and Herbert, D. R. (2016) Immune polarization by hookworms: taking cues from T helper type 2, type 2 innate lymphoid cells and alternatively activated macrophages. Immunology 148, 115-24.

19. Storr, M. A., Keenan, C. M., Zhang, H., Patel, K. D., Makriyannis, A., Sharkey, K. A. (2009) Activation of the cannabinoid 2 receptor (CB2) protects against experimental colitis. Inflamm Bowel Dis 15, 1678-85.

20. Chen, G., Wang, S. H., Jang, J. C., Odegaard, J. I., Nair, M. G. (2016) Comparison of RELMalpha and RELMbeta Single- and Double-Gene-Deficient Mice Reveals that RELMalpha Expression Dictates Inflammation and Worm Expulsion in Hookworm Infection. Infect Immun 84, 1100-11.

21. Jang, J. C., Chen, G., Wang, S. H., Barnes, M. A., Chung, J. I., Camberis, M., Le Gros, G., Cooper, P. J., Steel, C., Nutman, T. B., Lazar, M. A., Nair, M. G. (2015) Macrophage-derived human resistin is induced in multiple helminth infections and promotes inflammatory monocytes and increased parasite burden. PLoS Pathog 11, e1004579.

22. Dotsey, E., Ushach, I., Pone, E., Nakajima, R., Jasinskas, A., Argueta, D. A., Dillon, A., DiPatrizio, N., Davies, H., Zlotnik, A., Crompton, P. D., Felgner, P. L. (2017) Transient Cannabinoid Receptor 2 Blockade during Immunization Heightens Intensity and Breadth of Antigen-specific Antibody Responses in Young and Aged mice. Sci Rep 7, 42584.

23. Muse, E. D., Feldman, D. I., Blaha, M. J., Dardari, Z. A., Blumenthal, R. S., Budoff, M. J., Nasir, K., Criqui, M. H., Cushman, M., McClelland, R. L., Allison, M. A. (2015) The association of resistin with cardiovascular disease in the Multi-Ethnic Study of Atherosclerosis. Atherosclerosis 239, 101-8.

24. Schlosburg, J. E., Blankman, J. L., Long, J. Z., Nomura, D. K., Pan, B., Kinsey, S. G., Nguyen, P. T., Ramesh, D., Booker, L., Burston, J. J., Thomas, E. A., Selley, D. E., Sim-Selley, L. J., Liu, Q. S., Lichtman, A. H., Cravatt, B. F. (2010) Chronic monoacylglycerol lipase blockade causes functional antagonism of the endocannabinoid system. Nat Neurosci 13, 1113-9.

25. Li, L., Stoeckert, C. J., Roos, D. S. (2003) OrthoMCL: identification of ortholog groups for eukaryotic genomes. Genome Res 13, 2178-89.

26. Edgar, R. C. (2004) MUSCLE: multiple sequence alignment with high accuracy and high throughput. Nucleic Acids Res 32, 1792-7.

27. Letunic, I., Doerks, T., Bork, P. (2015) SMART: recent updates, new developments and status in 2015. Nucleic Acids Res 43, D257-60.

28. Zhu, X. Q., Korhonen, P. K., Cai, H., Young, N. D., Nejsum, P., von Samson-Himmelstjerna, G., Boag, P. R., Tan, P., Li, Q., Min, J., Yang, Y., Wang, X., Fang, X., Hall, R. S., Hofmann, A., Sternberg, P. W., Jex, A. R., Gasser, R. B. (2015) Genetic blueprint of the zoonotic pathogen Toxocara canis. Nat Commun 6, 6145.

29. Hunt, V. L., Tsai, I. J., Coghlan, A., Reid, A. J., Holroyd, N., Foth, B. J., Tracey, A., Cotton, J. A., Stanley, E. J., Beasley, H., Bennett, H. M., Brooks, K., Harsha, B., Kajitani, R., Kulkarni, A., Harbecke, D., Nagayasu, E., Nichol, S., Ogura, Y., Quail, M. A., Randle, N., Xia, D., Brattig, N. W., Soblik, H., Ribeiro, D. M., Sanchez-Flores, A., Hayashi, T., Itoh, T., Denver, D. R., Grant, W., Stoltzfus, J. D., Lok, J. B., Murayama, H., Wastling, J., Streit, A., Kikuchi, T., Viney, M., Berriman, M. (2016) The genomic basis of parasitism in the Strongyloides clade of nematodes. Nat Genet 48, 299-307.

30. Stoltzfus, J. D., Minot, S., Berriman, M., Nolan, T. J., Lok, J. B. (2012) RNAseq analysis of the parasitic nematode Strongyloides stercoralis reveals divergent regulation of canonical dauer pathways. PLoS Negl Trop Dis 6, e1854.

31. Rosa, B. A., Jasmer, D. P., Mitreva, M. (2014) Genome-wide tissue-specific gene expression, co-expression and regulation of co-expressed genes in adult nematode Ascaris suum. PLoS Negl Trop Dis 8, e2678.

32. Tang, Y. T., Gao, X., Rosa, B. A., Abubucker, S., Hallsworth-Pepin, K., Martin, J., Tyagi, R., Heizer, E., Zhang, X., Bhonagiri-Palsikar, V., Minx, P., Warren, W. C., Wang, Q., Zhan, B., Hotez, P. J., Sternberg, P. W., Dougall, A., Gaze, S. T., Mulvenna, J., Sotillo, J., Ranganathan, S., Rabelo, E. M., Wilson, R. W., Felgner, P. L., Bethony, J., Hawdon, J. M., Gasser, R. B., Loukas, A., Mitreva, M. (2014) Genome of the human hookworm Necator americanus. Nat Genet 46, 261-269.

33. Sotillo, J., Sanchez-Flores, A., Cantacessi, C., Harcus, Y., Pickering, D., Bouchery, T., Camberis, M., Tang, S. C., Giacomin, P., Mulvenna, J., Mitreva, M., Berriman, M., LeGros, G., Maizels, R. M., Loukas, A. (2014) Secreted proteomes of different developmental stages of the gastrointestinal nematode Nippostrongylus brasiliensis. Mol Cell Proteomics 13, 2736-51.

34. Schwarz, E. M., Hu, Y., Antoshechkin, I., Miller, M. M., Sternberg, P. W., Aroian, R. V. (2015) The genome and transcriptome of the zoonotic hookworm Ancylostoma ceylanicum identify infection-specific gene families. Nat Genet 47, 416-22.

35. Langmead, B., Trapnell, C., Pop, M., Salzberg, S. L. (2009) Ultrafast and memory-efficient alignment of short DNA sequences to the human genome. Genome Biol 10, R25.

36. Li, B. and Dewey, C. N. (2011) RSEM: accurate transcript quantification from RNA-Seq data with or without a reference genome. BMC Bioinformatics 12, 323.

37. Turcotte, C., Blanchet, M. R., Laviolette, M., Flamand, N. (2016) The CB2 receptor and its role as a regulator of inflammation. Cell Mol Life Sci 73, 4449-4470.

38. Bouchery, T., Filbey, K., Shepherd, A., Chandler, J., Patel, D., Schmidt, A., Camberis, M., Peignier, A., Smith, A. A. T., Johnston, K., Painter, G., Pearson, M., Giacomin, P., Loukas, A., Bottazzi, M. E., Hotez, P., LeGros, G. (2018) A novel blood-feeding detoxification pathway in Nippostrongylus brasiliensis L3 reveals a potential checkpoint for arresting hookworm development. PLoS Pathog 14, e1006931.

39. Klein, T. W. (2005) Cannabinoid-based drugs as anti-inflammatory therapeutics. Nat Rev Immunol 5, 400-11.

40. Randall, P. A., Vemuri, V. K., Segovia, K. N., Torres, E. F., Hosmer, S., Nunes, E. J., Santerre, J. L., Makriyannis, A., Salamone, J. D. (2010) The novel cannabinoid CB1 antagonist AM6545 suppresses food intake and food-reinforced behavior. Pharmacol Biochem Behav 97, 179-84.

41. Tam, J., Vemuri, V. K., Liu, J., Bátkai, S., Mukhopadhyay, B., Godlewski, G., Osei-Hyiaman, D., Ohnuma, S., Ambudkar, S. V., Pickel, J., Makriyannis, A., Kunos, G. (2010) Peripheral CB1 cannabinoid receptor blockade improves cardiometabolic risk in mouse models of obesity. J Clin Invest 120, 2953-66.

42. Elphick, M. R. (2012) The evolution and comparative neurobiology of endocannabinoid signalling. Philos Trans R Soc Lond B Biol Sci 367, 3201-15.

43. Galles, C., Prez, G. M., Penkov, S., Boland, S., Porta, E. O. J., Altabe, S. G., Labadie, G. R., Schmidt, U., Knölker, H. J., Kurzchalia, T. V., de Mendoza, D. (2018) Endocannabinoids in Caenorhabditis elegans are essential for the mobilization of cholesterol from internal reserves. Sci Rep 8, 6398.

44. Savinainen, J. R., Saario, S. M., Laitinen, J. T. (2012) The serine hydrolases MAGL, ABHD6 and ABHD12 as guardians of 2-arachidonoylglycerol signalling through cannabinoid receptors. Acta Physiol (Oxf) 204, 267-76.

45. Lehtonen, M., Reisner, K., Auriola, S., Wong, G., Callaway, J. C. (2008) Mass-spectrometric identification of anandamide and 2-arachidonoylglycerol in nematodes. Chem Biodivers 5, 2431-41.

46. McPartland, J. M., Matias, I., Di Marzo, V., Glass, M. (2006) Evolutionary origins of the endocannabinoid system. Gene 370, 64-74.

47. Lucanic, M., Held, J. M., Vantipalli, M. C., Klang, I. M., Graham, J. B., Gibson, B. W., Lithgow, G. J., Gill, M. S. (2011) N-acylethanolamine signalling mediates the effect of diet on lifespan in Caenorhabditis elegans. Nature 473, 226-9.

48. Oakes, M. D., Law, W. J., Clark, T., Bamber, B. A., Komuniecki, R. (2017) Cannabinoids Activate Monoaminergic Signaling to Modulate Key C. elegans Behaviors. J Neurosci 37, 2859-2869.

49. Reis Rodrigues, P., Kaul, T. K., Ho, J. H., Lucanic, M., Burkewitz, K., Mair, W. B., Held, J. M., Bohn, L. M., Gill, M. S. (2016) Synthetic Ligands of Cannabinoid Receptors Affect Dauer Formation in the Nematode Caenorhabditis elegans. G3 (Bethesda) 6, 1695-705.

50. Howe, K. L., Bolt, B. J., Shafie, M., Kersey, P., Berriman, M. (2017) WormBase ParaSite - a comprehensive resource for helminth genomics. Mol Biochem Parasitol 215, 2-10.

51. Holroyd, N. and Sanchez-Flores, A. (2012) Producing parasitic helminth reference and draft genomes at the Wellcome Trust Sanger Institute. Parasite Immunol 34, 100-7.

52. Di Marzo, V. and Izzo, A. A. (2006) Endocannabinoid overactivity and intestinal inflammation. Gut 55, 1373-1376.

53. Katz, D., Katz, I., Porat-Katz, B. S., Shoenfeld, Y. (2017) Medical cannabis: Another piece in the mosaic of autoimmunity? Clin Pharmacol Ther 101, 230-238.

54. Acharya, N., Penukonda, S., Shcheglova, T., Hagymasi, A. T., Basu, S., Srivastava, P. K. (2017) Endocannabinoid system acts as a regulator of immune homeostasis in the gut. Proc Natl Acad Sci U S A 114, 5005-5010.

55. Sykaras, A. G., Demenis, C., Case, R. M., McLaughlin, J. T., Smith, C. P. (2012) Duodenal enteroendocrine I-cells contain mRNA transcripts encoding key endocannabinoid and fatty acid receptors. PLoS One 7, e42373.

56. Senin, L. L., Al-Massadi, O., Folgueira, C., Castelao, C., Pardo, M., Barja-Fernandez, S., Roca-Rivada, A., Amil, M., Crujeiras, A. B., Garcia-Caballero, T., Gabellieri, E., Leis, R., Dieguez, C., Pagotto, U., Casanueva, F. F., Seoane, L. M. (2013) The gastric CB1 receptor modulates ghrelin production through the mTOR pathway to regulate food intake. PLoS One 8, e80339.

57. Else, K. J. (2005) Have gastrointestinal nematodes outwitted the immune system? Parasite Immunol 27, 407-15.

58. Goumon, Y., Casares, F., Pryor, S., Ferguson, L., Brownawell, B., Cadet, P., Rialas, C. M., Welters, I. D., Sonetti, D., Stefano, G. B. (2000) Ascaris suum, an intestinal parasite, produces morphine. J Immunol 165, 339-43.

59. Golabi, M., Naem, S., Imani, M., Dalirezh, N. (2016) Evidence of morphine like substance and mu-opioid receptor expression in Toxacara canis (Nematoda: Ascaridae). Veterinary Research Forum 7, 335-339.

60. Astarita, G., Rourke, B. C., Andersen, J. B., Fu, J., Kim, J. H., Bennett, A. F., Hicks, J. W., Piomelli, D. (2006) Postprandial increase of oleoylethanolamide mobilization in small intestine of the Burmese python (Python molurus). Am J Physiol Regul Integr Comp Physiol 290, R1407-12.

61. Cottone, E., Pomatto, V., Cerri, F., Campantico, E., Mackie, K., Delpero, M., Guastalla, A., Dati, C., Bovolin, P., Franzoni, M. F. (2013) Cannabinoid receptors are widely expressed in goldfish: molecular cloning of a CB2-like receptor and evaluation of CB1 and CB2 mRNA expression profiles in different organs. Fish Physiol Biochem 39, 1287-96.

62. Pacioni, G., Rapino, C., Zarivi, O., Falconi, A., Leonardi, M., Battista, N., Colafarina, S., Sergi, M., Bonfigli, A., Miranda, M., Barsacchi, D., Maccarrone, M. (2015) Truffles contain endocannabinoid metabolic enzymes and anandamide. Phytochemistry 110, 104-10.

63. Heng, T. S., Painter, M. W., Consortium, I. G. P. (2008) The Immunological Genome Project: networks of gene expression in immune cells. Nat Immunol 9, 1091-4.

64. DiPatrizio, N. V. (2016) Endocannabinoids in the Gut. Cannabis Cannabinoid Res 1, 67-77.

65. Izzo, A. A. and Sharkey, K. A. (2010) Cannabinoids and the gut: new developments and emerging concepts. Pharmacol Ther 126, 21-38.

66. Cani, P. D., Plovier, H., Van Hul, M., Geurts, L., Delzenne, N. M., Druart, C., Everard, A. (2016) Endocannabinoids--at the crossroads between the gut microbiota and host metabolism. Nat Rev Endocrinol 12, 133-43.

67. Goodridge, H. S., Marshall, F. A., Else, K. J., Houston, K. M., Egan, C., Al-Riyami, L., Liew, F. Y., Harnett, W., Harnett, M. M. (2005) Immunomodulation via novel use of TLR4 by the filarial nematode phosphorylcholine-containing secreted product, ES-62. J Immunol 174, 284-93.

68. Winter, A. D., Gillan, V., Maitland, K., Emes, R. D., Roberts, B., McCormack, G., Weir, W., Protasio, A. V., Holroyd, N., Berriman, M., Britton, C., Devaney, E. (2015) A novel member of the let-7 microRNA family is associated with developmental transitions in filarial nematode parasites. BMC Genomics 16, 331.

69. Riner, D. K., Ferragine, C. E., Maynard, S. K., Davies, S. J. (2013) Regulation of innate responses during pre-patent schistosome infection provides an immune environment permissive for parasite development. PLoS Pathog 9, e1003708.

CHAPTER FOUR - Conclusion

Summary

Macrophage-derived RELMα cell-intrinsically regulates macrophage functions during hookworm infection

Previous studies have identified the role of RELMα in limiting Th2 cytokine-induced inflammation in settings such as asthma and helminth infection. However, given that RELMα is produced by vastly distinct cell types such as lung airway epithelial cells and immune cells, in chapter two we investigated the functional contribution of RELMα derived from immune and non-immune cells. We took advantage of bone marrow chimera technology to show that immune cell-derived RELMα**,** but not non-immune cell-derived RELMα**,** downregulates the Th2 immune response against *Nb* hookworms and therefore impairs the host's ability to clear worms. Further, we identified $CD11c^{+}$ $F4/80^{+}$ macrophages as the primary source of immune cell-derived RELMα in hookworm infected lungs.

To investigate the mechanism by which RELMα inhibits worm expulsion, we utilized $CD11c^{+}$ macrophage-worm co-culture assays. We demonstrated that RELMα impairs macrophage attachment and subsequent killing of worms. We then utilized Nanostring technology to measure RELMα-induced changes in expression of over 700 myeloid specific genes in purified lung macrophages. We discovered that RELMα treatment downregulated genes involved in biological pathways such as cell adhesion and Fc receptor signaling, and upregulated genes associated biological pathways such as cycle and apoptosis and Th1 activation.

Collectively, these results suggest that macrophage-derived RELMα is an important host molecule for regulating immune cell functions and for controlling inflammation during hookworm infection.

Endocannabinoids promote host immune responses against hookworms

In chapter three we explored the impact of host and parasite endocannabinoid signaling during hookworm infection. Endocannabinoids are lipid-derived signaling molecules that signal through cannabinoid receptors that have impacts on physiological processes such as feeding. Previous studies have extensively studied the mammalian endocannabinoid system in the brain, gut and immune system. However, how endocannabinoids function in helminth infection and whether organisms such as hookworms were able to produce endocannabinoids was not explored. We utilized the *Nb* hookworm model and discovered that the host produces endocannabinoids in the lung and intestine, AEA, 2-AG and OEA.

To elucidate the function of endocannabinoid signaling, we utilized commercially available CB receptor antagonists and discovered that endocannabinoid signaling via CB1 and not CB2 receptor is important in host IL-5 cytokine expression and worm and egg clearance. Interestingly, we also observed *Nb* worms producing endocannabinoids at all lifecycle stages. Further, we also discovered that *Nb* and other parasitic worms encode genes for endocannabinoid biosynthetic and degradative enzymes. This was the first description of helminths producing endocannabinoids and of endocannabinoids promoting host immune responses and reduce parasite burden.

These data demonstrate that endocannabinoids are produced during hookworm infection by both the host and parasite. As a host molecule, endocannabinoids are important signaling molecules that regulate immune responses to ensure that the appropriate immune response is launched against parasitic worm invasion.

Future Directions

Why is immune cell-derived and not non-immune cell-derived RELMα immunomodulatory?

Our studies and others have shown that considerably higher levels of RELMα is expressed by airway epithelial cells and immune cells as measured in BAL fluid and serum, respectively. If without physiological consequences, why do epithelial cells produce RELMα and why does immune cell-derived RELMα have function on the immune system? There is currently no evidence that RELMα is produced as two isoforms by each of the cell types. Our prediction is that due to the mobility of immune cells, they can migrate in and out of the lungs during infection as well as draining lymph nodes, therefore have prime access for communication with other immune cells for immune regulation. Further, it is possible that RELMα produced by epithelial cells is secreted into the airways and not accessible to the lung parenchyma or immune cells therein. To delineate the contribution of macrophage and epithelial cell RELMα in worm infection, future studies should perform worm infections on novel RELMα reporter mice crossed with CRE/lox systems to generate cell specific RELMα deficient mice.

What is the function of host versus helminth endocannabinoids?

We and others show that endocannabinoids are produced in hookworm infected lungs and intestine. We separately show that hookworms at all development stages produce endocannabinoids as well. In our system we tested the function of endocannabinoids by using a CB1R antagonist *in vivo*. However, it is likely that this compound abrogated CB1 signaling in both host and parasite. To delineate the role of each source of endocannabinoids, future studies

should employ commercially available $CB1R^{-/-}$ as well as $CB2R^{-/-}$ mice. In these studies helminth infected mice and treated with or without endocannabinoid antagonistic drugs will identify the importance of host and parasite-derived endocannabinoids.

Conclusion

In this thesis, we investigated the role of two host factors for their role in regulating immune responses against hookworms. First, we investigated RELMα for its role in regulating immune responses in the lung during hookworm infection. In keeping with previous reports, we found that RELMα impaired Th2 immunity and consequently impaired the hosts ability to clear worms. Upon closer examination, we discovered that the cellular source of RELMα was critical for its function. RELMα sourced from immune cells, more accurately macrophages, functioned in a cell-intrinsic fashion where it inhibited anti-worm macrophage functions. Mechanistically, RELMα downregulated genes in macrophages involved in cell adhesion and upregulated genes involved in Th1 activation resulting in less Th2 polarized macrophages that were less able to attach to and kill worms. Given that heightened immune responses come at a cost of tissue damage, we predict that RELMα exists not to serve as a detriment to the host by retaining parasitic worms. Rather, it is possible that mammals evolved to express such a protein to ensure an 'immune check' during situations of aberrant inflammation for host protection. We next investigated the role of endocannabinoids in regulating immune responses to hookworm infection. We discovered a novel role of intestinal endocannabinoids in stimulating Th2 cytokines during worm infection that consequently promoted worm clearance by the host. We also discovered that parasitic worms are capable of endocannabinoid production. Why both host and parasite produce the same molecules with consequences against the parasite is yet unclear. Given that endocannabinoids dull pain responses, it is possible that burrowing parasitic worms produce these molecules to downplay host response to pain from lung tissue injury and that the host produces these molecules to stimulate immune responses to kill and expel worms. We propose a

mechanism where two disparate host molecules, RELMα and endocannabinoids, function in parallel for host protection during helminth infection (Figure 20).

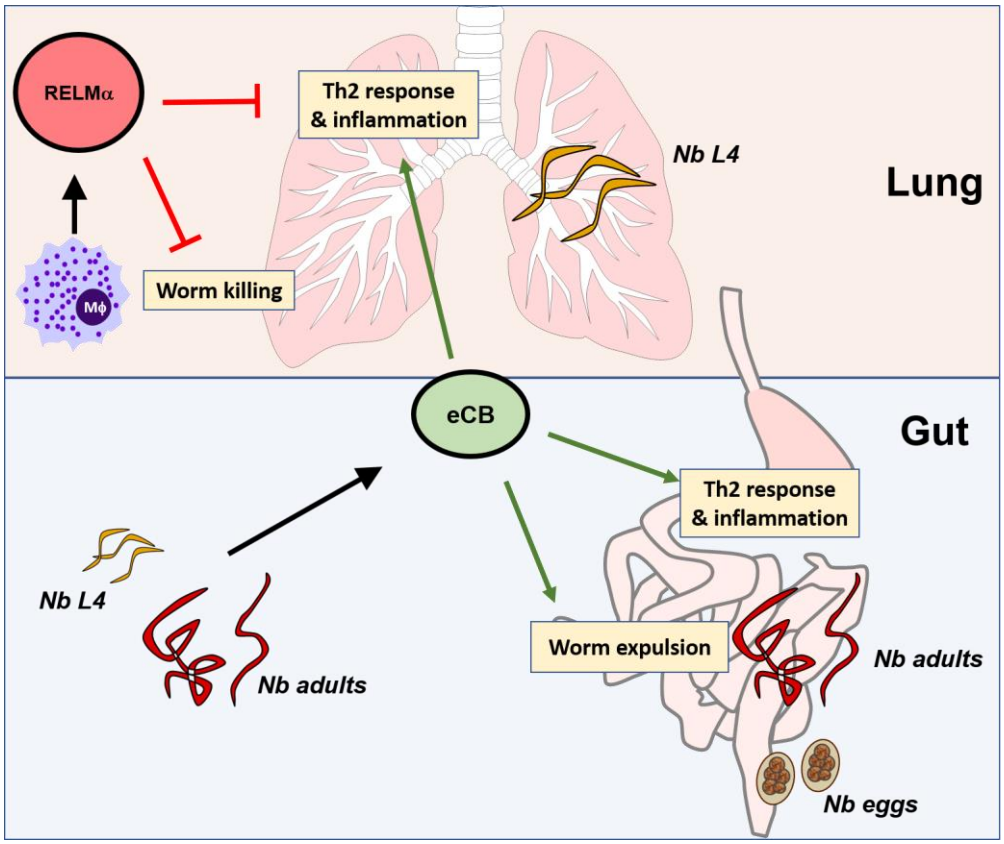

Figure 20. Immunomodulation by RELMα and endocannabinoids during helminth infection.